

2-
mix

Reports of the Department of Geodetic Science

Report No. 176

D K J 1

AN INVESTIGATION TO IMPROVE SELENODETIC CONTROL ON THE LUNAR LIMB UTILIZING APOLLO 15 TRANS-EARTH PHOTOGRAPHY

by

Wyndham Riette

Prepared for

National Aeronautics and Space Administration
Manned Spacecraft Center
Houston, Texas

Contract No. NAS 9-9695
OSURF Project No. 2841
Interim Report No. 7



NASA-CR-131264) AN INVESTIGATION TO
IMPROVE SELENODETIC CONTROL ON THE LUNAR
LIMB UTILIZING APOLLO 15 TRANS-EARTH
PHOTOGRAPHY (Ohio State Univ. Research
Foundation) 118 p HC \$8.00

(MOAD)
CSCL 03B

G3/30

N73-20846

Unclass

17239

The Ohio State University
Research Foundation
Columbus, Ohio 43212

June, 1972

118

Reports of the Department of Geodetic Science

Report No. 176

AN INVESTIGATION TO IMPROVE SELENODETIC CONTROL
ON THE LUNAR LIMB UTILIZING APOLLO 15
TRANS - EARTH PHOTOGRAPHY

by

Wyndham Riotte

Prepared for
National Aeronautics and Space Administration
Manned Spacecraft Center
Houston, Texas

Contract No. NAS 9-9695

OSURF Project No. 2841

Interim Report No. 7

The Ohio State University
Research Foundation
Columbus, Ohio 43212

June, 1972

PRECEDING PAGE BLANK NOT FILMED

PREFACE

This project is under the supervision of Ivan I. Mueller, Professor of the Department of Geodetic Science at The Ohio State University, and it is under the technical direction of Mr. Richard L. Nance, Photogrammetry and Cartography Section, NASA/MSC, Houston, Texas. The contract is administered by the Space Sciences Procurement Branch, NASA/MSC, Houston, Texas.

A revised version of this report has been submitted to the Graduate School of The Ohio State University in partial fulfillment of the requirements for degree Master of Science.

ACKNOWLEDGEMENT

I wish to express my appreciation to the faculty and staff of the Department of Geodetic Science, among whom professors Urho A. Uotila and Sanjib K. Ghosh were most influential in furthering my knowledge in adjustment computations and photogrammetry. Special thanks go to Dr. Dean C. Merchant who not only was instrumental in teaching computational photogrammetry but, for his guidance in the preparation of this report.

I am indebted to Mr. Richard Nance of the Photogrammetry and Cartography Section, NASA/MSC, Houston for providing the material required for this project; Mr. Lloyd Herd and Mr. Neal O'Brien of the Ohio Department of Highways for the instruction and use of the Analytical Plotter Commercial; the Ohio State University Computer Information Center for the use of the IBM 370 computer.

I would also like to express my thanks to Mr. James Reilly for invaluable programming assistance and Mrs. Evelyn Rist and Miss Susan Breslow for the typing of this report.

TABLE OF CONTENTS

	<u>Page</u>
PREFACE	ii
ACKNOWLEDGEMENT.....	iii
TABLE OF CONTENTS.....	iv
LIST OF FIGURES	vi
LIST OF TABLES	vii
LIST OF PLATES	viii
ABSTRACT	1
1. INTRODUCTION	2
2. HISTORY	4
2.1 Development of Earth-Based Heliometric and Photographic Measurements	4
2.2 Spacecraft Improvements in Selenodetic Control.....	8
3. APOLLO 15 MISSION	11
3.1 Summary of the Mission	11
3.2 Apollo 15 SIM Equipment	11
4. PROCEDURE	17
4.1 Evaluation of Metric Camera Film	17
4.2 Selection of Control and NEC (New Extended Control)	28
4.2.1 Selenographic Coordinate System	28
4.2.2 Visible Lunar Control	30
4.2.3 New Extended Control	33
4.3 Observation and Reduction of Observations	39
4.3.1 Observations of Photo Coordinates	39
4.3.2 Reduction of Observations	42
4.4 Block Adjustment Program (FORTBLOCK)	49
4.4.1 Input to FORTBLOCK.....	49
4.4.2 Results of FORTBLOCK	54
5. SUMMARY AND CONCLUSIONS	78
6. RECOMMENDATIONS	82

BIBLIOGRAPHY	85
APPENDICES	90
I. LIST OF ORBITER IV PHOTOGRAPHS WITH ACIC CONTROL INDICATED	90
II. TRANC 4 - PROGRAM FOR TRANSFORMING COMPARATOR COORDINATES INTO PHOTO COORDINATES	91
III. PROGRAM FOR CALCULATING ϕ , λ , h FROM X, Y, Z	105

LIST OF FIGURES

Page

1. Apollo 15 Trajectory from TEI + ~ 20 min to TEI + ~ 1 hr 42 min.	12
2. Scientific Instrument Module Configuration.	13
3. Film Format Diapositive Emulsion Up.	16
4. Frame 2753 at TEI + 20 min.	18
5. Frame 2765 at TEI + 25 min.	19
6. Frame 2780 at TEI + 30 min.	20
7. Frame 2795 at TEI + 35 min.	21
8. Frame 2810 at TEI + 40 min.	22
9. Frame 2825 at TEI + 54 min.	23
10. Selenographic Coordinate System Fixed to the Lunar Sphere.	29
11. Approximate Coordinates of NEC No. 15 $\phi = -50^{\circ}.8$ $\lambda = 82^{\circ}.0$.	34
12. Approximate Coordinates of NEC No. 13 $\phi = -41^{\circ}.3$ $\lambda = 97^{\circ}.6$.	35
13. Approximate Coordinates of NEC No. 12 $\phi = -33^{\circ}.5$ $\lambda = 96^{\circ}.2$ and NEC No. 17 $\phi = -36^{\circ}.8$ $\lambda = 99^{\circ}.1$.	36
14. Approximate Coordinates of NEC No. 16 $\phi = -56^{\circ}.2$ $\lambda = 90^{\circ}.4$.	37
15. Approximate Coordinates of NEC No. 14 $\phi = -39^{\circ}.7$ $\lambda = 84^{\circ}.5$.	37
16. Approximate Coordinates of NEC No. 11 $\phi = -4^{\circ}.4$ $\lambda = 93^{\circ}.3$.	38
17a. Plan View Of $\alpha = \tan^{-1} \frac{Y_0}{X_0}$.	50
17b. Perspective View Of Primary Rotation.	50
18. Secondary Rotation.	51
19. Tertiary Rotation.	52

LIST OF TABLES	<u>Page</u>
1. Mapping Camera Characteristics.	15
2. Selected Frames of Metric Camera SN - 003.	25
3. Coordinates of Control Points.	31
4. Selenographic Coordinates of Control Points .	32
5. NEC Coordinates.	33
6. NEC Selenographic Coordinates.	39
7. Frame Number and Measured Feature .	41
8. Estimates of Six Elements of Exterior Orientation .	53
9. Summary of Results 6 Photo Block Adjustment (3 iterations).	72
10. Summary of Results 6 Photo Block Adjustment (6 iterations).	73
11. Summary of Results 12 Photo Block Adjustment (3 iterations).	74
12. Summary of Results 12 Photo Block Adjustment (6 iterations).	75
13. Adjusted ϕ , λ , h of NEC Points.	76
14. Residuals and Standard Deviations of Control Points.	80

	LIST OF PLATES	<u>Page</u>
1.	Results of TRANC 4 for Photo Frames 2774 and 2777.	44
2.	Results of TRANC 4 for Photo Frames 2780 and 2785.	44
3.	Results of TRANC 4 for Photo Frames 2790 and 2795.	45
4.	Results of TRANC 4 for Photo Frames 2800 and 2805.	45
5.	Results of TRANC 4 for Photo Frames 2810 and 2815.	46
6.	Results of TRANC 4 for Photo Frames 2820 and 2825.	46
7.	FORTBLOCK Output Listing for 12 Photo Block Solution; Title Page.	55
8.	FORTBLOCK Output Listing for 12 Photo Block; Results of Exterior Oreintation for Photos 2774 and 2777.	56
9.	FORTBLOCK Output Listing for 12 Photo Block; Results of Exterior Orientation for Photos 2780 and 2785.	57
10.	FORTBLOCK Output Listing for 12 Photo Block; Results of Exterior Orientation for Photos 2790 and 2795.	58
11.	FORTBLOCK Output Listing for 12 Photo Block; Results of Exterior Orientation for Photos 2800 and 2805.	59
12.	FORTBLOCK Output Listing for 12 Photo Block; Results of Exterior Orientation for Photos 2810 and 2815.	60
13.	FORTBLOCK Output Listing for 12 Photo Block; Results of Exterior Orientation for Photos 2820 and 2825.	61
14.	FORTBLOCK Output Listing for 12 Photo Block; Results of Photo Coordinates.	62
15.	FORTBLOCK Output Listing for 12 Photo Block; Results of Photo Coordinates.	63
16.	FORTBLOCK Output Listing for Photo Block; Results of Photo Coordinates.	64

17.	FORTBLOCK Output Listing for 12 Photo Block; Results of Photo Coordinates.	65
18.	FORTBLOCK Output Listing for 12 Photo Block; Results of Control Points 1 and 2.	66
19.	FORTBLOCK Output Listing for 12 Photo Block; Results of Control Point 3 and NEC Point 11.	67
20.	FORTBLOCK Output Listing for 12 Photo Block; Results of NEC Points 12 and 13.	68
21.	FORTBLOCK Output Listing for 12 Photo Block; Results of NEC Points 14 and 15.	69
22.	FORTBLOCK Output Listing for 12 Photo Block; Results of NEC Points 16 and 17.	70
23.	FORTBLOCK Output Listing for 12 Photo Block; Results of Control Point 4.	71
I. (a-f)	Main Program for TRANC 4.	99-104
I. (g)	Subroutine RADIS for Computing Radial Distortion.	104
II. (a)	Main Program for Computing ϕ, λ , and h from X, Y, Z.	107
II. (b)	Subroutine CONVRT for Converting Degrees.	108

ABSTRACT

A study is made using actual metric photography taken by Apollo 15 after the Trans Earth Injection (TEI) when the spacecraft left the lunar orbit. After measurements on 12 frames were reduced for 11 known control and unknown points on the eastern limb, a least squares adjustment program provided the simultaneous solution for the selected points. The results indicate an improvement in selenodetic control may be achieved over a limited portion of the lunar limb; however, the solution could be further improved by strengthening the geometry of intersecting rays through additional observations of the same area using film from the succeeding Apollo missions.

1. INTRODUCTION

It was shown in an earlier report (Sprague [33]) that it is theoretically feasible to extend control from points of known location to unknown points on the lunar surface through the use of photogrammetric techniques with Apollo metric photography taken after the spacecraft leaves the moon's orbit. Specifically, this report used the theory with the data available from the Apollo 15 mission (July, 1971). Whenever possible, the nomenclature and the testing with real data followed the original report so that this is in part, a follow-on study; however, it is complete in that it stands alone on its own organization, results, conclusions and recommendations.

Measuring the moon, establishing lunar control, preparing lunar charts and solving for the physical shape, libration and orbiting parameters from earth-based telescopes and photographs had progressed to the limit of the observational capabilities of the equipment available when the first spacecraft approached the moon [8]. Determining plate constants, effects of atmospheric 'seeing,' and continuous reference to Franz's earliest heliometric measurements were some of the problems encountered and are discussed in the first section of the report.

The spacecraft, in particular, the Lunar Orbiter Series, provided a new perspective to the moon and consequently a new chapter was written on lunar chart preparation. The advent of man's venture to the surface forced to the forefront the requirement of having known control in order to prepare for a successful landing. The orbiting astronauts established landmark tracking points around the lunar equator. According to Robert M. Bizzell and Rigdon E. Joosten of NASA [4] these coordinates are felt to compose the most satisfactory control network available. The Apollo 15 was the first to carry a complete metric camera assembly designed to assist in the measure of the moon.

Twenty of the second generation frames showing the eastern limb of the moon receding from view with 100% overlap taken from TEI (Trans-Earth Injection) + ~20 minutes to TEI + ~47 minutes were selected for this study. Four control points, three lunar landmark tracking and one earth-base control point were found on the limb in the 'window' of visible features in the photo frames. Seven additional points whose positions were estimated from ACIC charts were selected as the NEC (New Extended Control) points which were solved for in the adjustment.

These eleven points on twelve photographs were measured on an AP/C (Analytical Plotter/Commercial) and the subsequent coordinates were reduced for the block adjustment program. The FORTBLOCK adjustment program processed 6 and 12 photo blocks and provided the adjusted coordinates for the eleven points and twelve exposure stations. Due to the unusual geometry of receding photography each of the 6 and 12 photo block adjustment was iterated six times. After the sixth iteration of the 12 photo block a follow on program provided the adjusted latitude and longitude of the seven NEC points from the adjusted selenographic coordinates.

Although the results were reasonable one area of concern was evident. The adjustment of the 6 and 12 photo block had an effect on the residuals and standard deviations of the four control points. In almost all cases the resulting standard deviations were larger than that provided by NASA. It is felt that this is attributed to the following causes: a) only four control points were located, b) the four control points were located on the limb of the photographed moon, c) the receding photography provided a very small horizontal base-height ratio. It is concluded that the resulting poor geometry could be improved by a) a more equatorial TEI trajectory which would allow the available control points to be centrally located, b) rephotographing the same NEC points on succeeding lunar flights, c) reaccomplishing the adjustment by using the film and data from succeeding Apollo missions.

2. HISTORY

The problem of unraveling the moon's history is a broad subject, covering as many areas of the physical sciences as any other. Since man has visited the ever present neighbor as many more questions have been raised as have been answered. The determination of the physical libration constants, the shape of the moon, the measurement of fundamental features and production of accurate lunar charts are all an interwoven part of this history and the answers are as varied as the authors. An outline of the problems and previous accomplishments is provided in earlier reports [8], [29], [33] and will not be repeated here; however, prior to the presentation of this project a brief introduction on measurement of lunar features and lunar charts is in order.

This chapter will describe the development of earth-based measurement of lunar coordinates using the heliometer and earth-based photographs in the first section. It will discuss the use of the heliometer by Franz, the measurements of earth based photographs by the University of Manchester, the problems that evolved, and ACIC's efforts at establishing lunar control coordinates. The second section will discuss the improvements provided by spacecraft photography.

2.1 Development of Earth-Based Heliometric and Photographic Measurements

Almost all notable efforts of measuring and establishing control on the moon started with the development of the heliometer, a device used for measuring angular separation from a reference point to the limb. The heliometer was invented in 1748 by Bouguer and was modified by Dolland. The device consisted of a telescope with two objectives mounted side by side so that two images of an object would be formed and the movement of one in relation to the other would provide measurement of angular distances. The modification consisted

of replacing the two lenses by two halves of a bisected lens so that only one superimposed image appeared at the focus. If one half moves in relation to the other similar angular separation can be measured. Since it was used for measuring the diameter of the sun it was called "heliometer." Bessel used the heliometer in 1839 to measure the distance between the center and lunar limb in order to solve for physical librations [15]. Although precise measurements have been made there are certain limitations. The largest aperture of any heliometer used is 8 inches and based on physical optics it cannot resolve angular separations smaller than one second of arc. Analysis of point locations refined further than this limitation is reaching for information inside diffraction patterns [14].

The basis for earth-based measurements of lunar features stems from Franz's 1890 heliometric measurement of eight craters in reference to the ninth - a center crater named Mösting A. These nine points with their accuracies and inaccuracies have formed the basis for numerous subsequent measurements. Franz measured an additional 141 points on five Lick Observatory plates in 1891 and inconsistencies were already established for the location of the assigned center point. In fact Ruffin and Meyer [31] show considerable discrepancies by seven prominent men in establishing the coordinates of this crater. A fundamental fault of Franz's measurements was the lack of determination of heights.

In 1958 Schrutka-Rechtenstamm reduced these 150 measurements and he developed absolute heights (i.e., absolute heights above and below a sphere with a radius of 1738.0 km). It is important to note that this was the first time that all heliometric readings were unified into a comprehensive mean to compute the libration constants. A list of these features, their coordinates and heights can be found in [31].

From this time all efforts were directed towards determining the heights of features. If one is given enough three dimensional coordinates one

can determine the shape of the moon, in particular the tidal bulge and then the answers to some of the questions may become possible. Of the numerous efforts several are of interest.

In 1963, Baldwin in the Measure of the Moon, showed the results of measurements on 696 lunar features, but the measurements were made on only five Lick Observatory plates. G. A. Mills of the Department of Astronomy, University of Manchester, England in 1967 increased the number of observations. He divided the visible portion into 96 zones and he provided the measured and reduced coordinates of 919 points. He also used the 'stereoscopic' method which involved the taking of photographs at different librations to utilize the apparent displacement effect. Although the displacement averages 15° , the effect provided measurements on at least 28 plates for each feature [20].

Three problems arise in the measuring and determining coordinates of these lunar features and are discussed in subsequent paragraphs, 1) determination of plate constants 2) coordinates were based on 38 selected Franz-Schratka-Rechtenstamm and Meyer-Ruffin points whose coordinates were felt to be well known 3) effects of atmospheric 'seeing.'

Zdenek Kopal, also of the Department of Astronomy, University of Manchester working for AFCRL in 1969 - 1970, recognized the problem of determining plate constants. His solution consisted of photographing the moon on pre-exposed stellar plates. The great advantage of the star calibrated lunar photographs is the ability to define the inclination of the lunar axis very precisely. "The plate constants which are defined by comparison of the stellar positions measured on the photographic plates to their equatorial coordinates include the rotation transformation which makes the axis of measures parallel to the projection of the ecliptic coordinates on the plate" [16].

A. A. Gurshtein and N. P. Slovokhotova of the Institute for Space Research, Moscow, recognized that well-established lunar control must be found independent of the original nine Franz points [11]. Their concept, though theoretical,

is to solve the libration problem by long and systematic earth-based observations, including the installation and use of cube-corner retro-reflectors and devices for observing from the lunar surface at approximately 20 points. These could be extended to 200 "first order" points for determining the moon's shape and for small scale mapping (1:1,000,000) such as the ACIC LAC series. This network could be further extended to 20,000 near side points for "third order" work. Since their concept involves a long-term solution, the authors evaluated six previous catalogues by men prominent in the field. The coordinates of 192 easily identifiable, symmetrical, well-distributed features were selected to be used as a fundamental network until their concept was attempted [11].

The 'seeing' problem was investigated by Donald L. Meyer when ACIC worked on establishing lunar control for their charting efforts prior to and during the Apollo missions. By experimenting and testing with different sequences and times of exposures, efforts were made at reducing the circular error of plate-to-plate transformation for mean plate coordinates. The purpose of the test was to demonstrate the distortions caused by 'seeing' effects as opposed to measurement and interpretation errors and it was shown that the error can be reduced from 22 microns to 8 microns when a particular sequence and time exposure is used - but the important point is that this is an additional problem area included in the solutions. These distortions can give a displacement of 1 - 2 km which is nearly as large as the departures from the lunar sphere (averages 1738 ± 3 km, Kopal) required for determination of the lunar shape, orbital motion and libration constants problem etc. [19].

The ACIC effort in 1965 at establishing lunar control is quite rigorous and is explained fully in [1], [6], [31]. The stereoscopic principal or intersection of perspective rays was used on a sequence of plates taken at Pic-du-Midi Observatory, France and U.S. Naval Observatory, Flagstaff. Even at the best resolution, the photographs only show features 1 - 3 km in size. The solution of the 'seeing' problem in using features of this size was attempted by taking different

sequences and exposures at these two observatories so that an averaging of the displacements could be performed. ACIC selected 196 points for measurement including 31 Franz-Schrutka points which were selected as fundamental points. This list of 196 plus an additional list of 89 point locations along with the associated standard errors in x , y , h were used for this report and are described in Chapter 3.

This brief outline of the efforts at establishing lunar control from earth-based procedures is not meant to be all inclusive nor is it meant to slight the important work by others such as Marchant, Arthur, Montsoulas, Hunt, AMS, DOD, etc., but its purpose was to show the underlying problems that have persisted in the development of obtaining feature positioning on the moon.

2.2 Spacecraft Improvements in Selenodetic Control

A large step forward was taken with the Lunar Orbiter spacecraft photos starting from 1966 through 1967, for now different perspectives were available and the problem of the earth's atmosphere could be circumvented. This made the first real procedure available where the control could be established away from the center of figure concept of Franz and true independent control could be established as discussed in [29]. The Orbiter photography, though not of photogrammetric quality, led to the development of the excellent series of ACIC charts which provided the first complete and relatively accurate picture of the entire lunar surface. However, it is not until the establishment of control points taken in an inertial system from the Apollo series which is dependent on the lunar motion and lunar datum defined by the center of mass are the resulting coordinates free from Franz's measurements [22], [30].

The history of the mapping of the moon is covered explicitly in [6] [17]. However, since the Orbiter IV photographs and the ACIC lunar charts were used as sources for selenodetic control in this project, a word of introduction is necessary. The Lunar Orbiter series and particularly Orbiter IV which was

placed in a near polar orbit provided the first complete detailed imagery of the lunar farside. Although the pictures were not designed for photogrammetric work, enough data, especially the orbital information data, was available in order that photogrammetric triangulation of areas near Apollo landing sites was accomplished which greatly enhanced the ACIC charts. The series of ACIC charts includes the first nearside 1:1,000,000 Lunar Astronautical Chart (LAC) based on the 196 fundamental points. This series of 1:1,000,000 appears to be the most popular international working scale for reasons described in [9]. The 1:2,500,000 Lunar Planning Chart (LOC) was devised by using the Orbiter II-V information for a positional reference system which related features from the near side to far side [4]. Ruffin explains in [32] the details of the positional reference system. He describes the Orbiter spacecraft orbiting information, the selected frames in matching the control photographed to the near side control points then extending to the far side regions. The extension was first to areas of photo coverage then into areas without photo coverage. The misclosures of the extensions were distributed linearly.

Now Apollo landmark tracking points are available to provide control in an equatorial region around the moon. The first attempt, procedure and coordinate results by Apollo 8 are covered in [22]. The addition of a number of points by succeeding Apollo missions through Apollo 12 is described in [4], [30], [33]. The reliability of these positions is such that they are now used for this project and for evaluation of current lunar cartographic work because...

" (1) the Apollo Landmark control points are in a center of mass system, (2) their values are consistent, (3) the orbital parameters used in their reduction are superior to previous programs, e.g., Lunar Orbiter, (4) the spacecraft optical sighting technique yields stronger and redundant geometry for improved solution and reliability determinations, (5) the control points extend to the lunar backside where no control existed previously, (6) no significant improvement in accuracy of future control systems are anticipated and (7) these

control points are consistent with the Apollo navigation system for which subsequent operational and mission planning is a primary requirement of lunar cartographic products." [4].

3. APOLLO 15 MISSION

3.1 Summary of Mission

The successful Apollo 15 mission, the first of three flights scheduled in the Apollo J series and the first to provide mapping quality photographs of the lunar surface was launched from Kennedy Space Center, Florida at 9:34:00 a.m. e.d.t. on July 26, 1971. The spacecraft was manned by Colonel David R. Scott, Commander; Major Alfred J. Worden, Command Module Pilot; and Lt. Col. James B. Irwin, Lunar Module Pilot.

Each Apollo mission has numerous time categories and two of interest are the Apollo Elapsed Time and Ground Elapsed Time. The Apollo Elapsed Time is the time from range zero and range zero is the integral second prior to lift off. The Ground Elapsed Time is the time monitored from actual space vehicle lift off. The difference between AET and GET was less than one second for Apollo 15 [23]. After a GET (Ground Elapsed Time) of 173.5 hours into the mission the ascent stage that lifted off the lunar surface docked with the command module. The lunar orbital phase of the Apollo 15 mission was terminated when the module's position was approximately 180° longitude, by the TEI (Trans-Earth Injection) maneuver at 223:48:45 which lasted 141.2 seconds [26]. The path of the orbit as projected to the lunar surface from TEI + ~ 20 minutes to TEI + ~ 1 hour 42 minutes is shown in Figure 1. The trans earth coast extravehicular activity began at about 242 hours and the Command Module Pilot retrieved the film cassettes and examined the SIM (Scientific Instrument Module). The mission terminated with the landing at a GET time of 295:11:53 [26].

3.2 Apollo 15 SIM Equipment

The location of the SIM in the Apollo15 service module is shown in Figure 2.

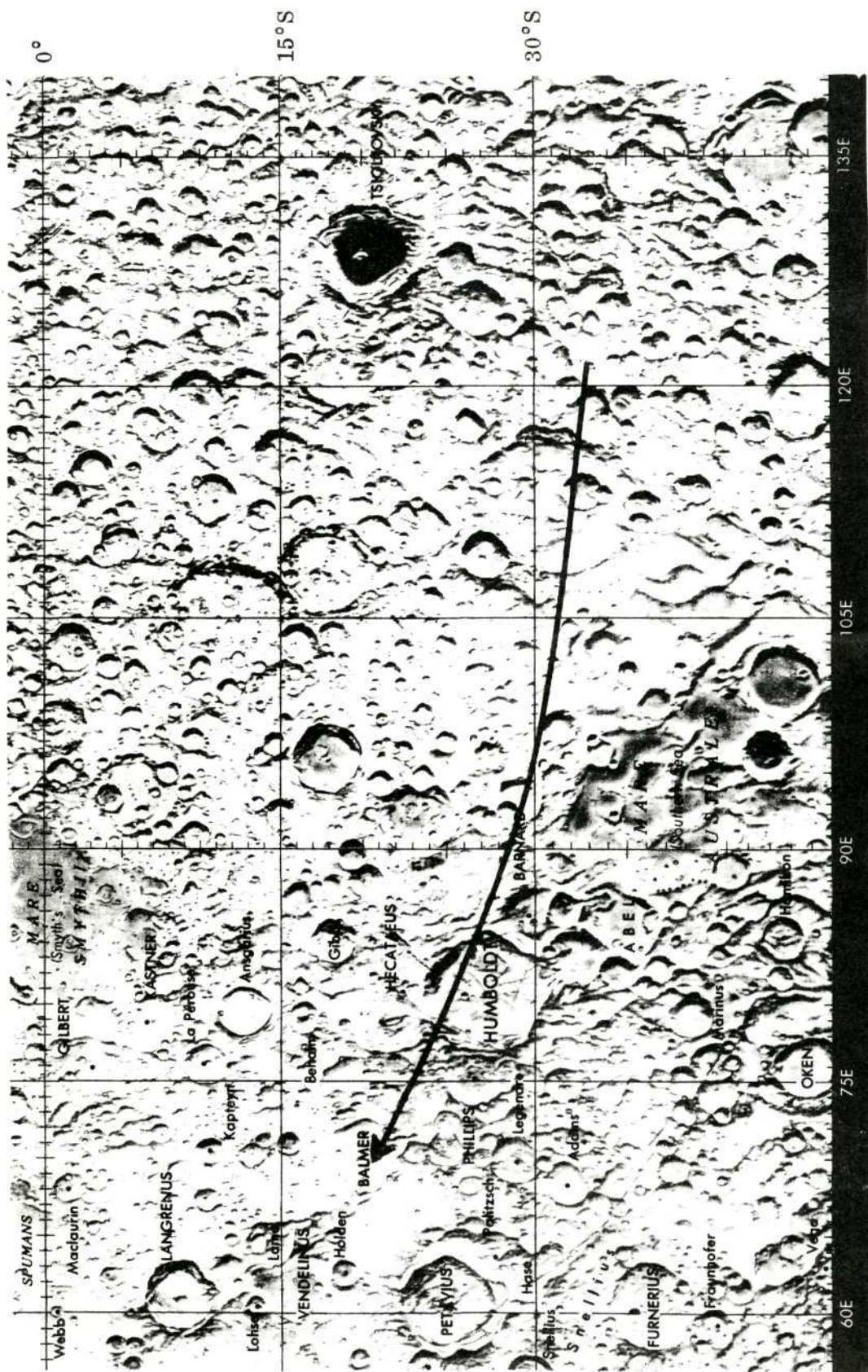


Figure 1.

Apollo 15 Trajectory from TEI + 20 min to TEI + 1 hr 42 min
Reproduction from ACIC Lunar Chart (scale 1:10,000,000)

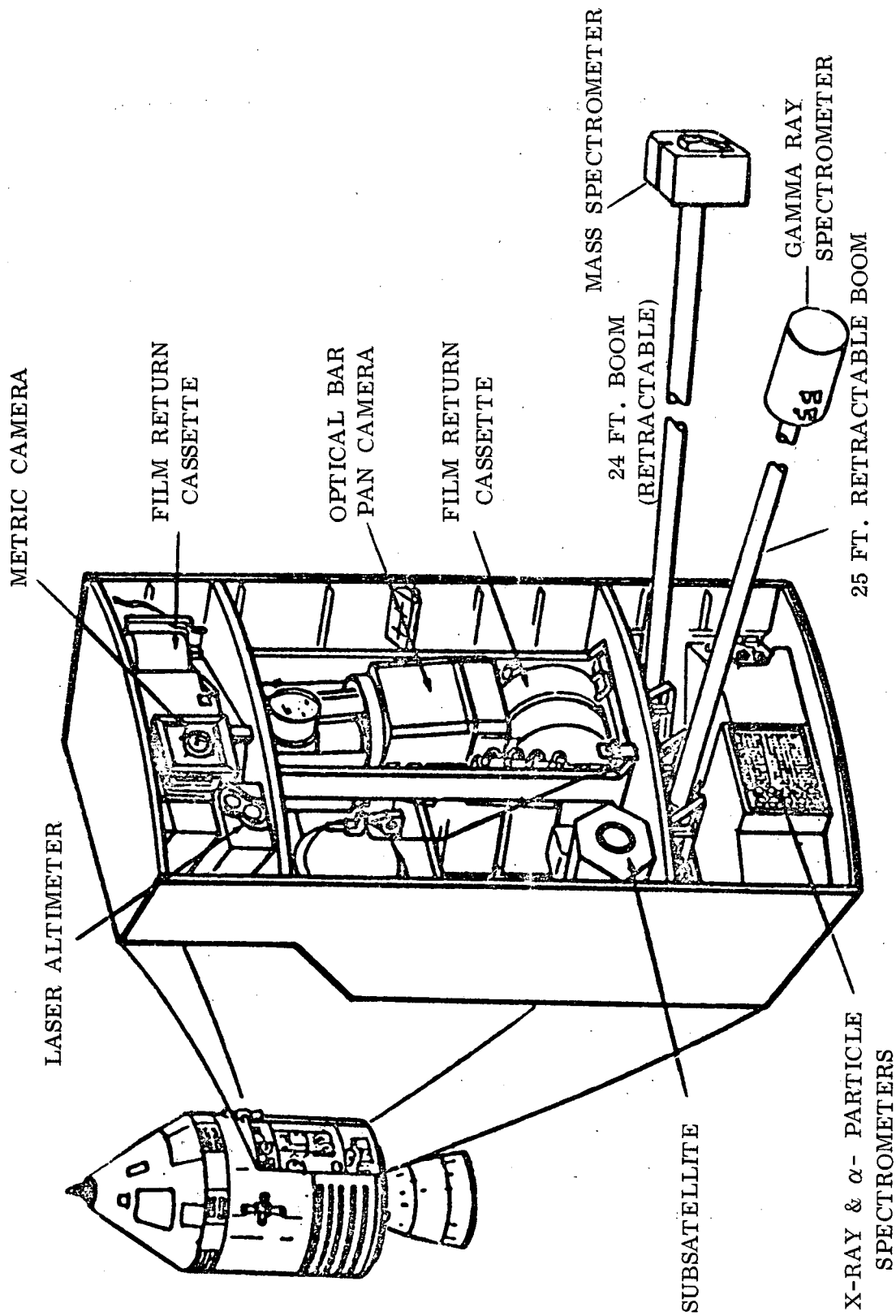


Figure 2: Scientific Instrument Module Configuration
(After NASA publication, Apollo 15 SIM Bay Photographic Equipment and Mission Summary)

The SIM contained the Fairchild 3 inch metric camera, the 3 inch stellar camera, the Itek 24 inch optical bar panoramic camera, the RCA ruby laser altimeter and equipment for the spectrometer experiments. The SIM bay was uncovered approximately 4.5 hours before insertion into lunar orbit. The orientation of the experiments with respect to the lunar surface was determined from the spacecraft trajectory and inboard gimbal angles.

The 3 inch mapping camera and the 3 inch stellar camera which were used for orientation made up the MCS (Mapping Camera Subsystem). The interlock angle between the cameras was $96^{\circ} \pm 30'$ [28]. This study only used the film from the 3 inch mapping camera. The parameters of the mapping camera are listed in Table 1. The complete camera specifications are found in [7].

Film flattening was accomplished by means of a glass focal platen and a movable pressure plate. The emulsion side of the film was in contact with the focal plane platen. There is a 121 square reseau pattern and eight fiducials. The reseaus are 10 mm apart, 2 mm in length and the line width is .005 mm. A diagram of the film format is shown in Figure 3.

The complete stellar calibration of the metric mapping camera is found in [28]. The report was prepared by Raytheon, Autometric, Alexandria, Virginia under contract to Fairchild Space and Defense Systems (FSDS). The stellar field calibration was performed at the NASA White Sands Test Facility, Las Cruces, New Mexico during 25 - 26 March, 1971. Certain values from the calibration report were extracted for use in this study and the details will be covered in succeeding sections. They include (1) calibrated focal length, (2) calibrated principal point, (3) radial distortion parameters, (4) lens distortion parameters, (5) calibrated coordinates of the reseau grid.

Type: Stationary film

Lens and Aperture: 3 in. f/4.5 (fixed)

Format: 4 1/2 x 4 1/2 in.

Coverage: 74° x 74°

Film: 5 in., 2.5 mil base unperforated

Altitude: 30 to 80 nautical miles *

Film Capacity: 1,500 feet

Cycle Time: 8.25 to 33.0 sec./cycle

Exposure Time: 1/15 to 1/250 sec.

Exposure Control: Automatic between lens shutter

Forward Motion Compensation: 12.1 to 16.1 milliradian/sec. (optional)
(in five discrete steps: 12.1, 13.1, 14.1, 15.1, 16.1 mill radian/sec.)

Resolution: 90 lines/mm AWAR, 2:1 contrast target EK 3404 film

Distortion: ± 50 microns radial **, 5 microns tangential

Overlap: 78% (nominal) or 58%, adjustable only prior to installation in spacecraft *

Fixed Data:

 Reseau
 Fiducial
 Camera Serial Number

Auxiliary Data:

 Coded Time
 Altitude ***
 Shutter Speed ***
 FMC on/off ***

* This study enlarges these values as explained in succeeding sections

** See section 3.3.2 for analysis of computed values

*** Not available for frames for this study

Table 1 Mapping Camera Characteristics

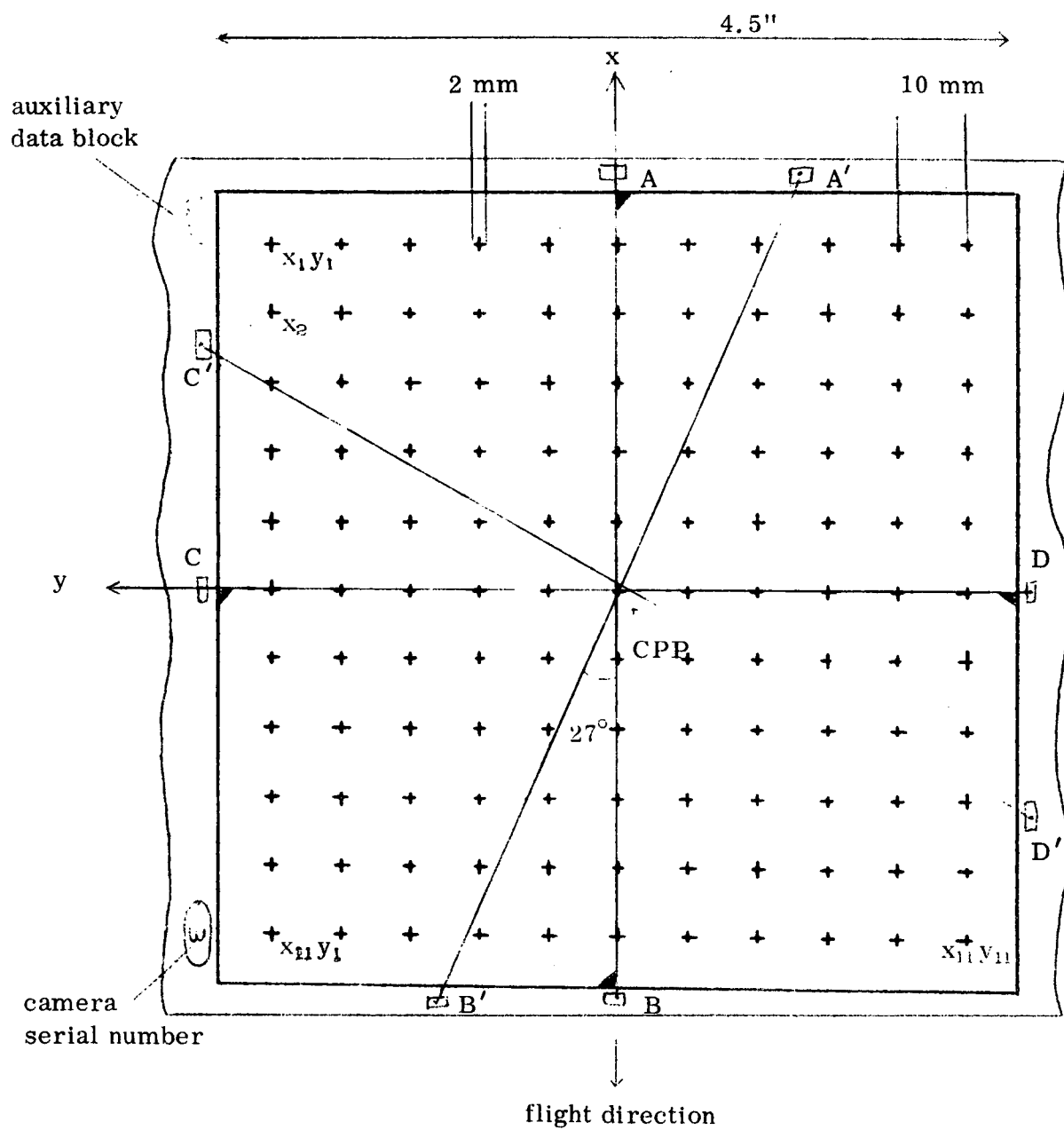


Figure 3. Film Format Diapositive Emulsion Up

4. PROCEDURE

The first section of this chapter describes the orientation of the visible portion of the moon and the evaluation of the selected frames taken by the Apollo 15 metric camera after the TEI. Examination of the selenographic system, the photo-interpretation of control points and the selection of NEC (New Extended Control) points is provided in Section 4.2.1 through 4.2.3. The observation and reduction of these features, the adjustment of the unknown parameters (i. e. , NEC points and exposure station elements) are discussed fully in Section 4.3 and 4.4.

4.1 Evaluation of Metric Camera Film

The fourth generation diapositive of the last roll of film taken by Apollo 15 was made available by the Mapping Science Branch, NASA, MSC, Houston, Texas. This roll contained the frames covering the lighted portion of the surface taken during the last few revolutions when the spacecraft was in its nominal 60 - 80 nautical mile orbit. Of interest to this project was the sequence of frames taken when the lighted surface appeared approximately 20 min. after the TEI. It is this sequence where the moon is receding from view in each successive frame that was used in attempting to extend control from the known to the unknown points. Drawings at actual scales of selected frames of this sequence are shown in Figures 4 - 9.

The problem of orientation of the visible portion of the lunar surface was difficult. There is only a narrow band of approximately 20° longitude where distinct craters can be discerned. The remainder is lost either due to high reflection or due to complete darkness beyond the terminator. That portion that is visible is approximately at 85° - 105° longitude east and is not visible from earth-based photography. The lunar orientation was solved by examination of the orbiter photos as described in [18]. There are two features immediately apparent from this sequence of pictures: 1) the trajectory and thus, the resulting pictures of the lunar surface are in an area much further to the east and south

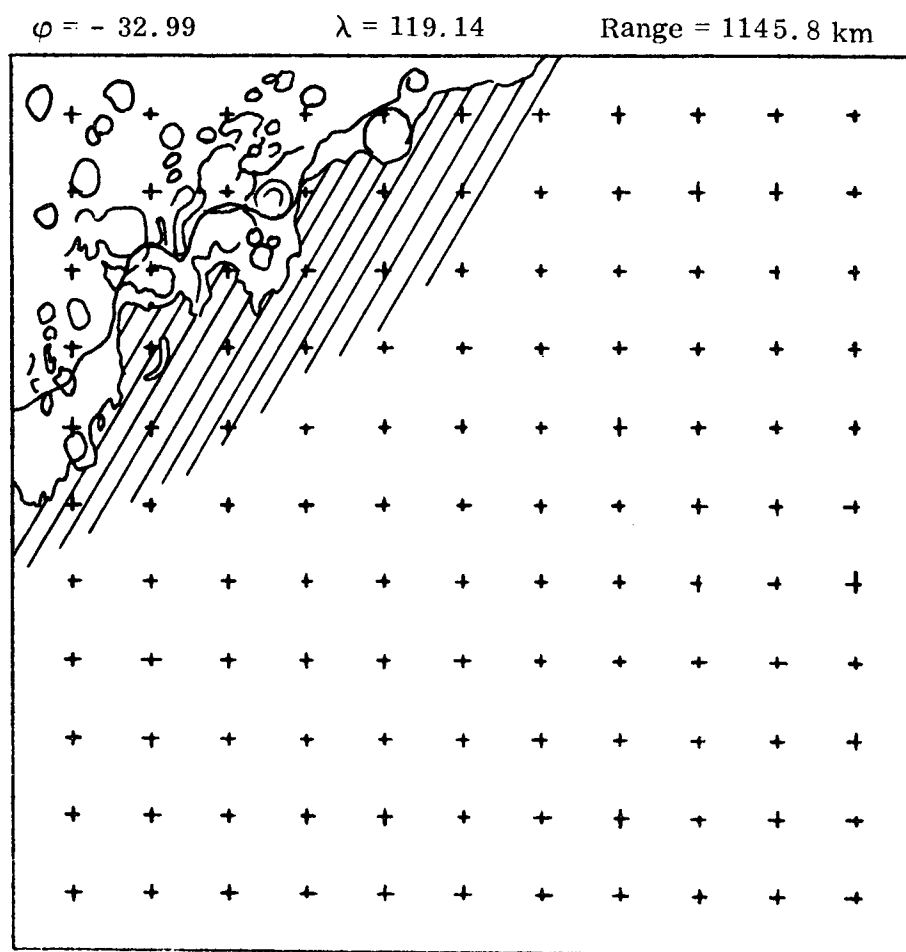


Figure 4. Frame 2753 at TEI + 20 min

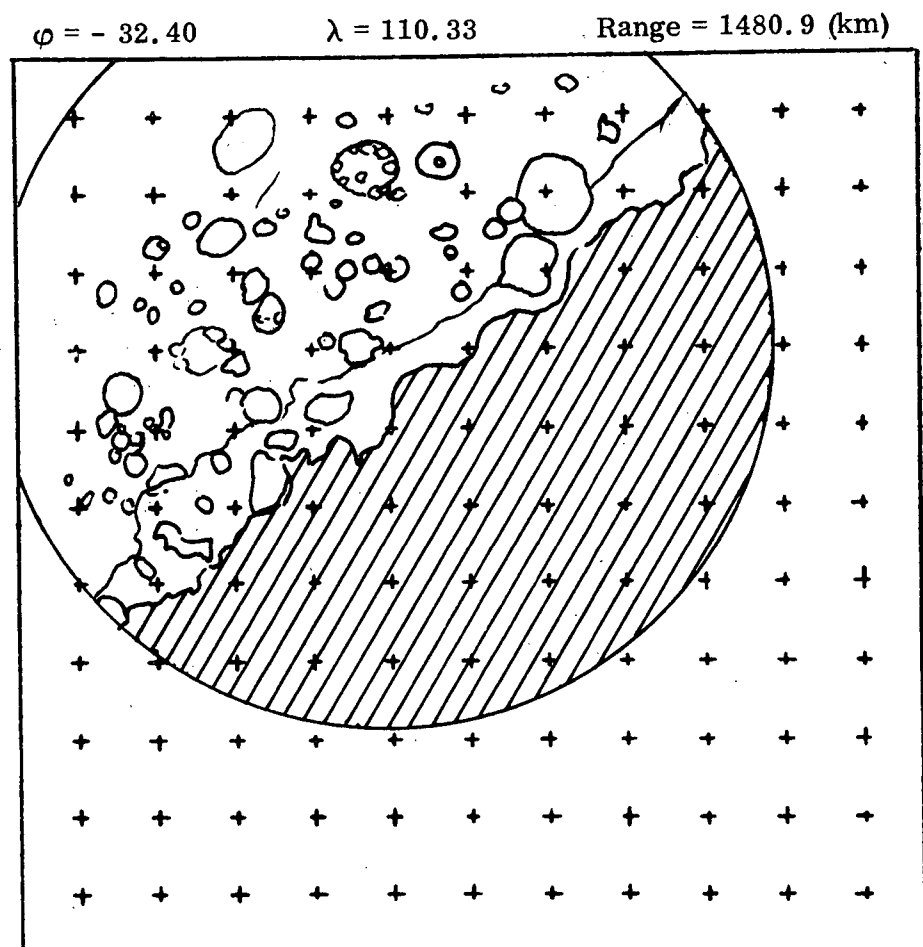


Figure 5. Frame 2765 at TEI + 25 min

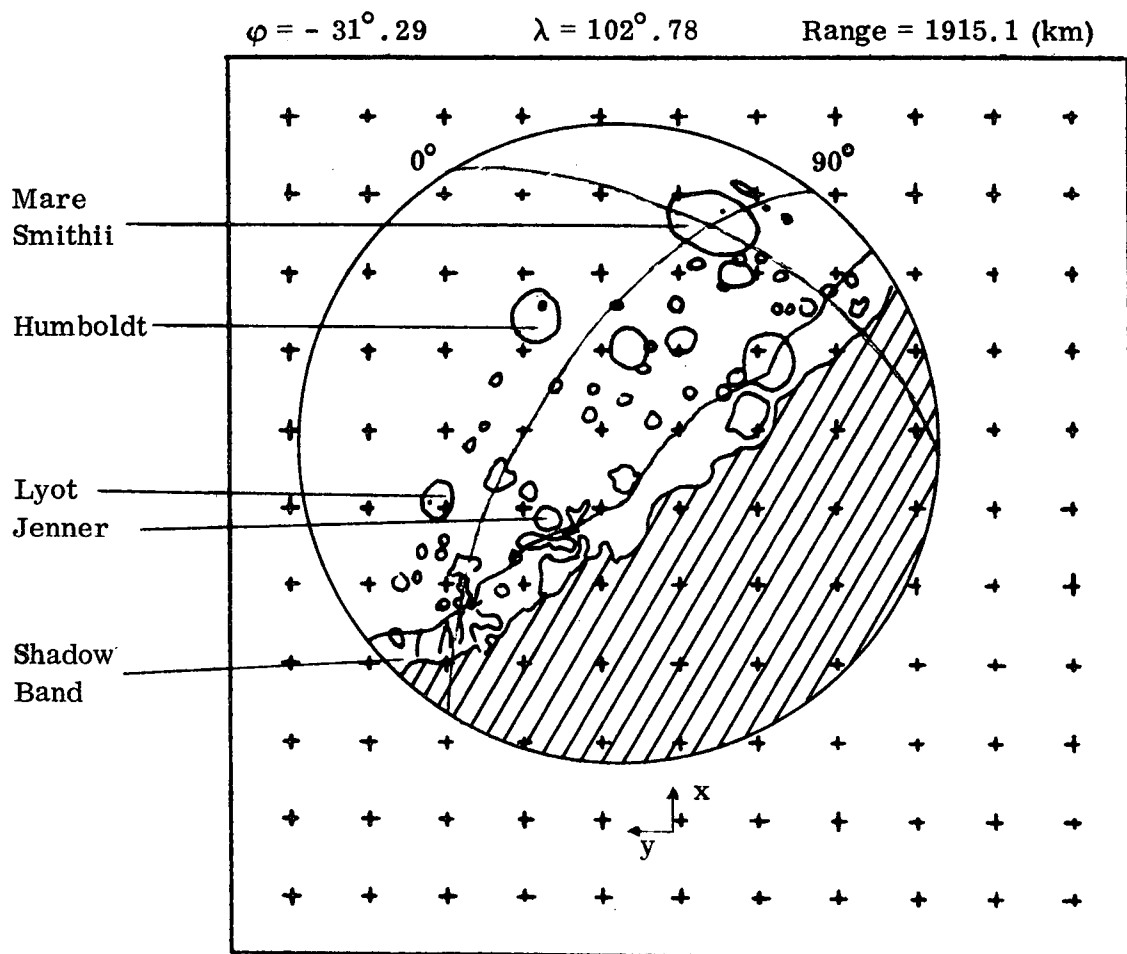


Figure 6. Frame 2780 at TEI + 30 min

$\varphi = -30^{\circ}.08$ $\lambda = 96^{\circ}.60$ Range = 2091.4 (km)

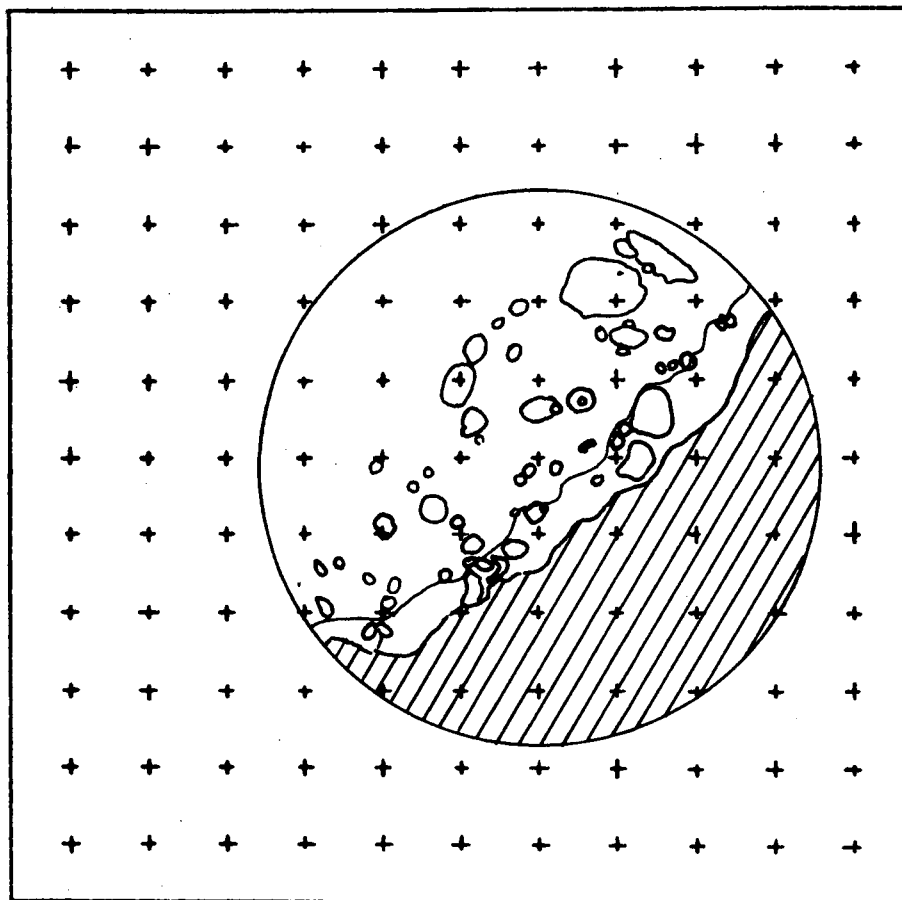


Figure 7. Frame 2795 at TEI + 35 min

$\varphi = -28^{\circ}.90$ $\lambda = 91^{\circ}.74$ Range = 2802.8 (km)

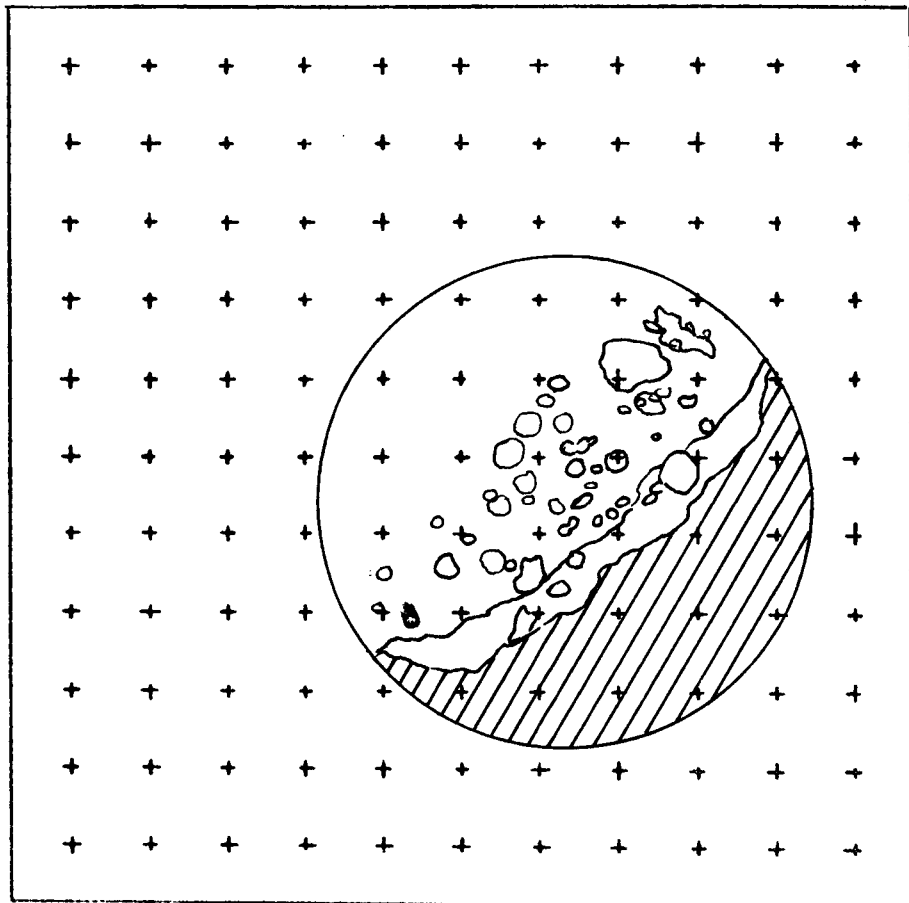


Figure 8. Frame 2810 at TEI + 40 min

$\varphi = -27^{\circ}.81$ $\lambda = 87^{\circ}.13$ Range = 3337.0 (km)

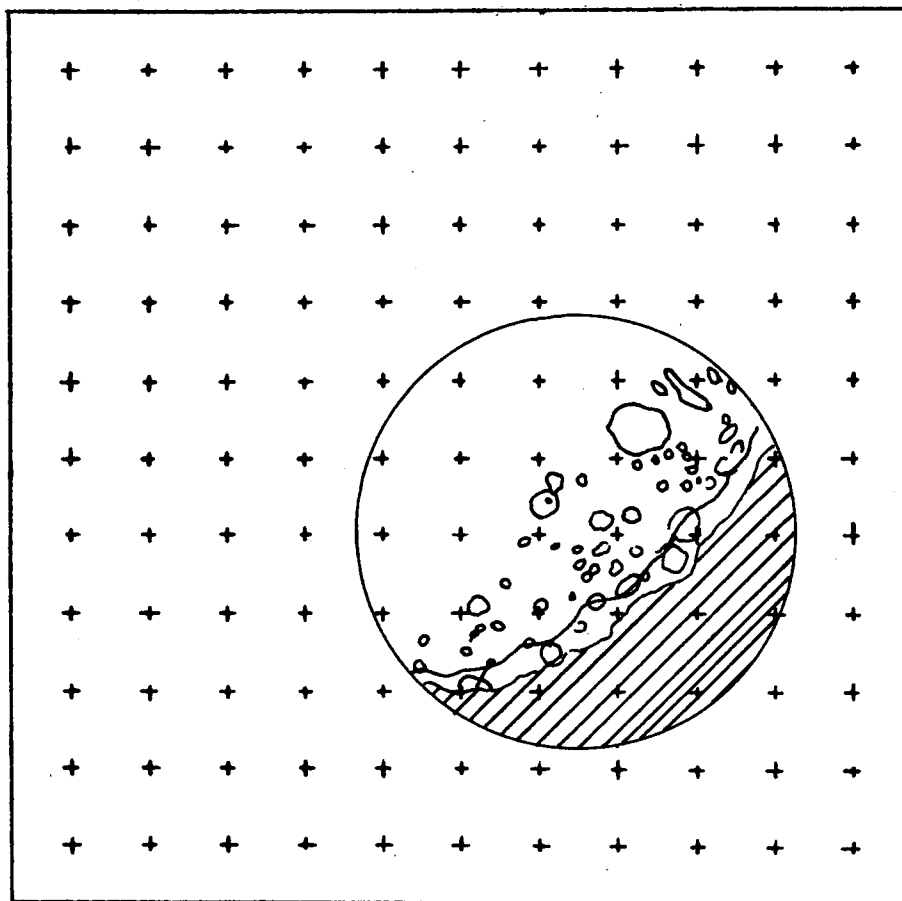


Figure 9. Frame 2825 at TEI + 45 min

than anticipated [27]. For example, Mare Crisium, a prominent feature shown in the pictures in [27], is not even clearly visible in the Apollo 15 frames because the spacecraft is above an area much further south and east. 2) one hundred percent overlap is visible almost immediately.

From the roll of film 20 frames were selected for further study. The guidelines in selecting the frames were as follows: 1) the selection should commence at approximately TEI + 20 minutes and continue for every few minutes as indicated in Sprague's original work [33]. It should be noted that this is the time of the first frame. 2) enough frames should be selected so that there would be an excess number of observations for the block adjustment program. 3) Sprague's project [33] showed that the block adjustment program results were not improved when the number of photos was increased beyond 14 - 16, consequently, the number 20 was selected to provide an overlap. A list of the selected frames are shown in Table 2. Frame number 2773 was the first after the TEI. The last frame, number 2830, was arbitrarily selected because it was felt that the view of the moon was becoming too small for any practical use in this study. After the selection, NASA provided second generation diapositives of the 20 frames for the actual measurements and the resolution was greatly improved.

The information for Table 2 came from the following sources:

- | | |
|--------------|---|
| Col. 1 | - frame number as it appears on the film. |
| Col. 2 | - the time extracted from the auxiliary data block on each frame. |
| Col. 3 | - this is an approximate number to the nearest minute. The time of the TEI is subtracted from the time of the photograph in Col. 2. |
| Col. 4, 5, 6 | - extracted from the Apollo Flight Data Report [25]. |
| Col. 7 | - the radius of the moon taken at 1,738.1 km was subtracted from the selenocentric distance in Col. 6 after conversion to kilometers. |

(1) Frame No.	(2) Time (G. E. T.)			(3) TEI + ~ min.	(4) Selenographic latitude	(5) Selenographic longitude
	hr.	min.	sec.			
1. 2753	224	8	58.0	20	- 32° 99	119° 14
2. 2756	224	9	59.0	21	- 32. 89	116. 87
3. 2759	224	11	0. 0	23	- 32. 75	114. 74
4. 2762	224	12	1. 0	24	- 32. 58	112. 73
5. 2765	224	13	2. 0	25	- 32. 40	110. 83
6. 2768	224	14	4. 0	26	- 32. 20	109. 04
7. 2771	224	15	5. 0	27	- 31. 98	107. 34
8. 2774	224	16	6. 0	28	- 31. 76	105. 74
9. 2777	224	17	7. 0	29	- 31. 53	104. 22
10. 2780	224	18	8. 0	30	- 31. 29	102. 78
11. 2785	224	19	50. 0	31	- 30. 81	100. 12
12. 2790	224	21	32. 0	33	- 30. 56	98. 89
13. 2795	224	23	14. 0	35	- 30. 08	96. 60
14. 2800	224	24	56. 0	36	- 29. 60	94. 52
15. 2805	224	26	38. 0	38	- 29. 13	92. 63
16. 2810	224	28	21. 0	40	- 28. 90	91. 74
17. 2815	224	30	2. 0	42	- 28. 45	90. 08
18. 2820	224	31	44. 0	43	- 28. 02	88. 55
19. 2825	224	33	26. 0	45	- 27. 60	87. 13
20. 2830	224	35	29. 0	47	- 27. 20	85. 82

Table 2 Selected Frames of Metric Camera SN - 003

	(5) Frame No.	(6) Selenocentric Dist. (ft.)	(7) Range to Surface (km)	(8) Scale approx.	(9) 10 microns = (meters approx)
1.	2753	9461741.6	1145.839	1:15,000,000	150
2.	2756	9731846.9	1228.167	1:16,000,000	160
3.	2759	10005413.0	1311.550	1:17,000,000	172
4.	2762	10281993.0	1395.851	1:18,000,000	184
5.	2765	10561192.0	1480.950	1:19,000,000	195
6.	2768	10842660.0	1566.743	1:21,000,000	206
7.	2771	11126086.0	1653.131	1:22,000,000	218
8.	2774	11411197.0	1740.033	1:23,000,000	229
9.	2777	11697749.0	1827.374	1:24,000,000	240
10.	2780	11985528.0	1915.089	1:25,000,000	252
11.	2785	12564023.0	2091.414	1:27,000,000	275
12.	2790	12854421.0	2179.928	1:29,000,000	287
13.	2795	13436853.0	2357.453	1:31,000,000	310
14.	2800	14020743.0	2535.422	1:33,000,000	334
15.	2805	14605387.0	2713.622	1:35,000,000	357
16.	2810	14897813.0	2802.753	1:37,000,000	369
17.	2815	15482583.0	2980.991	1:39,000,000	392
18.	2820	16066927.0	3159.099	1:42,000,000	416
19.	2825	16650539.0	3336.984	1:44,000,000	439
20.	2830	17233177.0	3514.572	1:46,000,000	462

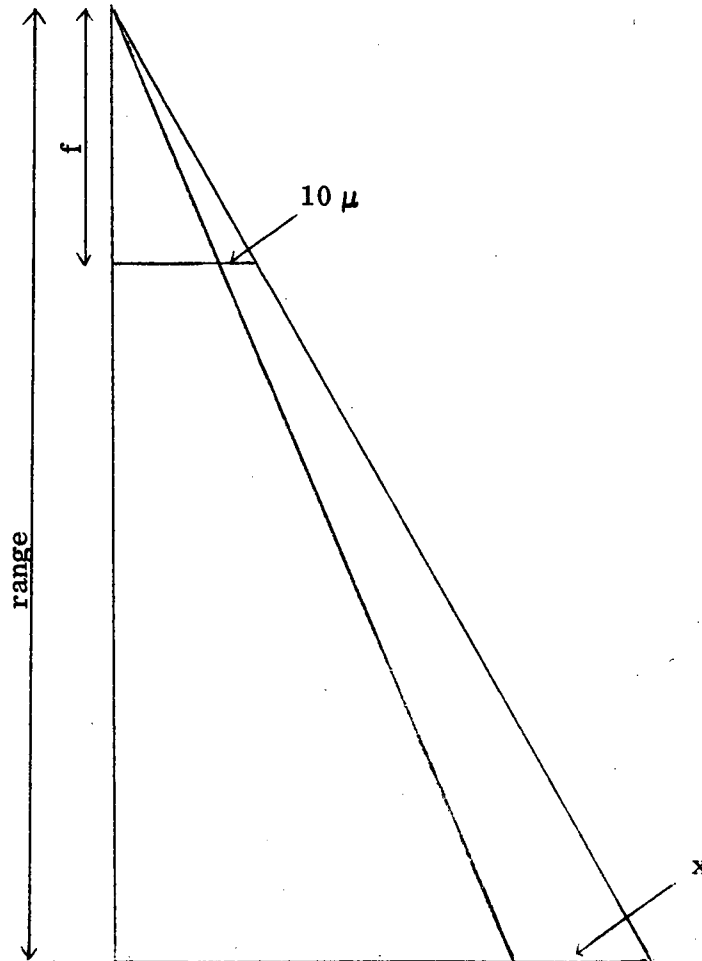
Table 2 Selected Frames of Metric Camera SN - 003 (con't)

Col. 8 - this is a rounded number computed from

$$\text{scale} = \frac{f}{h} = \frac{76 \text{ mm}}{\text{Col. 7}}$$

Col. 9 - this is a rounded number computed from

$$\frac{76 \text{ mm}}{10 \mu} = \frac{\text{range (Col. 7)}}{x}$$



It is merely a guideline to show what 10 microns on the film represents on the lunar surface.

Examination of the selected frames and the data in the Table 2 indicated several problems: 1) the scale is much smaller than any conventional mapping project, 2) it is apparent that the spacecraft is not traversing across the lunar surface as in the case of normal strip photogrammetry but appears to be coming straight out of the large prominent, dark center crater Jenner in Mare Australe. This near vertical trajectory provides very poor geometry of intersecting rays at the nadir region of the photographs. An indicator of good or poor geometry in photogrammetry is the base-height ratio and trouble is usually predicted when the base-height ratio is $< .3$ [10]. In this case the horizontal base is very small compared to the altitude and for all practical purposes the ratio is nearly zero, (approximately .04). The geometry of intersecting perspective rays from the exposure station is further compounded by the fact that the known control is grouped very closely together on the northern or upper limb and the selected unknown points range mostly in the southern area. This grouping of control in a small area coupled with large altitudes provides a very narrow cone for the intersection of rays in solving for the exposure station.

4.2 Selection of Control and NEC (New Extended Control)

4.2.1 Selenographic Coordinate System

The selenographic coordinate system as used here is not what some literature describes in the catalogues as the 'true' coordinate system but rather is the dynamical coordinate system. It is fixed to the lunar sphere with its origin at the center of mass [12]. This system is shown in Figure 10. It is right handed with the X axis positive towards the earth, the Z axis is lying on the rotational axis of the moon with positive to the north and the Y axis completing the system [33].

The selenocentric coordinates may be obtained from latitude (ϕ), longitude

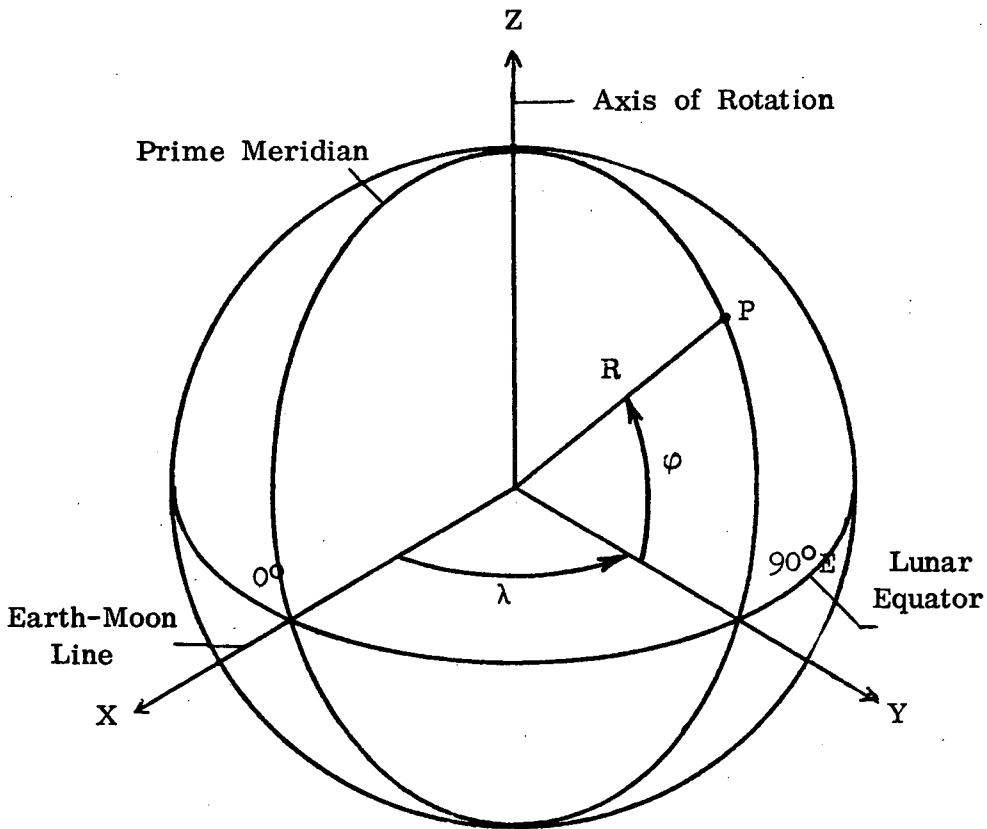


Figure 10 .

Selenographic Coordinate System Fixed to the Lunar Sphere

(λ) and radius (R) by the following[2] :

$$X_c = R \cos \varphi \cos \lambda$$

$$Y_c = R \cos \varphi \sin \lambda$$

$$Z_c = R \sin \varphi$$

The selenographic coordinates being center of mass oriented may be obtained by an appropriate origin shift in kilometers along the selenocentric axes [33] so that the transformation becomes:

$$X = R \cos \varphi \cos \lambda - 2.5$$

$$Y = R \cos \varphi \sin \lambda + 1.0$$

$$Z = R \sin \varphi - .5$$

From [33] the moon's radius in this report is also taken as 1738.1077 km.

4.2.2 Visible Lunar Control

Photointerpretation or identifying known points was accomplished by examination of other photographs with the points indicated. The known control identified and used in this project were of two types: 1) ACIC control and 2) Lunar Landmark Control.

NASA's Mapping Science Branch provided the enhanced Orbiter IV photographs of the frontside and eastern limb listed in Appendix I with ACIC's 196 fundamental and 89 additional identifiable control points circled [3]. Due to the attitude of the Apollo spacecraft there was only one control point, ACIC #69 on Orbiter IV photo 185H1, identifiable on the Apollo 15 film.

Fortunately, additional pictures were available of the Lunar Landmark Control [22] [30] [33]. In the 'window' of visible features on the Apollo 15 film three of these points were discernable. Three points were not visible in the first seven frames consequently the measurements began with frame number 2774. The following Table 3 shows the control used in this study. The source for points 1 and 2 is [30]; for point 3 which is a feature tracked by Apollo 14, the latitude and longitude were supplied by NASA; for point 4 [1].

Frame No.	Name	ϕ	$\sigma\phi$	λ	$\sigma\lambda$	R (km)	σR (km)
1.	F - 1/10	1°8722	°0203	88°2532	°0104	1733.007	.378
2.	CP - 3/8	- 8.8990	.0145	96.8915	.0226	1735.374	.430
3.	Ansgarius	-11.633	*	81.068	*	*	*
4.	ACIC 69	-18.478	.013	62.113	.034	1736.130	.540

* not available

Table 3 Coordinates of Control Points

The above coordinates were converted to selenographic X, Y, Z coordinates and are listed in Table 4. The standard errors (σ) were calculated by the following propagation of error [13][35]. Since no correlation was provided the ϕ , λ , and R covariance terms are omitted. The resulting covariance terms between X, Y, and Z are also neglected, since only the standard deviation (σ) is required for the diagonal weight matrix which is used in the adjustment. The weight matrix is discussed further in Section 4.4.1.

$$X = R \cos \phi \cos \lambda - 2.5$$

$$Y = R \cos \phi \sin \lambda + 1.0$$

$$Z = R \sin \phi - 0.5$$

$$\sigma_x^2 = \left(\frac{\sigma\phi}{\rho}\right)^2 \left(\frac{\partial X}{\partial \phi}\right)^2 + \left(\frac{\sigma\lambda}{\rho}\right)^2 \left(\frac{\partial X}{\partial \lambda}\right)^2 + \sigma_R^2 \left(\frac{\partial X}{\partial R}\right)^2$$

$$\sigma_y^2 = \left(\frac{\sigma\phi}{\rho}\right)^2 \left(\frac{\partial Y}{\partial \phi}\right)^2 + \left(\frac{\sigma\lambda}{\rho}\right)^2 \left(\frac{\partial Y}{\partial \lambda}\right)^2 + \sigma_R^2 \left(\frac{\partial Y}{\partial R}\right)^2$$

$$\sigma_z^2 = \left(\frac{\sigma\phi}{\rho}\right)^2 \left(\frac{\partial Z}{\partial \phi}\right)^2 + \sigma_R^2 \left(\frac{\partial Z}{\partial R}\right)^2$$

Where:

$$\frac{\partial X}{\partial \varphi} = R (-\sin \varphi) (\cos \lambda)$$

$$\frac{\partial X}{\partial \lambda} = R (\cos \varphi) (-\sin \lambda)$$

$$\frac{\partial X}{\partial R} = (\cos \varphi) (\cos \lambda)$$

$$\frac{\partial Y}{\partial \varphi} = R (-\sin \varphi) (\sin \lambda)$$

$$\frac{\partial Y}{\partial \lambda} = R (\cos \varphi) (\sin \lambda)$$

$$\frac{\partial Y}{\partial R} = (\cos \varphi) (\sin \lambda)$$

$$\frac{\partial Z}{\partial \varphi} = R (\sin \varphi)$$

$$\frac{\partial Z}{\partial R} = \sin \varphi$$

Point No.	Name	X (km)	σ_x (km)	Y (km)	σ_y (km)	Z (km)	σ_z (km)
1.	F - 1/10	50.2985	.3145	1732.2770	.3783	56.1178	.6138
2.	CP - 3/8	- 208.2202	.6734	1703.0977	.4348	- 268.9505	.4390
3.	Ansgarius	261.8195	.600*	1682.7634	.600*	- 350.9761	.600*
4.	ACIC 69	769.6745	.8912	1456.4050	.6537	- 550.7500	.4109

* assigned based on radius of 1738.11 (km)

Table 4 Selenographic Coordinates of Control Points

It is important to remember that the above control points are the only control points available for this block adjustment, consequently any solution is due in part to this fact.

4.2.3 New Extended Control (NEC)

The points whose coordinates were desired were selected at the time of measurement. The following seven points were selected because 1) they were small circular features easily identifiable on all measured frames and because of their distinct location they should be easily located on photographs of the same area on succeeding Apollo missions, 2) their general location can be identified on ACIC's Lunar Planning Chart LOC - 3, Lunar Polar Chart LMP - 3, Lunar Farside Chart LMP - 2, 3) it was desired to have at least one feature within the bracket of four reseaus. Diagrams of these points at eight times enlargement from frame 2780 are found in Figures 11 - 16. Table 5 shows the coordinates' approximate positions as extracted from the above mentioned charts.

Point No.	ϕ	λ
11	- 4 ^o .4	93 ^o .3
12	-33.5	96.2
13	-41.3	97.6
14	-39.7	84.5
15	-50.8	82.0
16	-56.2	90.4
17	-36.8	99.1

Table 5 NEC Coordinates

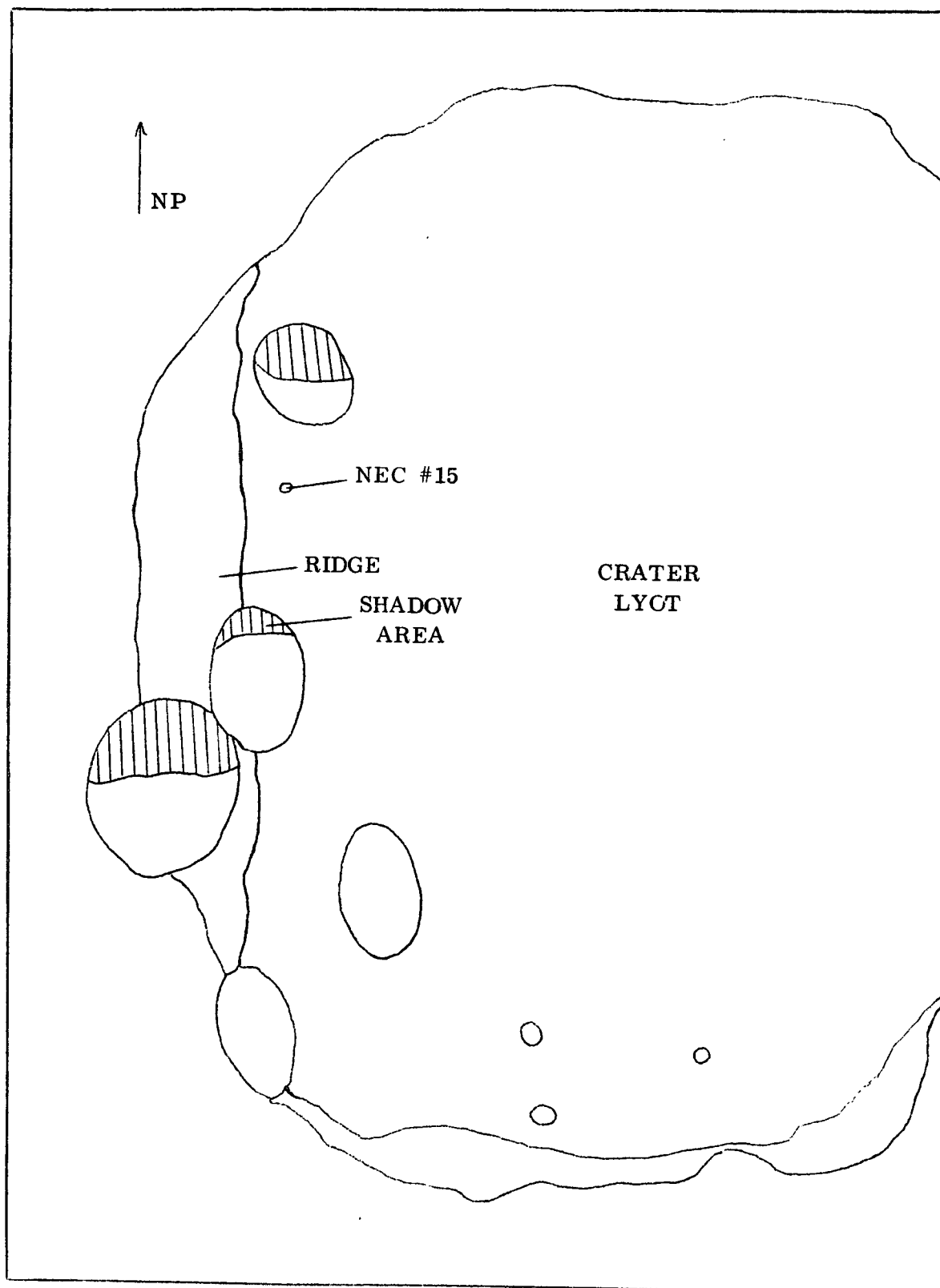


Figure 11. Approximate Coordinates of NEC No. 15 $\phi = -50^{\circ}8$ $\lambda = 82^{\circ}0$

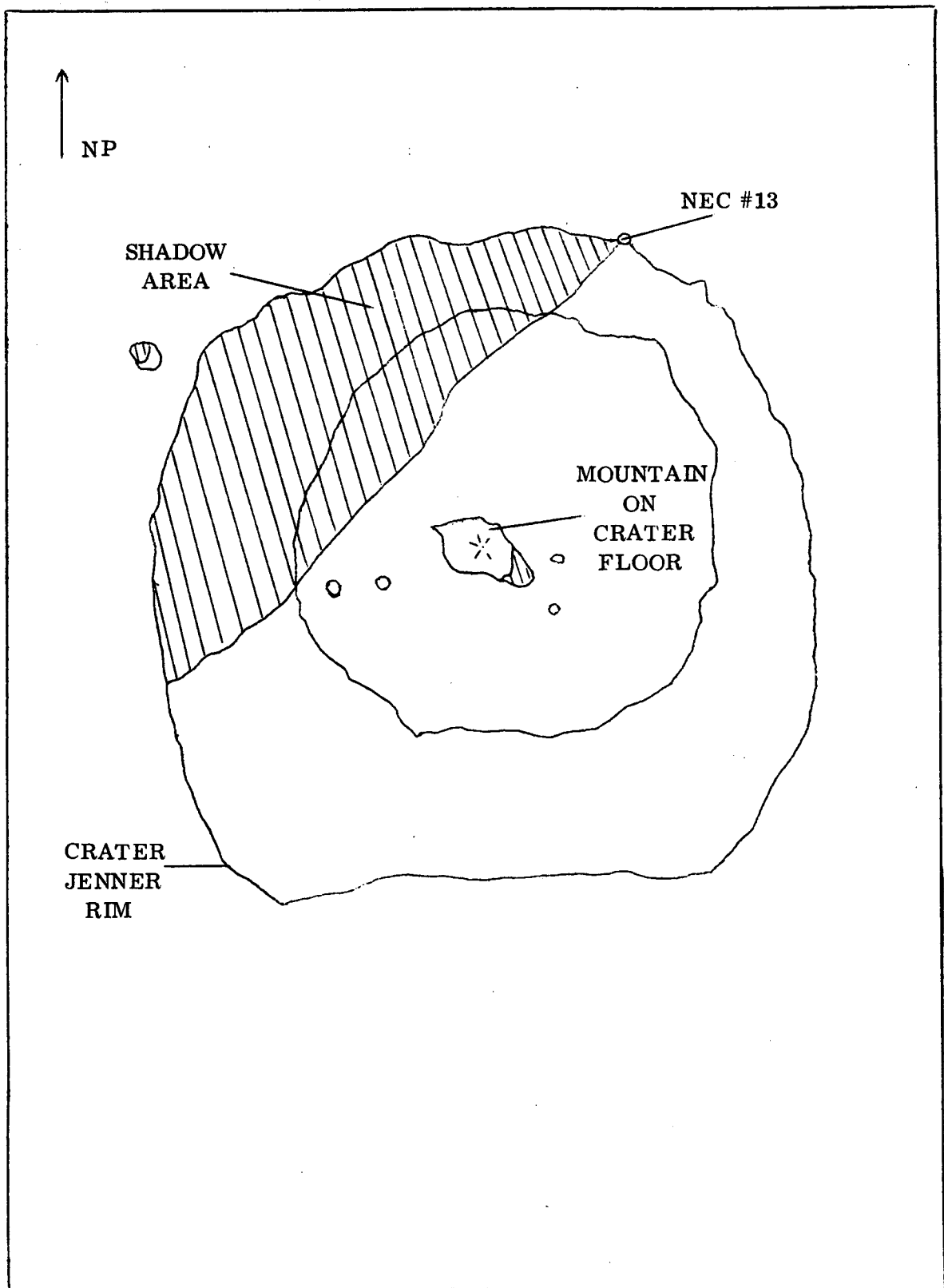


Figure 12. Approximate Coordinates of NEC No. 13 $\phi = -41^{\circ}3$ $\lambda = 97^{\circ}6$

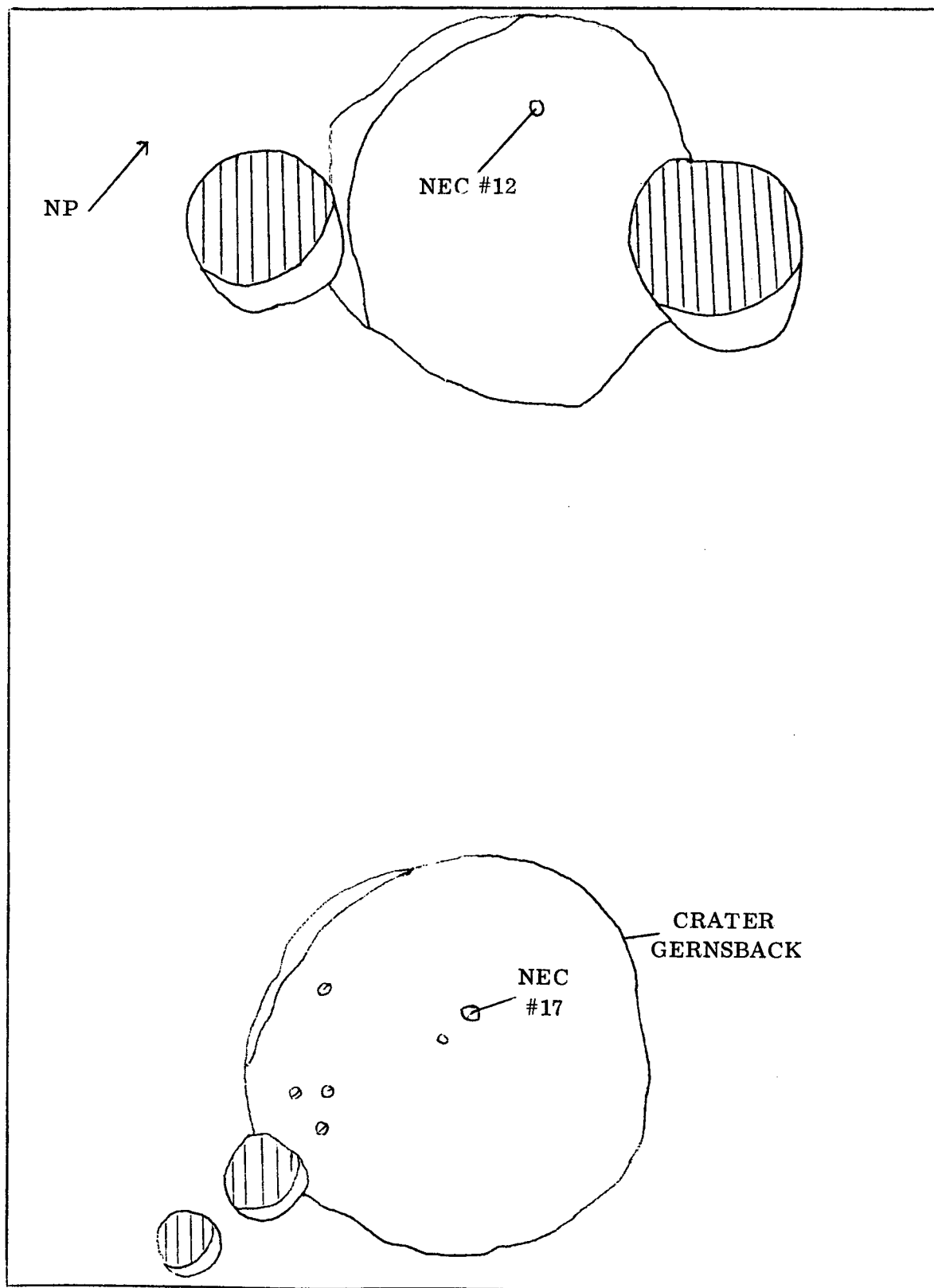


Figure 13. Approximate Coordinates of NEC No. 12 (above) $\phi = -33^{\circ}.5$ $\lambda = 96^{\circ}.2$

NEC No. 17 $\phi = -36^{\circ}.8$ $\lambda = 99^{\circ}.1$

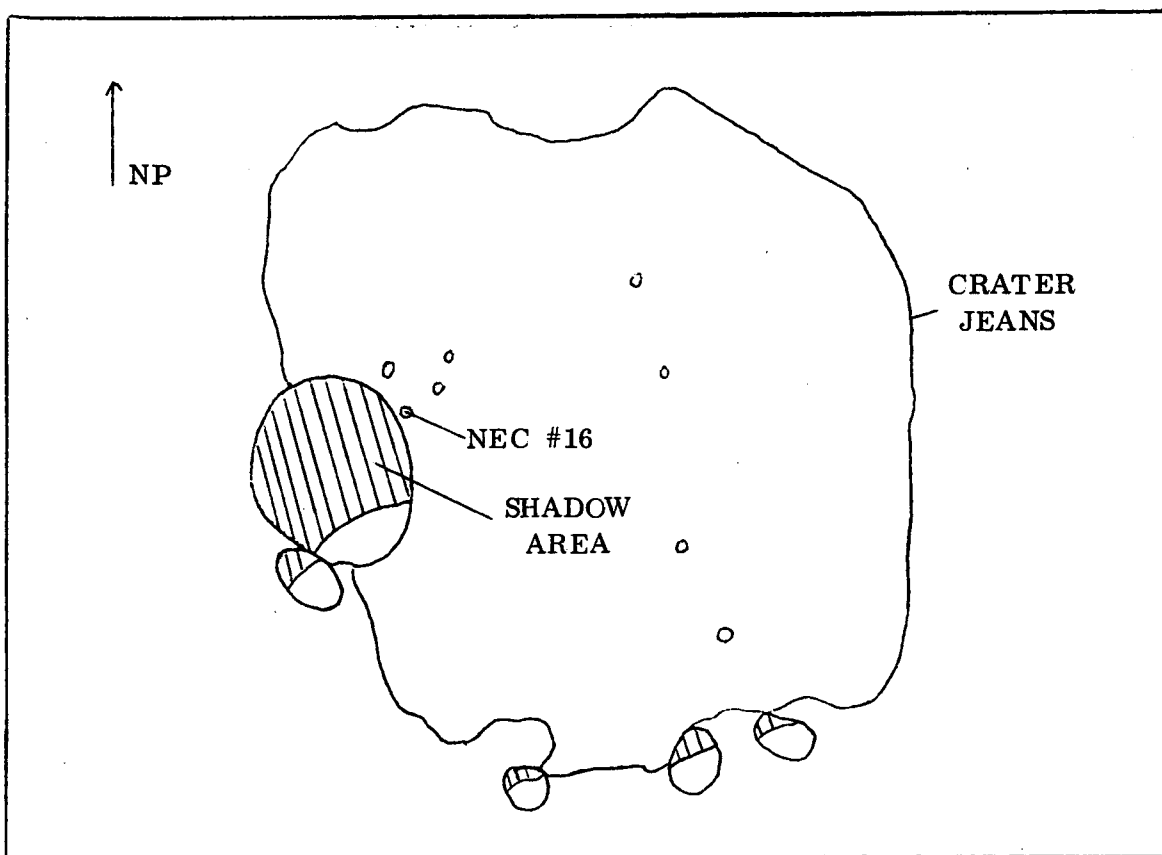


Figure 14. Approximate Coordinates of NEC No. 16 $\phi = -56^{\circ}2$ $\lambda = 90^{\circ}4$

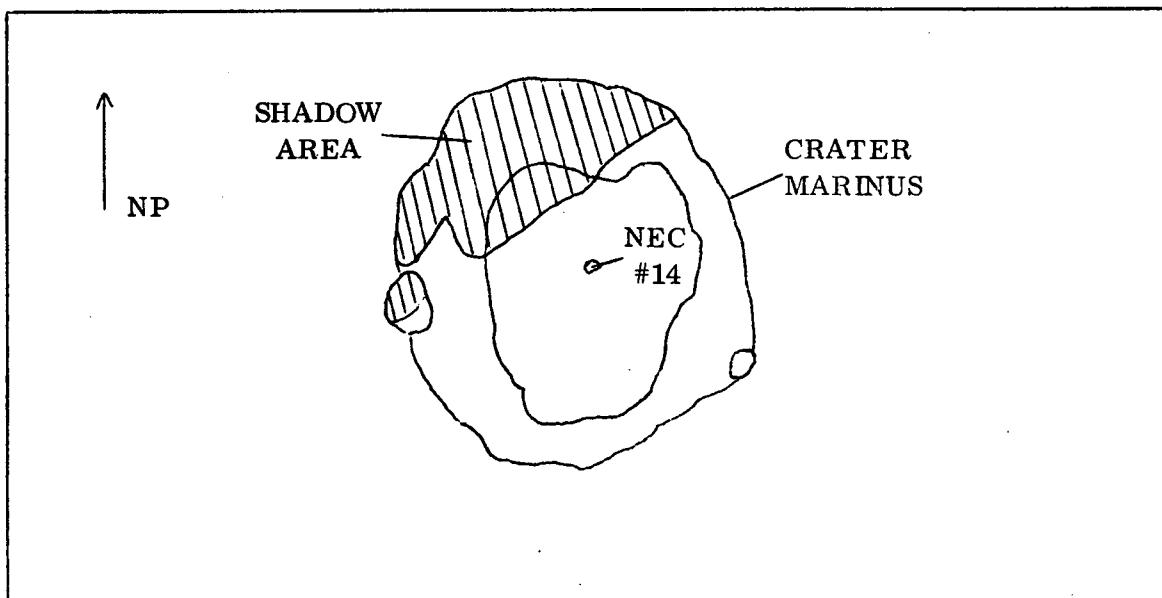


Figure 15. Approximate Coordinates of NEC No. 14 $\phi = -39^{\circ}7$ $\lambda = 84^{\circ}5$

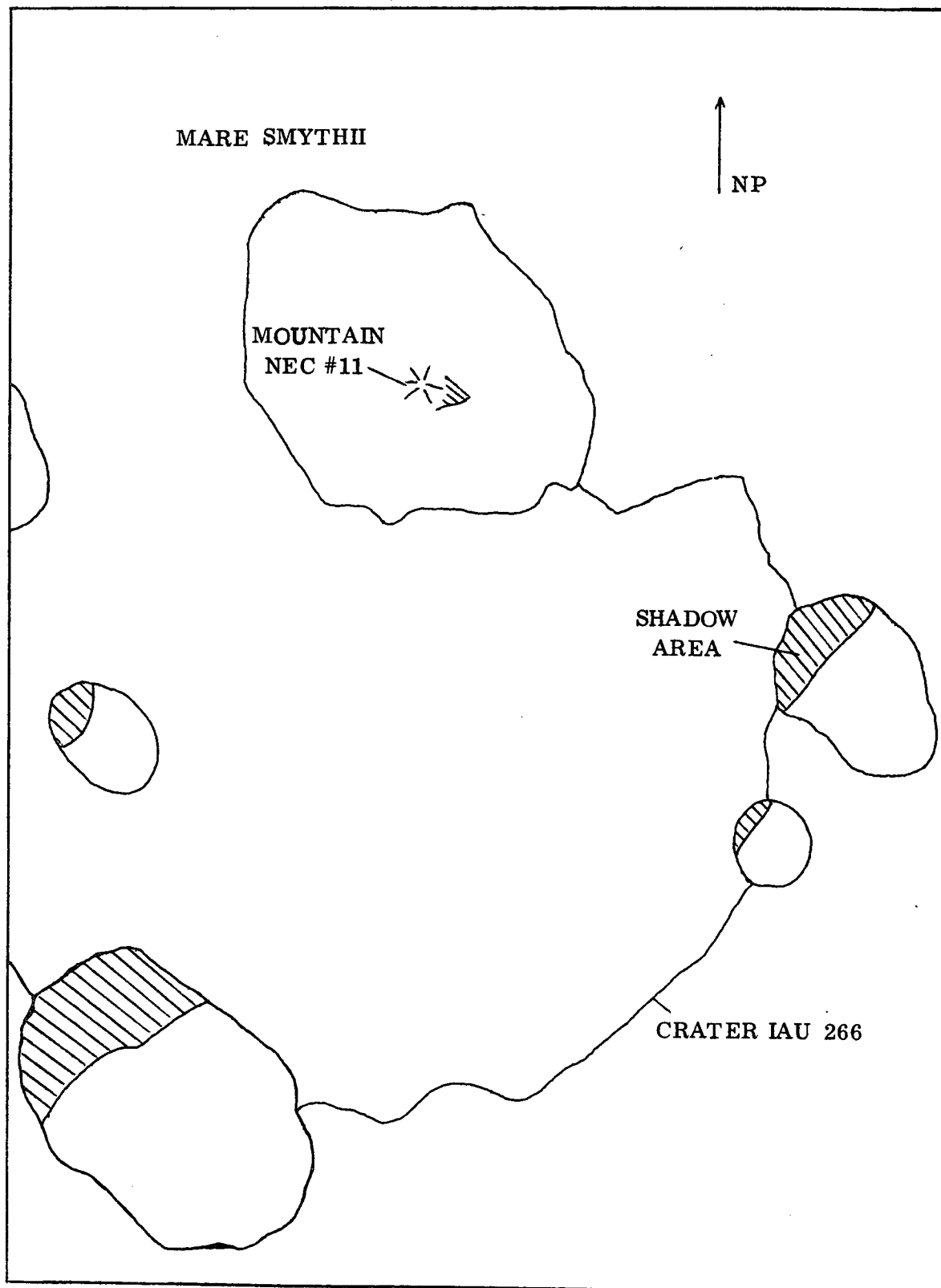


Figure 16. Approximate Coordinates of NEC No. 11 $\phi = -4^{\circ}.4$ $\lambda = 93^{\circ}.3$

These coordinates were reduced to selenographic coordinates and are shown in Table 6. The computations included the use of the moon's radius as 1738.1077 km.

Point No.	X (km)	Y (km)	Z (km)
11	- 102.2576	1731.1115	- 133.8459
12	- 159.0325	1441.9059	- 959.8259
13	- 175.1975	1295.3074	- 1147.6540
14	125.6745	1332.1426	- 1110.7473
15	150.3865	1088.8441	- 1347.4370
16	9.2502	967.8781	- 1444.8405
17	- 222.6177	1375.2404	- 1041.6675

Table 6 NEC Selenographic Coordinates

Based on the accuracy of the ACIC charts a standard deviation of 20 km was assigned to each of the above NEC points.

4.3 Observations and Reduction of Observations

4.3.1 Observations of Photo Coordinates (AP/C)

It is fortunate that Mr. Lloyd Herd and Mr. Neal O'brien of the Aerial Engineering Section of the Ohio Department of Highways made available their department's AP/C (Analytical Plotter/Commercial). The AP/C is a first order measuring instrument manufactured by OMI (Ottico Meccanica Italiana, Rome) with a least count of one micron. In a test for stability of an AP/C by Toglatti and Solaini a standard deviation of coordinates of $\pm 2 \mu$ was obtained

with calibration plates [34]. The AP/C consists of a stereo comparator built by the Nistri Company of Italy with an on line computer built by the Bendix Corporation. In this project the AP/C was used as a comparator with the computer serving as a digitized readout function. The observations were made in stereo by increasing numbered pairs of photographs. The AP/C does not have a 'zoom' lens feature but the scale difference between pairs of photographs is within the eye accomodation range of 10 - 12% [10]. Table 7 shows the photo frame and the feature whose coordinates were recorded.

It can be seen from the table on the following page that the number of measurements/frame is generally decreasing. This is due to two interrelated causes. As the moon is receding from view fewer features can be discerned due to scale, resolution and altitude and there are fewer features surrounded by four visible reseaus.

Each point or feature was measured four times on each frame and each of the four bracketing reseaus was measured once for a total of 1728 measurements. Four reseaus are required for the reduction process covered in the next section. Examination of Figures 4 - 9 show that some features that could be selected for measurement are lost when the surrounding reseaus which are black are lost in the blackness of space or the blackness near or beyond the terminator. The use of the fiducials or reseaus for determination of film shrinkage and lens distortion is a clear cut procedure when the entire diapositive film format shows contrast of the lighted surface and black fiducials and/or reseaus. In this project the fiducials are completely unuseable and only certain patterns of four reseaus are useable.

An interesting and unexpected facet occurred during the observations. Control points 1 - 3, the Lunar Landmark craters were tracked by the Apollo astronauts while the spacecraft was in a 60 - 80 nautical mile orbit. These are relatively small features (250 - 1,500 meters [30]) and easily discernable at that altitude; however their locations are not as clear during the time span of the

Frame No.	Control				NEC						
	1	2	3	4	11	12	13	14	15	16	17
2774	X	X	X		X	X	X	X	X	X	X
2777	X	X	X		X	X	X	X	X	X	X
2780	X	X			X	X	X	X	X	X	
2785	X	X			X	X	X	X	X	X	
2790	X			X	X	X	X	X	X		X
2795	X			X	X	X	X	X	X		X
2800	X	X	X	X	X	X	X	X	X	X	X
2805	X	X	X	X	X	X	X	X	X	X	X
2810	X	X	X	X	X		X	X	X	X	
2815	X	X	X	X	X		X	X	X	X	
2820	X	X	X	X	X		X	X	X		
2825	X	X	X	X	X		X	X	X		
Total	12	10	8	8	12	8	12	12	12	8	6 = 108

Table 7 Frame Number and Measured Feature

TEI photographs when the altitude is increasing from 1145 km to 3500 km. In fact this is approaching the limit of the film resolution and surface detail and this coupled with the shadows, made placing the measuring mark in some cases a judgement decision based on the placement in the previous pair of photographs. Control point number 4, an earth-based control feature is a crater whose appearance is extremely large. The placement of the measuring mark can 'swim' several microns, (i. e. , there was a range of 12μ) inside the crater walls, not only on each pair of photographs but also on each repeated measurement. On the other hand, the features selected for extending control are clearly visible very distinct features approximately the same size as the measuring mark (20μ) and thus these NEC points were easier to measure. An analysis of the observation residuals shows that the pointing precision in planimetry for the control points was 16.53μ compared to 12.77μ for the selected NEC points. Admittedly there were fewer measurements on the control points, 38 compared to 70, but the results are justified when the film is examined.

4.3.2 Reduction of Observations

The measured coordinates were processed by a modified TRANC 4 program. The details and a program listing are given in Appendix II. The program transforms the coordinates from the comparator system to coordinates in the calibrated reseau grid system through an affine transformation. The source for the calibrated reseau was [24]. The general affine transformation for which the coefficients are solved for is (see [2]):

$$(1) \quad \begin{aligned} x &= AO + A_1 x' + A_2 y' \\ y &= BO + B_1 x' + B_2 y' \end{aligned}$$

where:

x', y' = photo coordinates

x, y = stereocomparator coordinates

AO, BO = origin shift

A1, B1, A2, B2 = coefficients solved for by least squares adjustment of the 4 (x) and 4 (y) comparator coordinates of the bracketing reseaus.

These coefficients are then used in solving for the coordinates of the object point. The four observations on the object are averaged and the coordinates are solved by a back solution in the transformation as shown in Appendix II.

$$(2) \quad \begin{aligned} x' &= \frac{A_2 (y - BO) - B_2 (x - AO)}{A_2 \cdot B1 - A1 \cdot B2} \\ y' &= \frac{B1 (x - AO) - A1 (y - BO)}{A_2 \cdot B1 - A1 \cdot B2} \end{aligned}$$

Each point within a reseau is handled in the same manner and the results are shown in Plates 1 - 6.

The program computes for each point the unit standard error

$$\sigma_o = \sqrt{\frac{[VV]}{n - u}} = \sqrt{\frac{E_x^2 + E_y^2}{n - u}}$$

where: E_x and E_y are vectors containing the residuals in x and y. These are the differences between each (x, y) comparator coordinate from the general affine transformation (1) prior to adjustment and the (x, y) observed comparator coordinate

n = number of observations (8)

u = number of unknowns (6)

The last column in Plates 1 - 6 show the result of the computation of the standard error of the mean for x and y computed from

$$\sigma_{mean} = \sqrt{\frac{[VV]}{n(n-2)}} = \sqrt{\frac{V_x V_x + V_y V_y}{n(n-2)}}$$

where: $V_x = (x - \bar{x})$ and $V_y = (y - \bar{y})$

\bar{x} = x average and \bar{y} = y average of point observations

JOB NUMBER 10

PHOTO COORDINATES CORRECTED FOR LENS AND FILM DISTORTIONS (FAIRCHILD MAPPING CAMERA #003)

PHOTO	POINT	X (MM)	Y (MM)	UNIT STANDARD ERROR (MM) AFTER AFFINE TRANSFORMATION	STANDARD ERROR OF MEAN OF X AND Y ON THE OBJECT SPACE POINT (MM)
2774.	1.	44.4632	-7.0753	0.806230-02	0.213609-02
2774.	2.	36.7541	-7.1087	0.412310-02	0.151380-02
2774.	3.	46.5731	9.6612	0.509900-02	0.250000-02
2774.	11.	42.0697	-7.2827	0.900000-02	0.278870-02
2774.	12.	16.6090	15.4192	0.670420-02	0.133850-02
2774.	13.	9.8949	22.7033	0.141420-02	0.292620-02
2774.	14.	17.8792	29.4370	0.707110-03	0.226480-02
2774.	15.	7.2805	37.7974	0.223610-02	0.125600-02
2774.	16.	-1.2497	39.7600	0.262840-02	0.692220-03
2774.	17.	11.0668	15.7874	0.254950-02	0.254950-02
2777.	1.	43.8596	-7.2060	0.200000-02	0.213609-02
2777.	2.	32.4454	-7.2757	0.777820-02	0.151380-02
2777.	3.	41.8613	8.5468	0.125100-01	0.418330-02
2777.	11.	37.5886	-7.4170	0.254950-02	0.268670-02
2777.	12.	13.2807	14.0258	0.700000-02	0.133850-02
2777.	13.	6.9755	20.9662	0.583100-02	0.292620-02
2777.	14.	14.5884	27.3965	0.156110-02	0.226480-02
2777.	15.	4.6947	35.5815	0.740570-02	0.125600-02
2777.	16.	-3.3797	33.7178	0.105120-01	0.692220-03
2777.	17.	9.0302	14.3839	0.148030-01	0.254950-02

Plate 1: Results of TRANC 4 for Photo Frames 2774 and 2777

JOB NUMBER 10

PHOTO COORDINATES CORRECTED FOR LENS AND FILM DISTORTIONS (FAIRCHILD MAPPING CAMERA #003)

PHOTO	POINT	X (MM)	Y (MM)	UNIT STANDARD ERROR (MM) AFTER AFFINE TRANSFORMATION	STANDARD ERROR OF MEAN OF X AND Y ON THE OBJECT SPACE POINT (MM)
2780.	1.	33.5767	-7.1657	0.100000-02	0.140680-02
2780.	2.	24.3351	-7.2504	0.412310-02	0.217470-02
2780.	11.	33.4083	-7.3966	0.452770-02	0.177360-02
2780.	12.	10.0956	12.8739	0.608280-02	0.107040-02
2780.	13.	4.1758	19.5253	0.583100-02	0.151380-02
2780.	14.	11.4716	25.6752	0.223610-02	0.221270-02
2780.	15.	2.1674	33.6659	0.494970-02	0.152750-02
2780.	16.	-5.5054	31.9283	0.705540-02	0.327550-02
2785.	1.	33.4444	-6.9248	0.707110-03	0.122470-02
2785.	2.	27.6204	-7.0940	0.154950-02	0.207670-02
2785.	11.	27.4420	-7.2005	0.667080-02	0.177360-02
2785.	12.	5.4528	11.4230	0.118530-01	0.113650-02
2785.	13.	0.2506	17.6556	0.125300-01	0.141800-02
2785.	14.	7.0352	23.3999	0.694430-02	0.221270-02
2785.	15.	-1.4277	31.0908	0.405540-02	0.152750-02
2785.	16.	-6.5395	29.5591	0.135930-01	0.327550-02

Plate 2: Results of TRANC 4 for Photo Frames 2780 and 2785

PHOTO COORDINATES CORRECTED FOR LENS AND FILM DISTORTIONS (FAIRCHILD MAPPING CAMERA #003)

PHOTO	POINT	X (MM)	Y (MM)	UNIT STANDARD ERROR (MM) AFTER AFFINE TRANSFORMATION	STANDARD ERROR OF MEAN OF X AND Y ON THE OBJECT SPACE POINT (MM)
2790.	1.	29.8579	-21.4213	0.300000-02	0.217470-02
2790.	4.	27.6834	9.7633	0.316230-02	0.170170-02
2790.	11.	23.8517	-21.7888	0.282840-02	0.143510-02
2790.	12.	2.1518	-4.2797	0.353550-02	0.139540-02
2790.	13.	-2.8036	1.3773	0.158110-02	0.204120-02
2790.	14.	3.2876	6.4819	0.728010-02	0.170780-02
2790.	15.	-4.2159	13.1615	0.412310-02	0.140580-02
2790.	17.	-2.0145	-3.9572	0.447210-02	0.193110-02
2795.	1.	24.1349	-21.9193	0.135090-01	0.217470-02
2795.	4.	22.4600	6.5007	0.180280-01	0.170170-02
2795.	11.	18.3452	-22.3044	0.147650-01	0.143510-02
2795.	12.	-2.0306	-5.9206	0.636400-02	0.139540-02
2795.	13.	-5.0463	-0.5706	0.168090-01	0.204120-02
2795.	14.	-0.8117	4.2532	0.291550-02	0.170780-02
2795.	15.	-7.7153	10.7080	0.604150-02	0.140580-02
2795.	17.	-5.9562	-5.6048	0.777520-02	0.193110-02

Plate 3: Results of TRANC 4 for Photo Frames 2790 and 2795

PHOTO COORDINATES CORRECTED FOR LENS AND FILM DISTORTIONS (FAIRCHILD MAPPING CAMERA #003)

PHOTO	POINT	X (MM)	Y (MM)	UNIT STANDARD ERROR (MM) AFTER AFFINE TRANSFORMATION	STANDARD ERROR OF MEAN OF X AND Y ON THE OBJECT SPACE POINT (MM)
2800.	1.	19.9669	-23.4031	0.360790-02	0.147200-02
2800.	2.	9.9589	-23.7644	0.632460-02	0.254130-02
2800.	3.	16.7280	-11.8095	0.282440-02	0.418080-02
2800.	4.	18.6205	3.6844	0.141420-02	0.154780-02
2800.	11.	14.3342	-23.7790	0.430120-02	0.378320-02
2800.	12.	-5.0431	-8.2753	0.430120-02	0.254130-02
2800.	13.	-9.3058	-3.1649	0.514780-02	0.211640-02
2800.	14.	-3.7510	1.4165	0.360560-02	0.170780-02
2800.	15.	-10.1436	7.6788	0.412310-02	0.100000-02
2800.	16.	-15.7402	6.6345	0.158110-02	0.151380-02
2800.	17.	-8.7123	-7.9428	0.291550-02	0.234080-02
2805.	1.	16.5881	-24.7487	0.159530-01	0.147200-02
2805.	2.	7.1408	-25.0964	0.721110-02	0.254130-02
2805.	3.	13.6853	-13.7183	0.961770-02	0.418080-02
2805.	4.	15.7819	1.1648	0.353550-02	0.154780-02
2805.	11.	11.3612	-25.1162	0.751660-02	0.378320-02
2805.	12.	-7.0960	-10.3882	0.223510-02	0.254130-02
2805.	13.	-11.1033	-5.4948	0.168090-01	0.211640-02
2805.	14.	-5.5040	-1.0984	0.704370-13	0.170780-02
2805.	15.	-11.7159	4.9075	0.600000-02	0.100000-02
2805.	16.	-17.0254	3.7672	0.790570-02	0.141380-02
2805.	17.	-10.5718	-10.0188	0.265420-01	0.234080-02

Plate 4: Results of TRANC 4 for Photo Frames 2800 and 2805

JOB NUMBER 10

PHOTO COORDINATES CORRECTED FOR LENS AND FILM DISTORTIONS (FAIRCHILD MAPPING CAMERA #003)

PHOTO	POINT	X (MM)	Y (MM)	UNIT STANDARD ERROR (MM) AFTER AFFINE TRANSFORMATION	STANDARD ERROR OF MEAN OF X AND Y ON THE OBJECT SPACE POINT (MM)
2810.	1.	13.7244	-25.0866	0.667080-02	0.146490-02
2810.	2.	4.2680	-25.5883	0.412310-02	0.125830-02
2810.	3.	10.4520	-14.6663	0.158110-02	0.363720-02
2810.	4.	12.4905	-0.3318	0.254950-02	0.233630-02
2810.	11.	6.3751	-25.5461	0.632460-02	0.299500-02
2810.	13.	-13.2865	-7.1749	0.447210-02	0.120760-02
2810.	14.	-3.2780	-2.9325	0.447210-02	0.125830-02
2810.	15.	-13.9343	2.9592	0.159110-02	0.190390-02
2810.	16.	-13.9352	1.9172	0.500000-02	0.113650-02
2815.	1.	10.9052	-25.5228	0.353550-02	0.146490-02
2815.	2.	1.7242	-25.9928	0.790570-02	0.125830-02
2815.	3.	7.7178	-15.5672	0.761540-02	0.363720-02
2815.	4.	9.9134	-1.8030	0.486000-02	0.213630-02
2815.	11.	5.5987	-25.5427	0.254950-02	0.185970-02
2815.	13.	-14.9462	-8.3803	0.721110-02	0.120760-02
2815.	14.	-10.1162	-4.3395	0.919240-02	0.125830-02
2815.	15.	-15.4091	1.2964	0.360550-02	0.190390-02
2815.	16.	-20.1816	0.4350	0.141470-01	0.113650-02

Plate 5: Results of TRANC 4 for Photo Frames 2810 and 2815

JOB NUMBER 10

PHOTO COORDINATES CORRECTED FOR LENS AND FILM DISTORTIONS (FAIRCHILD MAPPING CAMERA #003)

PHOTO	POINT	X (MM)	Y (MM)	UNIT STANDARD ERROR (MM) AFTER AFFINE TRANSFORMATION	STANDARD ERROR OF MEAN OF X AND Y ON THE OBJECT SPACE POINT (MM)
2820.	1.	8.1216	-26.1331	0.223610-02	0.379950-03
2820.	2.	-0.7880	-26.5218	0.707110-03	0.470370-02
2820.	3.	5.0697	-16.5938	0.380790-02	0.317210-02
2820.	4.	7.4606	-3.3352	0.400000-02	0.151380-02
2820.	11.	3.0431	-26.5170	0.223610-02	0.144770-02
2820.	13.	-16.5204	-9.5555	0.158110-02	0.107060-02
2820.	14.	-11.9538	-5.7106	0.291550-02	0.162660-02
2820.	15.	-16.9281	-0.2215	0.282840-02	0.110470-02
2825.	1.	5.7365	-26.5525	0.567080-02	0.978950-03
2825.	2.	-2.9410	-26.9825	0.851470-02	0.367140-02
2825.	3.	2.6815	-17.4872	0.200000-02	0.317210-02
2825.	4.	5.1104	-4.5014	0.400000-02	0.151380-02
2825.	11.	0.7821	-26.9502	0.424260-02	0.194720-02
2825.	13.	-18.1667	-10.7803	0.135010-01	0.107060-02
2825.	14.	-13.5493	-7.0575	0.764350-02	0.162660-02
2825.	15.	-18.4235	-1.7541	0.827650-02	0.110470-02

Plate 6: Results of TRANC 4 for Photo Frames 2820 and 2825

E

The program also computes the distortion parameters in a separate subroutine. The radial distortion (Δr) and the tangential distortion (Δt) are represented by the basic distortion equations [2] [5] [21]. Radial distortion is represented by an odd power polynomial in terms of r , the radial distance from the principal point [21] [28].

$$\Delta r = K_1 r^3 + K_2 r^5 + K_3 r^7$$

where the K terms are extracted from the calibration report [28]

$$K_1 = - 0.13361854 \times 10^{-5}$$

$$K_2 = 0.52261757 \times 10^{-9}$$

$$K_3 = - 0.50728336 \times 10^{-13}$$

The x and y components of r are:

$$\Delta x_r = \frac{\Delta r}{r} (x') = (K_1 r^2 + K_2 r^4 + K_3 r^6) (x')$$

$$\Delta y_r = \frac{\Delta r}{r} (y') = (K_1 r^2 + K_2 r^4 + K_3 r^6) (y')$$

where x' y' are the measured coordinates [21] [28]. For these measurements the radial distortion ranged from $.8 \mu$ to 44.4μ and averaged 15.48μ . This is within the 50μ distortion range established by Table 1. The radial distortion is positive outward as shown on the radial distortion curve in the calibration report [28] and the correction was applied with opposite sign.

The tangential distortion is represented by an even powered polynomial "thin prism" model as developed in [5] [21] [28].

$$\Delta t = J_1 r^2 + J_2 r^4$$

where the J terms are extracted from the calibration report [28].

$$J_1 = - 0.54958195 \times 10^{-6}$$

$$J_2 = - 0.46089420 \times 10^{-10}$$

The x and y components are

$$\begin{aligned}\Delta x_t &= -\Delta t \sin \varphi_o = -(J_1 r^2 + J_2 r^4) \sin \varphi_o \\ \Delta y_t &= -\Delta t \cos \varphi_o = -(J_1 r^2 + J_2 r^4) \cos \varphi_o\end{aligned}$$

where

$$\varphi_o = 2.9459070 \text{ rad, the angle of maximum tangential distortion [28].}$$

The corrected image coordinates are then represented [21] [28].

$$\begin{aligned}x &= (1 + K_1 r^2 + K_2 r^4 + K_3 r^6) x' - (J_1 r^2 + J_2 r^4) \sin \varphi_o \\ y &= (1 + K_1 r^2 + K_2 r^4 + K_3 r^6) y' + (J_1 r^2 + J_2 r^4) \cos \varphi_o\end{aligned}$$

The coordinates provided are used in the FORTBLOCK adjustment.

4.4 Block Adjustment Program

The FORTBLOCK block adjustment triangulation program performs a simultaneous least squares adjustment on the estimated parameters (i.e., elements of exterior orientation and survey coordinates) based on the observations of photo coordinates, interior orientation elements and the collinearity condition. A complete description of the theory is found in [5] [21] [33]. The program provides adjusted values of the parameters, standard deviations, residuals, correlation coefficients and variance - covariance matrices. It was designed for use in conventional earth-based strip and block aerotriangulation problems where the control is distributed along strips and around the perimeter of the block, however, the program was modified for this project. The strip and block in this case is a sequence of 100 % overlapping photographs of the same area receding from view with a very small horizontal base.

The collinearity condition states that a point in the object space, the nodal point in the camera lens and the imaged point all lie on a straight line. This is represented by the following equations:

$$\begin{aligned}x - x_0 &= c \frac{\Delta X_R}{\Delta Z_R} \\y - y_0 &= c \frac{\Delta Y_R}{\Delta Z_R}\end{aligned}$$

where x and y are the photo coordinates corrected for distortion; x_0 and y_0 are the translation to the principal point; c is the focal length; ΔX_R , ΔY_R , ΔZ_R are the survey or selenographic coordinates in the right hand cartesian coordinate system rotated to the photo system [2] [21].

4.4.1 Input to FORTBLOCK

The FORTBLOCK program requires the following input: a) observed photo coordinates, b) calibrated focal length, c) estimated values of the selenographic coordinates for each control and NEC parameter, d) estimated values of the

elements of exterior orientation parameters, e) weights for the photo observations and estimated parameters.

The source for the photo coordinates was described in Section 4.3.2. The calibrated focal length was extracted from [28]. The source of the control and NEC points was covered in Section 4.2.2.

The six elements of exterior orientation are X_0 , Y_0 , Z_0 , κ , φ , ω . These provide the location and attitude of the camera and in this case the spacecraft when each picture was taken. The positional elements can be estimated by using the latitude, longitude and geocentric radius listed in Table 2. The rotational elements which are used in rotational matrices can be described as those angles necessary to rotate the selenographic axes into alignment with the photograph axes so that vectors in the object space will correspond to those in the image space. Figures 17 - 19 show the descriptive geometry used in estimating these angles.

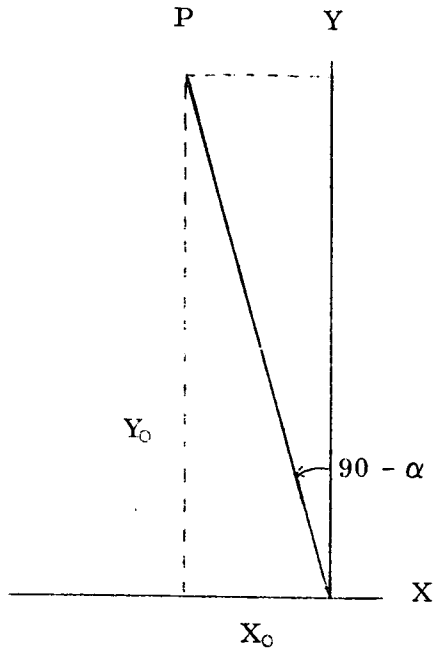


Figure 17a. Plan View Of

$$\alpha = \tan^{-1} \frac{Y_0}{X_0}$$

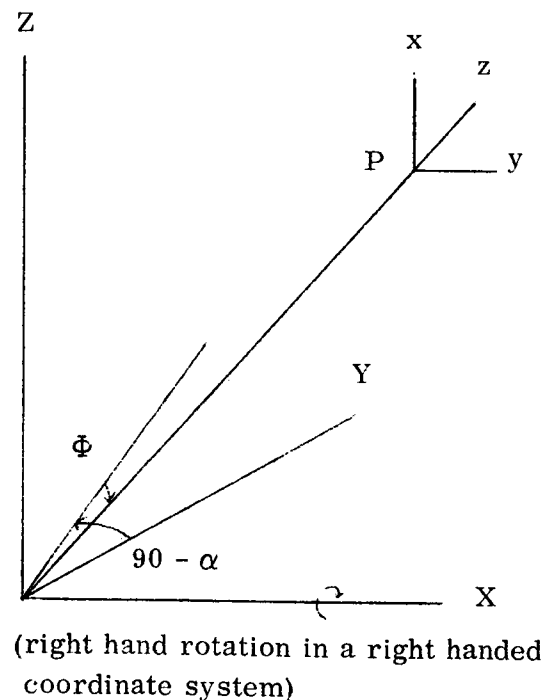


Figure 17b. Perspective View Of
Primary Rotation

The first rotation or primary rotation is a negative ω about the X axis which aligns Z into the camera y z plane. This rotation is by an amount $\Pi/2$ plus an additional amount equal to the latitude of the camera $\bar{\Phi}$.

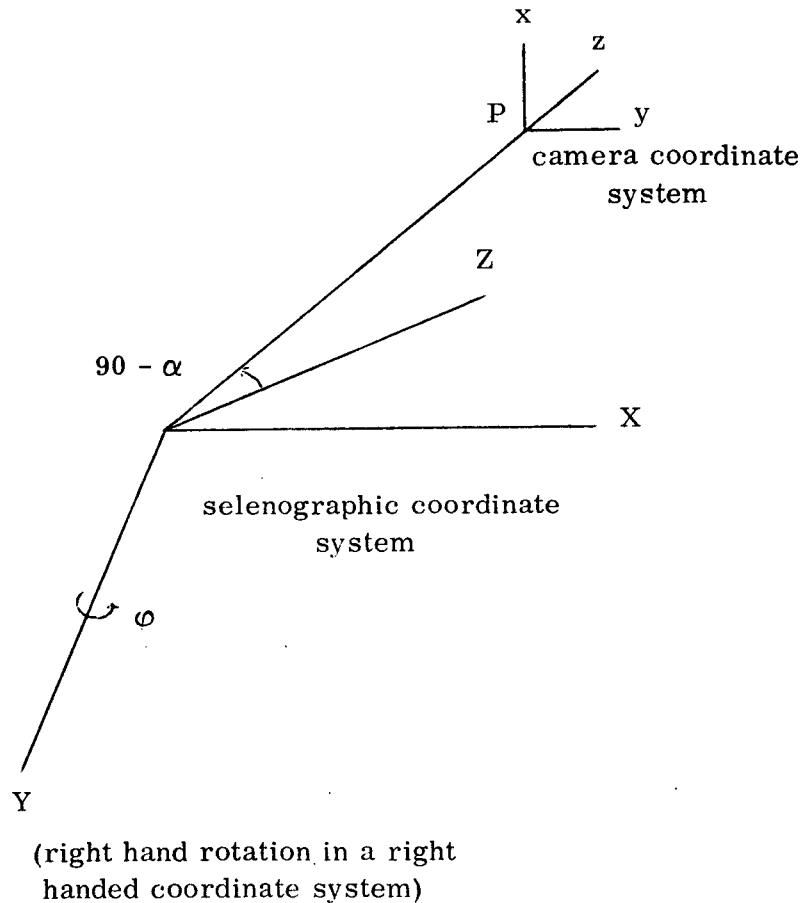


Figure 18. Secondary Rotation

The secondary rotation is a negative ϕ rotation of $90^\circ - \alpha$ about the once rotated Y axis in order to align the Z axis with the z camera axis. This is shown in Figure 18.

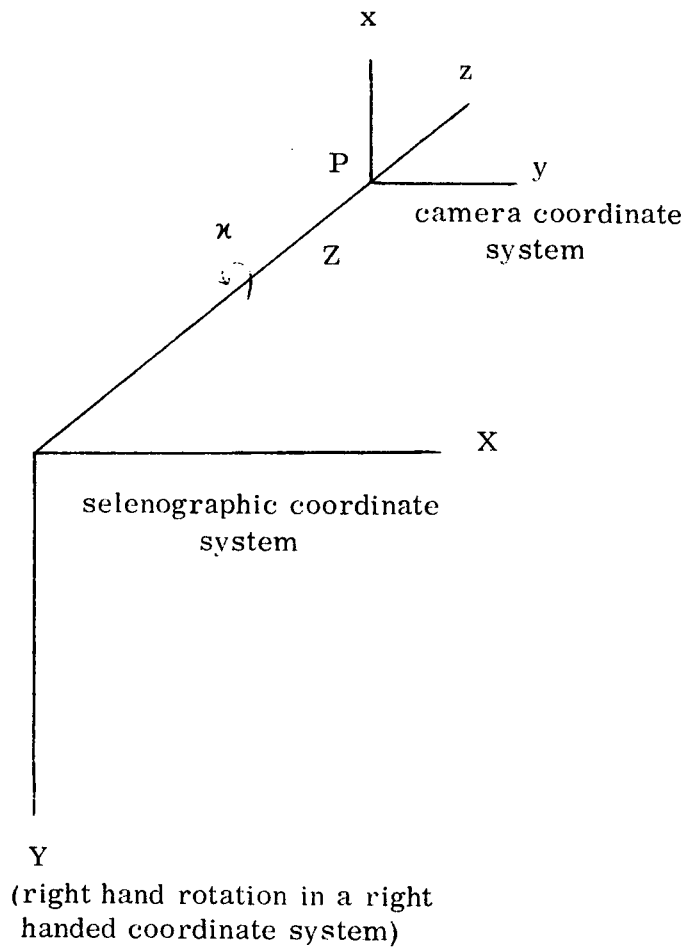


Figure 19. Tertiary Rotation

The tertiary and final rotation is a negative α rotation about the twice rotated Z axis by an amount $90 - \Phi$ as shown in Figure 19.

In summary, Table 8 shows all the estimated values of the exterior orientation used in the adjustment. The last required input, the weight which are the constraints are computed separately for observations and parameters.

The weights are derived from the inverse of the standard deviation squared. The standard deviations (σ) are extracted from external sources or estimated [35]. In all cases the a-priori value of the variance of unit weight is assumed to be unity. The standard deviation for all photo observations was 10μ consequently,

Frame No.	X ₀ (km)	Y ₀ (km)	Z ₀ (km)	κ (rad)	φ (rad)	ω (rad)
2774	- 804.74	2846.42	- 1831.25	- 1.020	- .276	- 2.125
2777	- 749.04	2944.97	- 1865.04	- 1.020	- .249	- 2.121
2780	- 693.07	3043.49	- 1897.85	- 1.024	- .244	- 2.117
2785	- 648.68	3619.24	- 2193.62	- 1.033	- .177	- 2.109
2790	- 585.46	3725.97	- 2227.87	- 1.037	- .156	- 2.104
2795	- 457.95	3935.33	- 2295.69	- 1.046	- .116	- 2.096
2800	- 329.92	4140.76	- 2360.69	- 1.054	- .080	- 2.088
2805	- 266.48	4242.10	- 2392.10	- 1.058	- .063	- 2.083
2810	- 137.46	4441.84	- 2454.20	- 1.066	- .031	- 2.075
2815	- 8.99	4651.33	- 2489.84	- 1.079	- .002	- 2.062
2820	119.82	4831.23	- 2572.83	- 1.082	- .025	- 2.060
2825	184.22	4926.63	- 7601.51	- 1.085	- .037	- 2.056

Table 8 Estimates of Six Elements of Exterior Orientation

the corresponding weight was:

$$W = \frac{1}{\sigma^2} = \frac{1}{(.010 \text{ mm})^2} = 10,000$$

The standard deviations for the control points came from Table 4. The standard deviation for the NEC points was assigned 20 km and was based on the ACIC charts used in estimating the longitude and latitude. No constraints were placed on the estimated elements of exterior orientation. The symplifying assumption is made that no correlation exists internally between control points, exposure stations and photo coordinates.

4.4.2 Results of FORTBLOCK

The FORTBLOCK adjustment program iterates internally three times and this is considered sufficient for most cases (i.e., normal earth-based aerial photography). There are a number of guidelines available on the number of iterations required [21]. "The number of iterations required will depend on how well the initial approximations are selected, the geometric strength of the triangulation, and the total number of parameters in the problem" [2]. Due to the unusual conditions of the receding photography the six and twelve photo block adjustments were iterated three times and then also for an additional three times. Six iterations were considered sufficient since only small differences were detected between the standard deviations of the control and NEC points on the third and sixth iterations (Tables 9 - 12).

To save space only one set of the FORTBLOCK output, the 12 photo block with six iterations, is shown in Plates 7 - 23. This adjustment with 12 photos provided the greatest number of observations, the greatest number of degrees of freedom and the lowest standard deviation for the adjusted NEC points, consequently, this solution was selected as the most favorable.

The succeeding tables (Tables 9 - 12) present a summary of the output for the NEC points. It should be noted that the column headed 'Residuals' are not

APOLLO 15 MISSION
JOB NUMBER 1
DATE 20 APR. 1972
TIME 21:29:17.3
NUMBER OF PHOTOS = 12
DEGREES OF FREEDOM = 144
UNIT STANDARD ERROR = 0.156560+01

Plate 7: FORTBLOCK Output Listing for 12 Photo Block Solution; Title Page

RESULTS
EXTERIOR ORIENTATION

PHOTO NO. 2774	X0 (METERS)	Y0 (METERS)	Z0 (METERS)	KAPPA (RAD.)	PHI (RAD.)	OMEGA (RAD.)
	-787125.754	2852024.756	-1839426.555	-0.8549090+00	-0.7507710-01	-0.2079610+01
STD.ERROR	0.51710+04	0.55570+04	0.41340+04	0.12270-02	0.26610-02	0.27370-02
RESIDUALS	-0.17610+05	-0.56050+04	0.81270+04	-0.16510+00	-0.20090+00	-0.25370-01
WEIGHTS	0.000000000	0.000000000	0.000000000	0.000000000	0.000000000	0.000000000

VARIANCE/COVARIANCE MATRIX

0.267360+08	0.998070+07	-0.519170+07	-0.172740+01	0.131850+02	0.894080+00
0.998070+07	0.308810+08	0.891890+07	0.497920+00	0.668900+01	0.134840+02
-0.519170+07	0.891890+07	0.170870+08	0.230350+01	-0.309110+01	0.826630+01
-0.172740+01	0.497920+00	0.230350+01	0.150630-05	-0.367410-06	0.444400-06
0.131850+02	0.668900+01	-0.309110+01	-0.367410-06	0.708250-05	0.721920-06
0.894080+00	0.134840+02	0.826630+01	0.444400-06	0.721920-06	0.747300-05

PHOTO NO. 2777	X0 (METERS)	Y0 (METERS)	Z0 (METERS)	KAPPA (RAD.)	PHI (RAD.)	OMEGA (RAD.)
	-732147.253	2952460.096	-1873651.717	-0.8526780+00	-0.6743570-01	-0.2107770+01
STD.ERROR	0.55270+04	0.57470+04	0.43590+04	0.11990-02	0.27260-02	0.27770-02
RESIDUALS	-0.14870+05	-0.74700+04	0.85520+04	-0.16730+00	-0.18160+00	-0.13010-01
WEIGHTS	0.000000000	0.000000000	0.000000000	0.000000000	0.000000000	0.000000000

VARIANCE/COVARIANCE MATRIX

0.305490+08	0.113400+08	-0.508720+07	-0.157820+01	0.145820+02	0.132710+01
0.113800+08	0.330300+08	0.107810+08	0.543180+00	0.704240+01	0.142230+02
-0.508720+07	0.107810+08	0.190040+08	0.226060+01	-0.286760+01	0.924350+01
-0.157820+01	0.543180+00	0.226060+01	0.143770-05	-0.320080-06	0.475020-06
0.145820+02	0.704240+01	-0.286760+01	-0.320080-06	0.743190-05	0.877360-06
0.132710+01	0.142230+02	0.924350+01	0.475020-06	0.899360-06	0.772230-05

Plate 8: FORTBLOCK Output Listing for 12 Photo Block;

Results of Exterior Orientation for Photos 2774 and 2777

PHOTO NO. 2780	XU (METERS)	YU (METERS)	ZU (METERS)	KAPPA (RAD.)	PHI (RAD.)	OMEGA (RAD.)
	-666343.150	3059186.145	-1906697.696	-0.851000+00	-0.5500660-01	-0.2115840+01
STD. ERROR	0.62610+04	0.59730+04	0.46680+04	0.11830-02	0.29730-02	0.28430-02
RESIDUALS	-0.26730+05	-0.15700+05	0.88980+04	-0.17300+00	-0.16900+00	-0.11570-02
WEIGHTS	0.000000000	0.000000000	0.000000000	0.000000000	0.000000000	0.000000000

VARIANCE/COVARIANCE MATRIX

0.391990+08	0.137730+08	-0.549450+07	-0.131960+01	0.182100+02	0.177300+01
0.137730+08	0.356720+08	0.131250+08	0.620080+00	0.780650+01	0.151470+02
-0.549450+07	0.131250+08	0.217860+08	0.226000+01	-0.289890+01	0.105580+02
-0.131960+01	0.620080+00	0.226000+01	0.140030-05	-0.220420-06	0.517910-06
0.182100+02	0.780650+01	-0.289890+01	-0.220420-06	0.883670-05	0.105720-05
0.177300+01	0.151470+02	0.105580+02	0.517910-06	0.105720-05	0.803390-05

PHOTO NO. 2785	XU (METERS)	YU (METERS)	ZU (METERS)	KAPPA (RAD.)	PHI (RAD.)	OMEGA (RAD.)
	-564671.050	3222234.496	-1965292.891	-0.8484350+00	-0.3804660-01	-0.2132030+01
STD. ERROR	0.72360+04	0.63220+04	0.51160+04	0.11400-02	0.32020-02	0.29270-02
RESIDUALS	-0.84010+05	0.39700+06	-0.22830+06	-0.14460+00	-0.13900+00	0.23030-01
WEIGHTS	0.000000000	0.000000000	0.000000000	0.000000000	0.000000000	0.000000000

VARIANCE/COVARIANCE MATRIX

0.523600+08	0.179760+08	-0.437540+07	-0.822430+00	0.228730+02	0.316010+01
0.179760+08	0.399700+08	0.171230+08	0.698970+00	0.899620+01	0.165060+02
-0.437540+07	0.171230+08	0.261780+08	0.214040+01	-0.216450+01	0.124900+02
-0.822430+00	0.698970+00	0.214040+01	0.129900-05	-0.406340-07	0.528260-06
0.228730+02	0.899620+01	-0.216450+01	-0.406340-07	0.102510-04	0.156650-05
0.316010+01	0.166060+02	0.124900+02	0.528260-06	0.156650-05	0.856700-05

Plate 9: FORTBLOCK Output Listing for 12 Photo Block;

Results of Exterior Orientation for Photos 2780 and 2785

PHOTO NO. 2790	XU (METERS)	YU (METERS)	ZU (METERS)	KAPPA (RAD.)	PHI (RAD.)	OMEGA (RAD.)
	-471434.720	3382315.806	-2014442.206	-0.8463290+00	-0.1663460+00	-0.2012610+01
STD.ERROR	0.71150+04	0.69780+04	0.56100+04	0.11750-02	0.28990-02	0.31190-02
RESIDUALS	-0.11400+06	0.34370+06	-0.21350+06	-0.19070+00	0.10350-01	-0.91390-01
WEIGHTS	0.000000000	0.000000000	0.000000000	0.000000000	0.000000000	0.000000000

VARIANCE/COVARIANCE MATRIX

0.506190+08	0.256120+08	0.402290+07	-0.335490+01	0.202990+02	0.709410+01
0.256120+08	0.486910+08	0.239700+08	-0.457180+00	0.116920+02	0.196660+02
0.402290+07	0.239700+08	0.314750+08	0.213440+01	0.195010+01	0.154050+02
-0.335490+01	-0.457180+00	0.213440+01	0.138030-05	-0.959970-06	0.444950-06
0.202990+02	0.116920+02	0.195010+01	-0.959970-06	0.840710-05	0.324450-05
0.709410+01	0.196660+02	0.154050+02	0.446850-06	0.328450-05	0.767120-05

PHOTO NO. 2795	XU (METERS)	YU (METERS)	ZU (METERS)	KAPPA (RAD.)	PHI (RAD.)	OMEGA (RAD.)
	-373114.645	3545468.435	-2060708.015	-0.8440460+00	-0.1682580+00	-0.2024000+01
STD.ERROR	0.83610+04	0.73680+04	0.63410+04	0.11540-02	0.32110-02	0.32670-02
RESIDUALS	-0.84940+05	0.38990+06	-0.23500+06	-0.20200+00	0.52760-01	-0.72000-01
WEIGHTS	0.000000000	0.000000000	0.000000000	0.000000000	0.000000000	0.000000000

VARIANCE/COVARIANCE MATRIX

0.699040+08	0.310910+08	0.704370+07	-0.344530+01	0.265910+02	0.868670+01
0.310910+08	0.542350+08	0.308440+08	-0.518990+00	0.129270+02	0.218350+02
0.704370+07	0.308440+08	0.402090+08	0.194810+01	0.300880+01	0.188760+02
-0.344530+01	-0.518990+00	0.194810+01	0.133110-05	-0.964430-06	0.414920-06
0.265910+02	0.129270+02	0.300880+01	-0.964430-06	0.103140-04	0.365540-05
0.868670+01	0.218350+02	0.188760+02	0.414920-06	0.365540-05	0.106760-04

Plate 10: FORTBLOCK Output Listing for 12 Photo Block;
Results of Exterior Orientation for Photos 2790 and 2795

PHOTO NO. 2800	XU (METERS)	YU (METERS)	ZU (METERS)	KAPPA (RAD.)	PHI (RAD.)	OMEGA (RAD.)
	-269008.167	3698683.213	-2112284.468	-0.8396040+00	-0.1703050+00	-0.2022410+01
STD.ERROR	0.95330+04	0.72180+04	0.67950+04	0.11270-02	0.34340-02	0.32040-02
RESIDUALS	-0.63910+05	0.44210+06	-0.24840+06	-0.21440+00	0.90310-01	-0.65570-01
WEIGHTS	0.000000000	0.000000000	0.000000000	0.000000000	0.000000000	0.000000000

VARIANCE/COVARIANCE MATRIX						
0.908790+06	0.317600+08	0.812390+07	-0.440100+01	0.325530+02	0.856190+01	
0.317600+08	0.521060+08	0.328010+08	-0.111260+01	0.120020+02	0.207690+02	
0.812390+07	0.328010+08	0.460390+08	0.144150+01	0.308590+01	0.201070+02	
-0.440100+01	-0.111260+01	0.144150+01	0.127420-05	-0.127470-05	0.189360-06	
0.325530+02	0.120020+02	0.308590+01	-0.127470-05	0.118070-04	0.326190-05	
0.856190+01	0.207690+02	0.201090+02	0.189360-06	0.326190-05	0.102640-04	

PHOTO NO. 2805	XU (METERS)	YU (METERS)	ZU (METERS)	KAPPA (RAD.)	PHI (RAD.)	OMEGA (RAD.)
	-163282.344	3854287.230	-2160023.236	-0.8360710+00	-0.1663110+00	-0.2013260+01
STD.ERROR	0.11130+05	0.74760+04	0.75000+04	0.11380-02	0.37950-02	0.32970-02
RESIDUALS	-0.10320+06	0.38780+06	-0.23210+06	-0.22190+00	0.10330+00	-0.69740-01
WEIGHTS	0.000000000	0.000000000	0.000000000	0.000000000	0.000000000	0.000000000

VARIANCE/COVARIANCE MATRIX						
0.123790+09	0.361440+08	0.132990+08	-0.549280+01	0.420460+02	0.102210+02	
0.361440+08	0.558880+08	0.393650+08	-0.154870+01	0.126290+02	0.221690+02	
0.132990+08	0.393650+08	0.562550+08	0.910130+00	0.468340+01	0.232730+02	
-0.549280+01	-0.154870+01	0.910130+00	0.129580-05	-0.157120-05	0.293660-09	
0.420460+02	0.126290+02	0.468340+01	-0.157120-05	0.144050-04	0.360430-05	
0.102210+02	0.221690+02	0.232730+02	0.293660-09	0.360430-05	0.109830-04	

Plate 11: FORTBLOCK Output Listing for 12 Photo Block;

Results of Exterior Orientation for Photos 2800 and 2805

PHOTO NO. 2810	X0 (METERS)	Y0 (METERS)	Z0 (METERS)	KAPPA (RAD.)	PHI (RAD.)	OMEGA (RAD.)
	-58788.743	4003245.096	-2207544.590	-0.8491210+00	-0.1634410+00	-0.2017800+01
STD. ERROR	0.13000+05	0.77580+04	0.84220+04	0.11440-02	0.42210-02	0.34450-02
RESIDUALS	-0.78470+05	0.43860+06	-0.24670+06	-0.21690+00	0.13240+00	-0.57200-01
WEIGHTS	0.000000000	0.000000000	0.000000000	0.000000000	0.000000000	0.000000000

VARIANCE/COVARIANCE MATRIX

0.169110+09	0.382090+08	0.182930+08	-0.633930+01	0.547310+02	0.113270+02
0.382090+08	0.601870+08	0.477000+08	-0.170200+01	0.124780+02	0.240430+02
0.182930+08	0.477000+08	0.709320+08	0.535630+00	0.607090+01	0.276470+02
-0.633930+01	-0.170200+01	0.539630+00	0.130770-05	-0.177070-05	-0.807150-07
0.547310+02	0.124780+02	0.607090+01	-0.177070-05	0.178180-04	0.374930-05
0.113270+02	0.240430+02	0.276470+02	-0.807150-07	0.374930-05	0.118670-04

PHOTO NO. 2815	X0 (METERS)	Y0 (METERS)	Z0 (METERS)	KAPPA (RAD.)	PHI (RAD.)	OMEGA (RAD.)
	34791.597	4155945.560	-2248419.551	-0.8448770+00	-0.1591060+00	-0.2014370+01
STD. ERROR	0.14860+05	0.79700+04	0.92040+04	0.11550-02	0.46010-02	0.35230-02
RESIDUALS	-0.43790+05	0.49540+06	-0.24140+06	-0.23410+00	0.15710+00	-0.45630-01
WEIGHTS	0.000000000	0.000000000	0.000000000	0.000000000	0.000000000	0.000000000

VARIANCE/COVARIANCE MATRIX

0.220880+09	0.398950+08	0.265620+08	-0.737280+01	0.642250+02	0.131020+02
0.398950+08	0.635220+08	0.547700+08	-0.202060+01	0.122130+02	0.252200+02
0.265620+08	0.547700+08	0.847120+08	-0.138230+00	0.832110+01	0.311540+02
-0.737280+01	-0.202060+01	-0.138230+00	0.133410-05	-0.200570-05	-0.263330-06
0.642250+02	0.122130+02	0.832110+01	-0.200570-05	0.211680-04	0.408440-05
0.131020+02	0.252200+02	0.311540+02	-0.263330-06	0.408440-05	0.124110-04

Plate 12: FORTBLOCK Output Listing for 12 Photo Block;

Results of Exterior Orientation for Photos 2810 and 2815

F

PHOTO NO. 2820	XU (METERS)	YU (METERS)	ZU (METERS)	KAPPA (RAD.)	PHI (RAD.)	OMEGA (RAD.)
	138215.442	4300913.091	-2292476.487	-0.8372350+00	-0.1549110+00	-0.2016520+01
STD.ERROR	0.17570+05	0.91190+04	0.11140+05	0.11710-02	0.52190-02	0.40610-02
RESIDUALS	-0.18400+05	0.53070+06	-0.28040+06	-0.24480+00	0.12990+00	-0.43490-01
WEIGHTS	0.000000000	0.000000000	0.000000000	0.000000000	0.000000000	0.000000000

VARIANCE/COVARIANCE MATRIX

0.109580+09	0.539260+08	0.560620+08	-0.833220+01	0.915290+02	0.221840+02
0.539260+08	0.831570+08	0.817890+08	-0.261810+01	0.156960+02	0.339590+02
0.560620+08	0.817890+08	0.124150+09	-0.134640+01	0.167760+02	0.440150+02
-0.833220+01	-0.261810+01	-0.134640+01	0.137160-05	-0.219740-05	-0.605620-06
0.915290+02	0.156960+02	0.167760+02	-0.219740-05	0.272380-04	0.660000-05
0.221840+02	0.339590+02	0.440150+02	-0.605620-06	0.660000-05	0.164880-04

PHOTO NO. 2825	XU (METERS)	YU (METERS)	ZU (METERS)	KAPPA (RAD.)	PHI (RAD.)	OMEGA (RAD.)
	267504.814	4446070.208	-2332275.509	-0.8406030+00	-0.1440820+00	-0.2016920+01
STD.ERROR	0.20240+05	0.93380+04	0.12230+05	0.11930-02	0.57700-02	0.41670-02
RESIDUALS	-0.33290+05	0.48060+06	-0.26970+06	-0.24440+00	0.10710+00	-0.39180-01
WEIGHTS	0.000000000	0.000000000	0.000000000	0.000000000	0.000000000	0.000000000

VARIANCE/COVARIANCE MATRIX

0.409750+09	0.523460+08	0.826320+08	-0.977040+01	0.116650+03	0.275200+02
0.523460+08	0.871990+08	0.321180+09	-0.314680+01	0.142960+02	0.354890+02
0.826320+08	0.321180+09	0.149460+09	-0.280350+01	0.236180+02	0.497650+02
-0.977040+01	-0.314680+01	-0.280350+01	0.142320-05	-0.250590-05	-0.968040-06
0.116650+03	0.142960+02	0.236180+02	-0.250590-05	0.332950-04	0.780040-05
0.275200+02	0.354890+02	0.497650+02	-0.968040-06	0.780040-05	0.173830-04

Plate 13: FORTBLOCK Output Listing for 12 Photo Block;
Results of Exterior Orientation for Photos 2820 and 2825

RESULTS
PHOTO COORDINATES
(ALL HEIGHTS TAKEN AS 10000.0)

PHOTO NO.	POINT NO.	X (MM)	Y (MM)	VX (MM)	VY (MM)
2774	1	48.463	-7.075	-0.10250-01	-0.40830-02
2774	2	36.754	-7.109	0.55270-02	-0.17760-01
2774	3	46.573	9.661	0.12530-01	0.31720-01
2774	11	42.070	-7.283	-0.11770-01	-0.18830-02
2774	12	16.609	15.419	-0.14160-01	-0.47220-02
2774	13	9.895	22.703	-0.88120-02	0.11050-01
2774	14	17.879	29.437	0.31860-02	-0.71340-02
2774	15	7.281	37.797	0.48840-02	-0.88740-02
2774	16	-1.249	35.760	-0.24300-02	0.52980-05
2774	17	11.087	15.787	0.15280-01	0.13710-02
2777	1	43.860	-7.206	-0.93010-02	0.16850-02
2777	2	32.445	-7.276	0.28530-01	-0.81320-02
2777	3	41.862	8.547	-0.30070-02	-0.14240-01
2777	11	37.589	-7.417	-0.60780-03	0.16710-01
2777	12	13.281	14.030	0.77920-03	0.12980-01
2777	13	6.976	20.966	-0.97110-02	-0.81790-02
2777	14	14.588	27.396	-0.96040-02	-0.56590-02
2777	15	4.695	35.581	0.26360-02	0.29760-02
2777	16	-3.380	33.718	0.15390-01	-0.91520-02
2777	17	8.030	14.384	-0.14260-01	-0.63100-02
2780	1	39.577	-7.166	-0.10460-02	-0.11040-01
2780	2	28.335	-7.250	-0.23270-01	0.95300-02
2780	11	33.408	-7.397	0.17990-01	0.41390-02
2780	12	10.096	12.874	0.55140-02	0.32110-02
2780	13	4.176	19.525	-0.27160-03	-0.62890-02
2780	14	11.472	25.675	0.13560-01	0.19200-03
2780	15	2.167	33.666	-0.94040-02	0.54210-02
2780	16	-5.505	31.928	-0.36610-02	-0.58330-02

Plate 14: FORTBLOCK Output Listing for 12 Photo Block;

Results of Photo Coordinates

2785	1	33.444	-6.925	0.14950-01	0.49410-03
2785	2	22.620	-7.094	-0.31180-01	-0.20010-02
2785	11	27.442	-7.200	-0.13400-02	-0.28940-02
2785	12	5.653	11.423	0.15090-01	0.33700-02
2785	13	0.251	17.656	0.16500-01	-0.47450-02
2785	14	7.035	23.400	0.27120-02	0.13810-01
2785	15	-1.428	31.091	-0.10760-01	0.34210-02
2785	16	-8.540	29.559	-0.79980-02	-0.12290-01
2790	1	29.658	-21.421	0.28210-02	-0.56130-02
2790	4	27.683	8.763	-0.55960-02	0.11580-01
2790	11	23.852	-21.789	-0.43410-02	-0.25920-02
2790	12	2.152	-4.280	-0.10720-01	-0.72750-02
2790	13	-2.804	1.377	0.20150-01	0.21930-01
2790	14	3.288	6.482	-0.10110-01	-0.13990-01
2790	15	-4.216	13.161	-0.15150-02	0.16370-02
2790	17	-2.014	-3.957	0.86800-02	-0.38440-02
2795	1	24.135	-21.919	0.17300-02	0.39110-02
2795	4	22.460	6.501	-0.47950-02	0.22140-02
2795	11	18.345	-22.304	-0.24450-03	-0.38700-02
2795	12	-2.031	-5.921	0.71520-02	0.66520-02
2795	13	-6.646	-0.591	-0.10310-01	-0.41690-02
2795	14	-0.812	4.253	0.65460-02	-0.73480-03
2795	15	-7.715	10.708	0.10730-01	0.21090-02
2795	17	-5.956	-5.609	-0.10460-01	-0.53900-02
2800	1	19.967	-23.403	-0.20560-02	-0.20420-02
2800	2	9.959	-23.764	0.19530-01	0.91650-02
2800	3	16.728	-11.809	-0.11550-01	-0.23760-01
2800	4	18.620	3.684	-0.54080-02	0.82450-02
2800	11	14.334	-23.779	0.38000-02	0.16600-02
2800	12	-5.043	-8.275	-0.99450-02	-0.55720-03
2800	13	-9.306	-3.165	0.19130-02	0.44760-02
2800	14	-3.751	1.417	-0.16030-02	-0.18710-02
2800	15	-10.144	7.679	0.28510-02	0.37600-02

Plate 15: FORTBLOCK Output Listing for 12 Photo Block;

Results of Photo Coordinates

2800	16	-15.740	6.634	0.39190-02	0.60040-03
2800	17	-8.712	-7.943	-0.16360-02	0.67390-03
2805	1	16.888	-24.749	-0.42870-03	-0.20460-02
2805	2	7.141	-25.096	0.20070-01	0.13550-01
2805	3	13.685	-13.718	-0.60110-02	-0.14440-01
2805	4	15.782	1.165	0.85190-02	-0.16740-02
2805	11	11.361	-25.116	-0.13020-01	0.69560-03
2805	12	-7.098	-10.388	0.90590-02	-0.19170-01
2805	13	-11.103	-5.495	-0.85710-02	-0.61650-02
2805	14	-5.804	-1.098	-0.13500-01	0.27470-01
2805	15	-11.716	4.908	0.16290-01	-0.13340-01
2805	16	-17.025	3.967	-0.12910-01	-0.29560-02
2805	17	-10.572	-10.019	0.51470-03	0.17060-01
2810	1	13.724	-25.087	-0.21830-04	-0.16180-02
2810	2	4.268	-25.588	0.97320-03	0.13000-01
2810	3	10.452	-14.666	-0.14690-02	-0.63880-02
2810	4	12.491	-0.332	-0.25730-02	0.76240-03
2810	11	8.375	-25.544	0.48020-02	-0.92280-02
2810	13	-13.286	-7.175	0.99790-02	-0.14970-02
2810	14	-8.278	-2.932	-0.66490-02	0.92020-03
2810	15	-13.934	2.855	-0.76740-02	-0.50970-03
2810	16	-18.935	1.917	0.31990-02	0.44940-02
2815	1	10.905	-25.523	0.34800-02	-0.35030-02
2815	2	1.724	-25.493	-0.91030-03	-0.12530-02
2815	3	7.718	-15.567	-0.70410-02	0.92280-02
2815	4	9.913	-1.803	-0.75540-02	0.59150-03
2815	11	5.649	-25.943	0.69920-02	-0.18620-02
2815	13	-14.946	-8.360	-0.50390-02	-0.17330-02
2815	14	-10.116	-4.340	0.14330-02	-0.17250-01
2815	15	-15.409	1.296	0.68509-02	0.61150-02
2815	16	-20.182	0.439	0.18150-02	0.10410-01
2820	1	8.122	-26.133	-0.36100-02	-0.78360-02
2820	2	-0.788	-26.522	0.80340-02	0.17710-01
2820	3	5.070	-16.594	-0.22560-02	0.14070-01

Plate 16: FORTBLOCK Output Listing for Photo Block;

Results of Photo Coordinates

2820	4	7.461	-3.335	0.12250-01	-0.98840-02
2820	11	3.043	-26.517	-0.31480-02	-0.72530-02
2820	13	-16.620	-9.556	-0.50670-02	-0.50940-02
2820	14	-11.954	-5.711	0.11350-03	-0.33490-02
2820	15	-16.928	-0.221	-0.59360-02	0.17040-02
2825	1	5.736	-26.553	-0.12320-02	-0.77510-02
2825	2	-2.941	-26.982	0.99530-02	0.17670-01
2825	3	2.682	-17.487	-0.95640-02	-0.17520-01
2825	4	5.110	-4.601	0.11590-02	0.13610-02
2825	11	0.782	-26.950	0.38570-02	-0.60130-03
2825	13	-18.167	-10.760	0.93040-03	-0.10260-02
2825	14	-13.699	-7.057	0.31110-02	0.12600-01
2825	15	-18.423	-1.754	-0.84860-02	-0.53680-02

Plate 17: FORTBLOCK Output Listing for 12 Photo Block;

Results of Photo Coordinates

RESULTS
SURVEY COORDINATES

POINT NO.	1	X	Y	Z
		49278.137	1732571.951	58209.811
STD. ERROR		0.46250+03	0.58290+03	0.80900+03
RESIDUALS		0.10200+04	-0.29500+03	-0.20920+04
WEIGHT		0.000010117	0.000006988	0.000002654

VARIANCE/COVARIANCE MATRIX

0.213910+06	0.513770+04	0.197760+05
0.190250-01	0.340910+06	-0.216330+05
0.528540-01	-0.457990-01	0.654450+06

Correlation Coefficient

POINT NO.	2	X	Y	Z
		-201644.386	1702873.190	-268744.551
STD. ERROR		0.64150+03	0.64650+03	0.62020+03
RESIDUALS		-0.65760+04	0.22450+03	-0.20590+03
WEIGHT		0.000002205	0.000005292	0.000005191

VARIANCE/COVARIANCE MATRIX

0.411490+06	0.280080+05	-0.118130+05
0.675350-01	0.417970+06	-0.366450+05
-0.296940-01	-0.913990-01	0.384600+06

Plate 18: FORTBLOCK Output Listing for 12 Photo Block:

Results of Control Points 1 and 2

POINT NO.	3	X	Y	Z
		259480.319	1683091.248	-352071.437
STD. ERROR		0.70730+03	0.73660+03	0.61160+03
RESIDUALS		0.23390+04	-0.32700+03	0.10950+04
WEIGHT		0.000002778	0.000002778	0.000002778

VARIANCE/COVARIANCE MATRIX

0.500290+06	-0.815220+05	0.103240+06
-0.156460+00	0.542630+06	-0.166260+06
0.238660+00	-0.369040+00	0.374070+06

POINT NO.	11	X	Y	Z
		-100378.527	1723742.914	-133724.700
STD. ERROR		0.53840+03	0.80970+03	0.92840+03
RESIDUALS		-0.18790+04	0.73690+04	-0.12120+03
WEIGHT		0.000000002	0.000000002	0.000000002

VARIANCE/COVARIANCE MATRIX

0.289910+06	-0.838800+05	0.590720+05
-0.192390+00	0.655690+06	-0.480430+06
0.118180+00	-0.639090+00	0.861860+06

Plate 19: FORTBLOCK Output Listing for 12 Photo Block;

Results of Control Point 3 and NEC Point 11

POINT NO. 12	X	Y	Z
	-152632.196	1438455.910	-950354.867
STD. ERROR	0.12910+04	0.25290+04	0.15580+04
RESIDUALS	-0.64000+04	0.34500+04	-0.94710+04
WEIGHT	0.000000002	0.000000002	0.000000002

VARIANCE/COVARIANCE MATRIX

0.166620+07	-0.169370+06	-0.259200+06
-0.518730-01	0.639820+07	-0.229790+07
-0.128910+00	-0.583180+00	0.242650+07

POINT NO. 13	X	Y	Z
	-119109.219	1306499.336	-1132545.875
STD. ERROR	0.13890+04	0.29220+04	0.17570+04
RESIDUALS	-0.56090+05	-0.11190+05	-0.15110+05
WEIGHT	0.000000002	0.000000002	0.000000002

VARIANCE/COVARIANCE MATRIX

0.194010+07	0.732470+05	-0.686320+06
0.180440-01	0.853730+07	-0.281200+07
-0.281120+00	-0.547660+00	0.308810+07

Plate 20: FORTBLOCK Output Listing for 12 Photo Block;

Results of NEC Points 12 and 13

POINT NO. 14	X	Y	Z
	123220.364	1327733.623	-1104416.700
STD. ERROR	0.14940+04	0.26940+04	0.15260+04
RESIDUALS	0.24540+04	0.44090+04	-0.63310+04
WEIGHT	0.000000002	0.000000002	0.000000002

VARIANCE/COVARIANCE MATRIX

0.223290+07	-0.429330+06	-0.466600+06
-0.106660+00	0.725620+07	-0.222720+07
-0.204590+00	-0.541720+00	0.232950+07

POINT NO. 15	X	Y	Z
	154425.771	1083854.930	-1347756.507
STD. ERROR	0.16110+04	0.36020+04	0.22230+04
RESIDUALS	-0.40390+04	0.49890+04	0.31950+03
WEIGHT	0.000000002	0.000000002	0.000000002

VARIANCE/COVARIANCE MATRIX

0.259600+07	-0.596580+06	-0.881310+06
-0.102800+00	0.129720+08	-0.445020+07
-0.246090+00	-0.555880+00	0.494060+07

Plate 21: FORTBLOCK Output Listing for 12 Photo Block;

Results of NEC Points 14 and 15

POINT NO. 16	X	Y	Z
	-1244.288	970961.940	-1439079.114
STD. ERROR	0.1632D+04	0.4253D+04	0.2658D+04
RESIDUALS	-0.8006D+04	-0.3084D+04	-0.5761D+04
WEIGHT	0.000000002	0.000000002	0.000000002

VARIANCE/COVARIANCE MATRIX

0.26646D+07	-0.66379D+06	-0.84357D+06
-0.45607D-01	0.18090D+08	-0.62983D+07
-0.19443D+00	-0.55714D+00	0.70643D+07

POINT NO. 17	X	Y	Z
	-224672.699	1373794.078	-1028307.070
STD. ERROR	0.1311D+04	0.2852D+04	0.1753D+04
RESIDUALS	0.2055D+04	0.1446D+04	-0.1336D+05
WEIGHT	0.000000002	0.000000002	0.000000002

VARIANCE/COVARIANCE MATRIX

0.17195D+07	0.22312D+05	-0.48008D+06
0.59651D-02	0.81363D+07	-0.29553D+07
-0.20482D+00	-0.59096D+00	0.30738D+07

Plate 22: FORTBLOCK Output Listing for 12 Photo Block;

Results of NEC Points 16 and 17

POINT NO.	4	X	Y	Z
		769400.527	1455652.861	-551375.275
STD. ERROR		0.1182D+04	0.9736D+03	0.6213D+03
RESIDUALS		-0.1726D+04	0.7521D+03	0.6254D+03
WEIGHT		0.000001240	0.000002347	0.000005923

VARIANCE/COVARIANCE MATRIX			
0.13981D+07	-0.41145D+05	0.90692D+04	
-0.35741D-01	0.94790D+06	-0.30840D+05	
0.12345D-01	-0.50986D-01	0.38599D+06	

Plate 23: FORTBLOCK Output Listing for 12 Photo Block;

Results of Control Point 4

NEC Point No.	No. of Photos App. On	Adjusted Values of Survey Coordinates (km)			Residuals (km)			Standard Deviation (km)		
		X_a	Y_a	Z_a	V_x	V_y	V_z	σ_x	σ_y	σ_z
11	6	- 100.420	1720.477	- 130.456	- 1.838	10.630	- 3.390	.977	1.746	2.315
12	6	- 156.410	1431.031	- 941.362	- 2.623	10.870	- 18.460	2.564	4.835	2.891
13	6	- 123.250	1299.695	- 1124.436	- 5.195	- 4.387	- 23.220	2.808	5.835	2.805
14	6	118.268	1326.885	- 1100.232	7.406	5.257	- 10.520	3.378	5.674	2.607
15	6	149.443	1084.973	- 1344.909	.944	3.871	- 2.528	3.646	7.989	2.887
16	4	- 6.231	971.865	- 1434.771	- 3.019	- 3.987	- 10.070	3.688	9.824	3.279
17	6	- 229.101	1367.037	- 1019.347	6.483	8.204	- 22.320	2.437	5.283	2.960
$\sigma_0 = 1.56$ Average $\rho_{xy} = - .67400$ Average $\rho_{xz} = .32656$ Average $\rho_{yz} = - .75927$										

Table 9 Summary of Results 6 Photo Block Adjustment (3 iterations)

NEC Point No.	No. of Photos App. On	Adjusted Values of Survey Coordinates (km)			Residuals (km)			Standard Deviation (km)		
		X _a	Y _a	Z _a	V _x	y _y	z _z	σ _x	σ _y	σ _z
11	6	- 100.444	1720.488	- 1304.840	- 1.813	10.620	- 3.362	.970	1.733	2.297
12	6	- 156.575	1431.195	- 941.455	- 2.457	10.710	- 18.370	2.546	4.799	2.869
13	6	- 123.407	1299.905	- 1124.519	- 5.179	- 4.598	- 23.130	2.789	5.791	2.784
14	6	117.992	1327.173	- 1100.376	7.682	4.970	- 10.370	3.355	5.631	2.587
15	6	149.132	1085.382	- 1345.043	1.255	3.462	- 2.394	3.621	7.928	2.863
16	4	- 6.484	972.239	- 1434.869	- 2.765	- 4.361	- 9.972	3.663	9.748	3.253
17	6	- 229.232	1367.179	- 1019.410	6.614	8.061	- 22.260	2.420	5.243	2.937
<p> $\sigma_0 = 1.55$ Average $\rho_{xy} = - .67425$ Average $\rho_{xz} = .32673$ Average $\rho_{yz} = - .75930$ </p>										

Table 10 Summary of Results 6 Photo Block Adjustment (6 iterations)

NEC Point No.	No. of Photos App. On	Adjusted Values of Survey Coordinates (km)			Residuals (km)			Standard Deviation (km)		
		X_a	Y_a	Z_a	V_x	V_y	V_z	σ_x	σ_y	σ_z
11	12	- 100.393	1723.747	- 133.735	- 1.865	7.365	- .111	.548	.834	.945
12	8	- 152.689	1438.396	- 950.353	- 6.343	3.510	- 9.473	1.314	2.573	1.585
13	12	- 119.116	1306.364	- 1132.500	- 5.608	- 11.060	- 15.150	1.414	2.972	1.788
14	12	123.142	1327.636	- 1104.366	2.532	4.507	- 6.381	1.521	2.740	1.553
15	12	154.418	1083.646	- 1347.635	- 4.032	5.198	.198	1.639	3.663	2.261
16	8	- 1.201	970.784	- 1438.970	- 8.049	- 2.906	- 5.870	1.661	4.326	2.704
17	6	- 224.687	1373.710	- 1028.291	2.069	1.531	- 13.380	1.335	2.901	1.784
$\sigma_o = 1.59$ Average $\rho_{xy} = - .07563$ Average $\rho_{xz} = - .16332$ Average $\rho_{yz} = - .57380$										

Table 11 Summary of Results 12 Photo Block Adjustment (3 iterations)

NEC Point No.	No. of Photos App. On	Adjusted Values of Survey Coordinates (km)			Residuals (km)			Standard Deviation (km)		
		X _a	Y _a	Z _a	V _x	Y _y	Z _z	σ _x	σ _y	σ _z
11	12	-100.378	1723.743	-133.725	-1.879	7.369	-.121	.538	.810	.928
12	8	-152.632	1438.456	-950.355	-6.400	3.450	-9.471	1.291	2.529	1.558
13	12	-119.109	1306.499	-1132.546	-5.609	-11.190	-15.110	1.389	2.922	1.757
14	12	123.220	1327.734	-1104.417	2.454	4.409	-6.331	1.494	2.694	1.526
15	12	154.426	1083.855	-1347.756	-4.039	4.989	.320	1.611	3.602	2.223
16	8	-1.244	970.962	-1439.079	-8.006	-3.084	-5.761	1.632	4.253	2.658
17	6	-224.673	1373.941	-1028.307	2.055	-1.446	-1.336	1.311	2.852	1.753
<p> $\sigma_o = 1.56$ Average $\rho_{xy} = -.07504$ Average $\rho_{xz} = -.14994$ Average $\rho_{yz} = -.57366$ </p>										

Table 12 Summary of Results 12 Photo Block Adjustment (6 iterations)

residuals from the adjustment but are the differences between the adjusted value and the initial approximated value.

To complete the picture the adjusted values from the 12 photos with six iterations (Table 12) were processed with a program listed in Appendix III to provide the adjusted latitude, longitude and heights above or below a sphere of 1738.1077 km radius. The computer can provide a great number of decimals and this is sometimes misleading towards refinement. It is felt that based on the precision of the observations to one micron which represents a range of 15 - 40 meters on the lunar surface, the results are significant to three decimal places. The third decimal place of degrees also represents approximately the same surface coverage (≈ 30 meters) on the lunar surface. This means that the estimated positions of the NEC points can be precisely located through the photogrammetric procedures outlined in this study. The latitudes and longitudes listed in Table 13 can be compared to Table 5 to show the more precise NEC point location.

Point No.	ϕ	λ	h (km)
11	- 4.428	93.333	- 6.274
12	- 33.304	96.057	- 7.319
13	- 40.803	95.209	- 4.963
14	- 39.633	84.698	- 6.693
15	- 50.912	81.891	- 1.721
16	- 55.992	90.073	- 2.101
17	- 36.453	99.288	- 7.442

Table 13 Adjusted ϕ , λ , h of NEC Points

Perhaps it should be noted that all the heights are negative and represent elevations below a radius of 1738.1077 km. This corresponds to various contour maps such as the ones shown in [17]. These mathematically derived contour maps show a general depression of the lunar sphere on the eastern limb where these points are located.

5. SUMMARY AND CONCLUSIONS

The results show that the system originally specified in theory [33] is workable with real data; however, as in most real data investigations numerous problems arise that are different or not encountered in the smooth operation of theory.

The second generation Apollo 15 film which was of excellent quality was evaluated, points of known control were identified although the number and location were not ideal, and unknown points were selected. Measurements were made and the results were reduced prior to the adjustment. The results of the adjustment show the following:

a. As the number of photos increased through the 6 and 12 photo block the standard deviations of the NEC points as shown in Tables 9 - 12 always decrease. As the iterations in FORTBLOCK are processed the standard deviations also decrease, consequently the sixth iteration of the 12 photo block provides the most favorable solution.

b. There is no significant decrease in the standard deviations of the NEC points from the third iteration to the sixth iteration. This implies that the solution has reached its limitations in this project although further refinement could probably be attained with observations on additional control points if they were available and on additional photographs within the sequence of frames selected.

c. In all cases but one the standard deviation of the NEC Y coordinate is greater than the X, Z coordinate as found theoretically and explained by Sprague [33]. The one exception was NEC point number 11, the northern most selected point. Its location is near the northern limb in the photographs in the area similar to where the control is located. The other NEC points range further south towards the center and lower limb of the photographed moon

and are located closer to the nadir point of the photograph. All the photographs were taken with the selenographic Y axis nominally towards the spacecraft and camera, thus, the convergence is not as precise as in the X - Z direction. This is similar to the determination of heights problem in earth-bound photogrammetry where the standard deviations in planimetry are less than in vertical [10].

d. The correlation coefficient is shown on the lower triangle of the variance covariance matrix in Plates 18 - 23 and is averaged for NEC points on Tables 9 - 12. For the same reasons as (c) above the six photo block shows higher correlation between the X Y and Y Z coordinates than between the X Z coordinates. It should be noted that correlation is considered relatively strong when $> .5$. This is not as prevalent for the 12 photo block.

e. Analysis of the entire variance covariance matrix for the selenographic coordinates of the 6 photo block shows higher correlation coefficients among the NEC points located near the nadir of the photograph (NEC points 12 - 17) and very low correlation among points located further away from the center of the photographs (control points 1 - 4 and NEC point 11). Also the NEC points located near the nadir are very lightly correlated with the control points located away from the center. This can be attributed to the poor geometry of intersecting rays to points near the center and also due to the greater weights assigned to the control points.

Even though the procedure is workable and answers were obtained there is a questionable area that makes the solution less tenable.

Although not discussed in the main body of the report, the adjustment of the 6 and 12 photo block had an effect on the residuals and standard deviations of the four control points. It was expected that the relatively light weights and zero weights on the unknown or NEC points and exposure stations respectively would cause large residuals for these as they adjusted. In some cases the movement of the control points and the resulting standard deviations was greater than the

standard deviations provided by NASA. The residuals and standard deviations from the 12 photo block are shown in the following table for the control points.

Control Point		Residuals (km)			Standard Deviation (km)		
No.	Name	V_x	V_y	Z_z	σ_x	σ_y	σ_z
1	F - 1/10	1.020	- .295	- 2.092	.462	.584	.809
2	CP - 3/8	- 6.576	.224	- .206	.642	.646	.620
3	Ansgarius	2.334	- .328	1.095	.707	.737	.612
4	ACIC 69	- 1.726	.752	.625	1.182	.973	.621

Table 14 Residuals and Standard Deviations of Control Points

It is felt that the unique geometry not only from the spacecraft traversing away from the lunar surface instead of across as in the normal case but also the location of the control in just the northern limb creating a very narrow cone of intersecting rays contributed to this problem.

It is concluded that what could be done under the circumstances was accomplished with optimum results and that the additional effort to take pictures from the Apollo spacecraft from the TEI to TEI + \sim one hour is minimal. It provides an opportunity to use photogrammetry to extend lunar control to the limb and farside exclusive of the passpoint operation in normal traversing aerotriangulation. The problem of weak geometry can be handled by setting the trajectory in a near equatorial orbit in order to place the control in a more favorable position on the photograph and to use similar photography from

additional Apollo missions. This would also allow for a complete opportunity at locating and utilizing all the control points available and to provide improved solutions through additional perspective rays.

6. RECOMMENDATIONS

a. It is recommended that the remaining Apollo missions in the J series continue photographing the lunar surface with the same type of metric camera from the TEI on through TEI + 1.5 hours as in the Apollo 15 mission. Furthermore, this project should be repeated after the Apollo 17 mission with the combined information and film from the three Apollo flights in this series.

b. Since the 'window' of visible features is relatively narrow longitudinally every effort should be made to take advantage of available control locations. The trajectory of the Apollo spacecraft after TEI in a near equatorial orbit as in Apollo 12 and 14 would be ideal in allowing the control points, especially the lunar landmark control, to be centrally located on the photographed moon instead of being on the limb.

c. Even though it is recommended that the next Apollo mission TEI trajectory be more equatorial, the same area of approximately 90° longitude should be rephotographed. The addition of pictures taken from another perspective would provide improved geometry for lunar point solutions. "The results obtained through block adjustment of combined photo data taken from two or more simulated missions were much more promising than results secured through adjustment of single trajectory data " [33].

d. As discussed in Section 4.2.2 the lunar landmark control is the most significant network of known control yet established and it is recommended that the orbiting Apollo astronauts continue their sightings on similar features, particularly on the far side, in order to densify this network.

e. In order to take advantage of all visible features photographed and the bracketing reseau system of photo coordinate reduction it is recommended that the TRANC 4 program be modified. The current procedure of requiring four bracketing reseaus should be changed in order to accomodate all visible

features near the terminator and limb by using a variable number of reseaus. For example, if only three reseaus surrounding an image are available the feature and reseaus would not be measured. Because of the particular nature of the photography a refinement would allow the use of a variable number of surrounding or nearby reseaus, thus making all visible features eligible for measurement.

f) An alternative method of solving for the adjusted control and NEC points is to constrain the coordinates of the exposure station. NASA has recently made available for each photo frame a myriad of details on computer output termed APE (Apollo Photographic Evaluation). Part of the data includes the six elements of exterior orientation including the standard deviations as computed from various external sources [24]. It is recommended that the next real data report include the processing of these data using the following form:

$$\begin{bmatrix} x \\ y \\ z \end{bmatrix}_{\text{PHOTO}} = \begin{bmatrix} M \end{bmatrix} \begin{bmatrix} X_{\text{LH}} \\ Y_{\text{LH}} \\ Z_{\text{LH}} \end{bmatrix} = \begin{bmatrix} F \end{bmatrix}^{-1} \begin{bmatrix} X_{\text{SG}} \\ Y_{\text{SG}} \\ Z_{\text{SG}} \end{bmatrix}$$

where:

$$\begin{bmatrix} F \end{bmatrix}^{-1} = \begin{matrix} \text{a transformation matrix of unit vectors from} \\ \text{selenographic coordinate system (SG) to local} \\ \text{horizontal coordinate system (LH)} \end{matrix}$$

$$\begin{bmatrix} M \end{bmatrix} = \begin{bmatrix} f(\varphi, \omega, \kappa) \end{bmatrix}^T = \begin{bmatrix} R\varphi \end{bmatrix}^T \begin{bmatrix} R\omega \end{bmatrix}^T \begin{bmatrix} R\kappa \end{bmatrix}^T$$

The selenographic coordinates of the points and exposure stations must be transformed to the local horizontal coordinate system since the rotation angles are

from local horizontal coordinate system to the camera axes. It should be noted that the orientation angles as described in [24] are of a rotation sequence with ϕ primary instead of ω primary as used in the programs in this study. Prior to use of the APE data the partials of the observation equations leading to the normals would have to be reevaluated; however, this has been accomplished and is available.

g) It is recommended that a project similar to the Orbiter series be initiated and designed specifically for investigating and mapping the moon. Unmanned orbiting spacecraft with mapping cameras in orbits similar to Orbiter IV and V would be closer to the surface and would provide better perspectives than the post - TEI trajectory used in this study. With maximum utilization of the Lunar Landmark Control Network, extension of control over the surface using photogrammetric procedures would be both feasible and reliable.

BIBLIOGRAPHY

1. ACIC, "Coordinates of Lunar Features," ACIC Technical Paper No. 15, ACIC, St. Louis, Missouri, March, 1965.
2. American Society of Photogrammetry, Manual of Photogrammetry, Falls Church, Virginia, 1966.
3. Boeing, Lunar Orbiter IV Photography, The Boeing Company under NASA contract NASA CR - 1093, NASA, Washington, D.C., July, 1968.
4. Bizzell, Robert M. and Joosten, Rigdon E., "Lunar Mapping - A Position Evaluation," Surveying and Mapping, Vol. 31, No. 3, September, 1971.
5. Brown, Duane C., An Advanced Reduction and Calibration for Photogrammetric Cameras, Contract for AFRCL No. AF19 (604) - 8493, January 10, 1964.
6. Doyle, Frederick J., "Photogrammetric Mapping of the Moon," a paper from the Proceedings of Photogrammetric Engineering, 9th Annual Photogrammetry Short Course, University of Illinois, June 7 - 13, 1969.
7. Fairchild, 3 Inch Mapping Camera, Contract No. NAS 9 - 10201, Fairchild Space and Defense Systems, Syossett, New York, February, 1970.
8. Fajemirokun, Francis A., Applications of Laser Ranging and VLBI Observations for Selenodetic Control, Department of Geodetic Science Report No. 157, The Ohio State University, Columbus, Ohio, November, 1971.

9. Florensky, K.P., Gurshtein, A.A., Korablev, V.I., Bougaevsky, L.M. and Shingareva, K.B., "Classification, Scales, Sequence and Nomenclature of Lunar Maps," The Moon, Vol. 3, No. 1, D. Reidel Publishing Company, Dordrecht, Holland, July, 1971.
10. Ghosh, S.K., "Unpublished Notes on Aerial Triangulation," The Ohio State University, Columbus, Ohio, 1971.
11. Gurshtein, A.A. and Slovokhotova, N.P., "Selection of Points for the Development of a Fundamental Control System on the Lunar Surface," The Moon, Vol. 3, No. 3, D. Reidel Publishing Company, Dordrecht, Holland, December, 1971.
12. Habibullin, Sh T., "On the Systems of Selenographic Coordinates, Their Determination and Terminology," The Moon, Vol. 3, No. 2, D. Reidel Publishing Company, Dordrecht, Holland, August, 1971.
13. Hirvonen, R.A., Adjustment by Least Squares in Geodesy and Photogrammetry, Ungar Publishing Company, New York, 1971.
14. Hopmann, J., "What Can We Say About the Shape of the Moon?," A paper presented at the Proceedings of the Second International Conference on Selenodesy and Lunar Topography, University of Manchester, England, May 30 - June 4, 1966, Published under Measure of the Moon, D. Reidel Publishing Company, Dordrecht, Holland, 1967.
15. Kopal, Zdenek, Relative Heights of Photographic Features of the Moon, Scientific Report No. 1 under AFCRL Contract F 61052-68-C-0002, June, 1969.

16. Kopal, Zdenek, Relative Heights of Photographic Features of the Moon, Scientific Report No. 2 under AFCRL Contract F 61025-68-C-0002, June, 1970.
17. Kopal, Zdenek, The Moon, D. Reidel Publishing Company, Dordrecht, Holland, 1969.
18. Kosofsky, L. J. and El-Baz, Farouk, The Moon as Viewed by Lunar Orbiter, NASA, Washington, 1970.
19. Meyer, Donald L., "Observational Uncertainties in Lunar Control Systems," A paper presented at the Proceedings of the Second International Conference on Selenodesy and Lunar Topography, University of Manchester, England, May 30 - June 4, 1966, Published under Measure of the Moon, D. Reidel Publishing Company, Dordrecht, Holland, 1967.
20. Mills, G. A., "Absolute Coordinates of Lunar Features," Icarus, Vol. 7, January 23, 1967.
21. Merchant, Dean C., "Unpublished Analytical Photogrammetry Lecture Notes," The Ohio State University, Columbus, Ohio, 1971.
22. Nance, Richard, "Positions of Lunar Features from Apollo 9," Journal of Geophysical Research, Vol. 75, No. 11, April 10, 1970.
23. NASA, Apollo 15 SIM Bay Photographic Equipment and Mission Summary Supplement, Mapping Sciences Branch, NASA, Houston, Texas, February, 1972 .

24. NASA, Apollo Photograph Evaluation Program Engineering Manual, NASA MSC Internal Note No. 72-FM-23, Houston, Texas, February 24, 1972.
25. NASA, Apollo Flight Data, Data Processing Branch, Computation and Analysis Division, MSC, Houston, Texas, July 26, 1971.
26. NASA, Apollo 15 Mission 5 Day Report, MSC, Houston, Texas, August, 1971.
27. NASA, Apollo 15 (Mission J-1) Post - TEI Views of the Moon (for July 26, 1971, Launch), MSC Internal Note No. 71-FM-105, NASA, MSC, Houston, Texas, March 22, 1971.
28. NASA, Apollo 15 SIM Bay Photographic Equipment and Mission Summary, Mapping Sciences Branch, NASA, MSC, Houston, Texas, August, 1971, and ammended by Minutes of Meeting, Data Interpretation between NASA/USGS/TOPOCOM/ACIC/Raytheon/Autometrics/FSDS, Syosset, New York, January 24, 1972.
29. Papo, Haim B., "Optimal Selenodetic Control," Department of Geodetic Science Report No. 156, The Ohio State University, Columbus, Ohio, August, 1971.
30. Ransford, G.A., Wollenhaupt, W.R. and Bizzell, R.M., Lunar Landmark Locations Apollo 8, 10, 11, and 12 Missions, NASA Technical Note S-249, Houston, Texas, August, 1970.
31. Ruffin, Byron W., and Meyer, Donald L., Coordinates of Lunar Features, Unpublished Article, ACIC, St. Louis, Missouri.

32. Ruffin, Byron W., A Positional Reference System of Lunar Features Determined From Lunar Orbiter Photography, Unpublished paper under NASA Contract P.R. W-12374-1, ACIC, St. Louis, Missouri, May, 1969.
33. Sprague, Michael D., An Investigation to Improve Selenodetic Control on the Lunar Far Side Utilizing Apollo Trans-Earth Trajectory Photography, Department of Geodetic Science Report No. 155, The Ohio State University, Columbus, Ohio, June, 1971.
34. Togliatti, G. and Solaini, L., "AP/C - Stability Tests," Vol. 33, No. 4, Photogrammetric Engineering, 1967.
35. Uotila, U.A., "Unpublished Notes on Adjustment Computations," The Ohio State University, Columbus, Ohio, 1971.

APPENDIX I

LIST OF ORBITER IV PHOTOGRAPHS WITH ACIC CONTROL INDICATED

39H3	73H2	90H3	109H2	131H3	151H3
46	76H2	95	109H3	133	156
47	77H1	95H2	110H1	134H1	156H2
53H2	77H2	96	112	134H2	156H3
53H3	78	97	113	136H3	157H2
54	78H1	97H1	113H1	137H1	157H3
59H3	78H3	97H3	113H2	137H3	158H2
60	79	98H1	114H1	138	160H2
60H2	79H1	98H2	114H3	138H3	162
61	80H1	100H3	115	139	163H3
61H1	84	101H1	120	139H2	168
64	84H1	101H2	120H3	143	177H1
66H1	85	101H3	121	143H1	184
66H2	85H1	102H1	121H1	143H2	185H1
66H3	85H3	102H2	122	144	
67	86H1	102H3	122H1	144H2	
67H1	86H2	103H3	122H2	145H3	
72	86H3	104	125	148H2	
72H1	88H2	106H3	125H2	149	
72H2	89	107	125H3	149H3	
72H3	89H1	108H2	126	150	
73	89H3	108H3	127	151H1	
73H1	90	109H1	130H3	151H2	

APPENDIX II

(Programmed by Mr. Deward R. Watts May, 1970)

TRANC 4 - PROGRAM FOR TRANSFORMING COMPARATOR COORDINATES INTO PHOTO COORDINATES

PURPOSE: The purpose of the program is to perform a general affine transformation between the observed comparator coordinates and the required photo coordinates.

THEORY: The program consists of four steps:

- (1) the input of the standard reseau grid and the photo coordinate input,
- (2) the formation and application of the transformation parameters,
- (3) the application of corrections for radial distortions,
- (4) the output of the photo coordinates in a form compatible with the input for the FORTBLOCK adjustment program.

The reseau grid is set up by reading cards containing the reseau identification number which serves as a subscript in the CR array and the x and y coordinates of that point as taken from the calibration report.

After the reseau grid has been set up the control parameters INFO (1), COND, TYPE are input. COND may be either RIGHT, LEFT or BOTH, depending on the position within the comparator, of the plate (s) viewed. TYPE indicates whether the plate (s) were positive or negative (POS or NEG). Following the control parameters, the center cross and photo coordinates are entered in the order described in the section title INPUT/OUTPUT FORMATS.

During the second phase of the program, the control parameters COND and TYPE are checked. If an invalid keyword was input, the program accepts COND = LEFT and TYPE = NEG by default. Because of the different possible operating conditions, a second array, TFORM, is formed. TFORM contains all of the necessary information to transform one point. In order to begin the transformation, it is necessary to retrieve the coordinates of the bracketing reseau

point from storage in the CR array. This is done by computing ID1 and ID2, where ID1 is the Jth element and ID2 is the Ith element of the CR (I, J, K) array. Prior to computing ID1 and ID2 the y comparator coordinate of a TYPE = POS plate has been shifted by 1000. This insures the proper reseau point will be retrieved from storage. From this point on, the affine transformation, based on four reseau points, proceeds.

The adopted general affine transformation is represented by:

$$x = AO + A1x' + A2y'$$

$$y = BO + B1x' + B2y'$$

where

x', y' = photo coordinates (center cross origin)

x, y = comparator coordinates

AO, BO = origin shift

$A1, B1, A2, B2$ = remaining coefficients of the
affine transformations

The coefficients of the affine transformation are computed by adjustment of the four x and four y comparator coordinates of the bracketing reseau points.

The average of the four repeated comparator observations of the object point image is computed and then transformed to its photo coordinates values. Use is made of the parameters determined in the above adjustment in the following back solution equations derived from the original affine equations above.

$$x = AO + A1x' + A2y'$$

$$y = BO + B1x' + B2y'$$

$$\begin{bmatrix} x \\ y \end{bmatrix} = \begin{bmatrix} AO \\ BO \end{bmatrix} + \begin{bmatrix} A1 & A2 \\ B1 & B2 \end{bmatrix} \begin{bmatrix} x' \\ y' \end{bmatrix}$$

$$\begin{bmatrix} x' \\ y' \end{bmatrix} = \begin{bmatrix} A1 & A2 \\ B1 & B2 \end{bmatrix}^{-1} \left\{ \begin{bmatrix} x \\ y \end{bmatrix} - \begin{bmatrix} AO \\ BO \end{bmatrix} \right\}$$

$$\begin{bmatrix} x' \\ y' \end{bmatrix} = \begin{bmatrix} B2 & -A2 \\ -B1 & A1 \end{bmatrix} \left(\frac{1}{A1B2 - A2B1} \right) \begin{bmatrix} x - AO \\ y - BO \end{bmatrix}$$

$$x' = \frac{B2 (x - AO) - A2 (y - BO)}{A1B2 - A2B1}$$

$$y' = \frac{-B1 (x - AO) + A1 (y - BO)}{A2B2 - A2B1}$$

$$x' = \frac{A2 (y - BO) - B2 (x - AO)}{A2B1 - A1B2}$$

$$y' = \frac{B1 (x - AO) - A1 (y - BO)}{A2B1 - A1B2}$$

All image points lying within the common bracketing reseau region are then processed by the above affine transformation. Subsequent points are then processed entirely independently using new adjustments for each new reseau region.

After the transformation parameters have been computed and applied, corrections for radial distortion are applied. The output array, CP, is formed and the point counter incremented. If COND = BOTH was specified, the counter is incremented after the photo coordinates for the second plate have been processed. The CP array is then printed and punched and control returned to the main program.

LANGUAGE AND COMPUTER: Fortran IV IBM System 370/165

AVERAGE COMPUTATION TIME: 12 seconds

INPUT/OUTPUT PARAMETERS

SUBROUTINES:

DGMTRA	Transposes a double precision, general matrix.
DGMRRD	Returns the product of two double precision general matrices.
RADISI	Applies a correction for radial distortion to the photo coordinates.

DSQRT Returns the double precision square root of an argument.

ARRAYS:

INFO (4) A vector which contains the following information:

- (1) the job number
- (2) the number of points on the photograph
- (3) the image photo number of the left comparator plate
- (4) the photo number of the right plate.

CR (11, 11, 2) An array which contains the coordinates of the reseau points generated by the Reseau Measurement Task, project (RMT).

CCO (50, 10, 4) In the form CCO (I, J, K) the array contains the following information. I = 1, 50 is a counter for the number of points on the photograph. J = 1, the point identification number. J = 2, the x comparator coordinate of an object space point in the left photo. J = 3, the y coordinate of an object space point in the left photo. J = 5, the x coordinate of an object space point in the right photo, J = 6, the y coordinate of an object space point in the right photo, J = 7, the x coordinate of a bracketing reseau point in the left photo, J = 8, the y coordinate of bracketing reseau point in the left photo, J = 9, the x coordinate of a bracketing reseau in the right photo and J = 10 the y coordinate of a bracketing reseau in the right photo. K = 1, 4 the identifying numbers of the bracketing reseau points.

CP (50, 12)	An array containing the elements to be output by the array in the form indicated in the TRANC 4 subroutine, of the program listing.
CC (4)	A vector containing (1) the x coordinate of the left plate center cross, (2) the y coordinate of the left plate center cross, (3) the x coordinate of the right plate center cross, (4) the y coordinate of the right plate center cross.
FIMAGE (4)	A vector which aids the input of the standard reseau grid generated by the RMT project.
INDEX (4)	A vector which aids the input of the standard reseau grid generated by the RMT project.
B (4, 3)	An array containing the partials of the observation function with respect to the transformation parameters.
EX (4), EX (4)	Two vectors containing the residuals in x and y.
BT (3,4)	The transpose of the B matrix.
UX (3), UY (3)	Two vectors representing the constant vector of the normal equations.
C (3, 3)	An array representing coefficient matrix of the normal equations.
TFORM (4, 4)	An array containing (1) the x coordinate of an object space point, (2) the y coordinate of an object space point, (3) the x comparator coordinate of a reseau point, (4) the y comparator coordinate. The above information is stored for all four reseau points bracketing the object space point, whose coordinates are to be transformed into the photo coordinate system.
PARX (3) PARY (3)	Two vectors containing the corrections to the initial approximations of AO, A1, A2, and BO, B1, B2.

SCALARS

COND	A variable indicating whether the routine is to operate on the values from the left or right plates or both.
TYPE	A variable containing the type of processing which produced the plate, positive or negative.
EOD	An indicator used to show the END OF FILE condition has been encountered.
NPOINT	A counter based on the number of points on a photo and used to index the CCO array.
RIGHT	A variable containing the hexadecimal representation of the word "RIGHT."
BOTH	A variable containing the hexadecimal representation of the word "BOTH."
LEFT	A variable containing the hexadecimal representation of the word "LEFT."
NEG	A variable containing the hexadecimal abbreviation "NEG."
POS	A variable containing the hexadecimal abbreviation "POS."
RI	A variable representing the reseau interval.
AO, A1, A2	Coefficients of the affine transformation from comparator to reseau (photo) coordinate system.
BO, B1, B2	
SUMX, SUMY	Variables containing the total of the X and Y coordinates of the object space coordinates summed over all four observations.
X, Y	Variables representing approximations of the point in the comparator coordinate system.

XAVG, YAVG	Variables containing the mean values of the object space point comparator coordinates.
D	The determinant of the C matrix.
DENOM	A variable containing the computed value of the denominator in the transformation equation.
TERM 1	A variable representing the difference in the mean of the Y object space comparator and the corrected initial approximation of the Y center cross-coordinate.
TERM 2	A variable representing the difference in the mean of the X object space comparator and the corrected initial approximation of the X center cross-coordinate.
XPRIME	A scaler variable containing the X coordinate of the object space point in the reseau system.
YPRIME	A scaler variable containing the Y coordinate of the object space point in the reseau system.
XP, YP	Variables representing the photo coordinates after corrections for radial distortion have been applied.
DISTOR	A variable representing the magnitude of the radial distortion has been applied.
INIT	A variable which serves as an indication of the information contained in COND, INIT = 0 for the left plate INIT = 2 for the right plate.
JPOINT	A counter based on the number of points processed by the routine for a given point.
ICOMP	An indicator on which to branch to the output section.
K 1, K 2	Variables representing which pair of center cross coordinates are to be used during computation.
ID1, ID2	An indicator on which to branch to the output section.

K 3	A variable containing the value of the increment applied to the Jth subscript of the CP (I, J) array. This value is dependent on the values stored in COND and INIT.
IPHOTO	A variable containing the photo number expressed in integer form.
I, J, K, L, IT, JJ, TEMP, TEMPI	Variables used as temporary storage and counters throughout the program.

```

0001      IMPLICIT REAL*8 (A-H,O-Z)
0002      DIMENSION CR(11,11,2),CCO(50,10,4),CP(50,12),CC(4)
0003      KLAL=8 COND,FIMAGE(4)
0004      INTEGER INFO(4),EUD,INDEX(4)
0005      EUD=0
0006      NPUNT=0
0007      1 READ(5,1004) (INDEX(1),I=1,2),(FIMAGE(1),I=1,2),(INDEX(1),I=3,4),(FIMAGE(1),I=3,4)
          *FIMAGE(1),I=3,4)
          1004  FORMAT(1X,I2,1X,I2,2(1X,F8.4),5X,I2,1X,I2,2(1X,F8.4))
0008      1004  FORMAT(1X,I2,1X,I2,2(1X,F8.4),5X,I2,1X,I2,2(1X,F8.4))
0009      IF(INDEX(1),I=1,2) GO TO 15
0010      IF(INDEX(3),NE=0) GO TO 5
0011      CR(INDEX(1),INDEX(2),1)=FIMAGE(1)
0012      CR(INDEX(1),INDEX(2),2)=FIMAGE(2)
0013      GO TO 1
0014      5 DO TO I=1,3,2
0015      CR(INDEX(1),INDEX(1+1),1)=FIMAGE(1)
0016      10 CR(INDEX(1),INDEX(1+1),2)=FIMAGE(1+1)
0017      GO TO 1
0018      15 READ(5,1001) INFO(1),COND,TYPE
0019      1001  FORMAT(15,2(1X,A8))
0020      20 READ(5,1002) INFO(3),CC(1),CC(2),INFO(4),CC(3),CC(4)
0021      1002  FORMAT(15,2(1X,F8.3),21X,15,14X,2(1X,F8.3))
0022      25 NPUNT=NPUNT+1
0023      DO 30 I=1,4
0024      1000  FORMAT(F8.0,4(1X,F8.3),7X,F4.0,1X,4(1X,F8.3))
0025      READ (5,1000,END=0) (CC(INPUNT,K,I),K=1,10)
          C
          C      TEST FOR END OF DATA
          C      TEST TYPE OF INPUT
          C
0026      IF(CC(INPUNT,1,1).EQ.0.0) GO TO 35
0027      30 CONTINUE
0028      GO TO 25
0029      35 INFO(2)=NPUNT-1
0030      L=INFO(2)
0031      CALL TRANC4(INFC,CCO,CP,CR,CC,COND,TYPE)
0032      IF(EUD.NE.0) GO TO 100
0033      NPUNT=0
0034      GO TO 20
0035      40 EUD=1
0036      GO TO 35
0037      100 STOP
0038      END
          TRNC4001
          TRNC4003
          TRNC4004
          TRNC4005
          TRNC4007
          TRNC4008
          TR
          TRNC4010
          TRNC4011
          TRNC4012
          TRNC4013
          TRNC4014
          TRNC4015
          TRNC4016
          TRNC4017
          TRNC4018
          TRNC4021
          TRNC4022
          TRNC4023
          TRNC4024
          TRNC4025
          TRNC4026
          TRNC4027
          TRNC4028
          TRNC4029
          TRNC4030
          TRNC4031
          TRNC4032
          TRNC4033
          TRNC4034
          TRNC4035
          TRNC4037
          TRNC4038
          TRNC4039
          TRNC4040
          TRNC4041
          TRNC4042
          TRNC4043

```

Plate Ia: Main Program for TRANC 4

COMPUTE THE RESEAU IDENTIFICATION NUMBER AND ESTABLISH THE CR MATRIX

TRNC4150

NC4151

IF TYPE=EQ,PUS,AND,JPOINT,EQ,1) CC(K2)=1000.0-CC(K2)

AC=CC(K1)

RG=CC(K2)

A1=1.0

A2=0.0

B1=0.0

B2=1.0

SUMX=0.0

SUMY=0.0

DO 100 J=1,4

101=(50.0+TFORM(J,3)-CC(K1))/RI+1.5

102=(50.0+TFORM(J,4)+CC(K2))/RI+1.5

IF NECESSARY, CONVERT TO THE POSITIVE SYSTEM

COMPUTE VALUES OF X,Y, AND ESTABLISH THE EX AND EY MATRICES

ASSUME THE FOLLOWING INITIAL CONDITIONS

AD=CCC

BO=YCC

A1=D2=1.0

A2=B1=0.0

X=AD+A1*CR(I02,I01,1)+A2*CR(I02,I01,2)

Y=BO+B1*CR(I02,I01,1)+B2*CR(I02,I01,2)

EX(J)=TFORM(J,3)-X

EY(J)=TFORM(J,4)-Y

IF (ICOMP,EQ,1) GO TO 100

ESTABLISH THE B MATRIX

B(J,1)=-1.0

B(J,2)=CR(I02,I01,1)*(-1.0)

B(J,3)=CR(I02,I01,2)*(-1.0)

COMPUTE THE SUM OF THE OBJECT IMAGE COORDINATES

SUMX=SUMX+TFORM(J,1)

SUMY=SUMY+TFORM(J,2)

TEST FOR FOURTH RESEAU POINT. IF TRUE CONTINUE. OTHERWISE,

RETURN FOR NEXT RESEAU POINT

100 CONTINUE

IF (ICOMP,EQ,1) GO TO 125

Reproduced from
Best available copy.

	C	COMPUTE THE AVERAGE OF THE OBJECT SPACE IMAGE COORDINATES	NC4197
	C		NC4198
0054	C	XAVG=SUMX/4.0	NC4199
0055	C	YAVG=SUMY/4.0	NC4200
	C		NC4201
	C		NC4202
	C	TRANSPOSE MATRIX B	NC4203
	C		NC4204
0056	C	CALL DGMFRA(B,UT,4,3)	NC4205
	C		NC4206
	C	OBTAIN THE UX AND UY MATRICES, WHERE UX=UTRANS*CX AND UY=UTRANS*EY	NC4207
	C		NC4208
0057	C	CALL DGMPC(C,UI,EX,UX,3,4,1)	NC4209
0058	C	CALL DGMPC(D,BT,EY,UY,3,4,1)	NC4210
	C		NC4211
	C	COMPUTE C MATRIX	NC4212
	C		NC4213
0059	C	CALL DGMPC(D,RT,RC,C,3,4,3)	NC4214
	C		NC4215
	C	COMPUTE INVERSE OF C MATRIX	NC4216
	C		NC4217
0060	C	CALL DMINV(C,3,0,PARX,PARY)	NC4218
	C		NC4219
	C	COMPUTE THE TRANSFORMATION PARAMETERS	NC4220
	C	FORM PAR MATRIX, WHERE PAR=-1.0*CINVR*U	NC4221
	C		NC4222
0061	C	DO 80 J=1,3	NC4223
0062	C	DU 80 J=1,3	NC4224
0063	C	80 C(I,J)=(-1.0)*C(I,J)	NC4225
0064	C	CALL DGMPC(C,UX,PARX,3,3,1)	NC4226
0065	C	CALL DGMPC(C,UY,PARY,3,3,1)	NC4227
0066	C	AC=PARX(1)+A0	NC4228
0067	C	A1=PARX(2)+A1	NC4229
0068	C	A2=PARX(3)+A2	NC4230
0069	C	HU=PARY(1)+B0	NC4231
0070	C	B1=PARY(2)+B1	NC4232
0071	C	B2=PARY(3)+B2	NC4233
	C		NC4234
	C	COMPUTE COORDINATES IN RESEAU SYSTEM (XPRIME,YPRIME)	NC4235
0072	C	ULNUV=A2*B1-A1*B2	NC4236
0073	C	TERM1=YAVG-R0	NC4237
0074	C	TERM2=XAVG-A0	NC4238
0075	C	APRIME=(A2*TERM1-B2*TERM2)/DENOM	NC4239
0076	C	YPRIME=(B1*TERM2-A1*TERM1)/DENOM	NC4240
	C		NC4241
	C	CORRECT FOR RADIAL AND TANGENTIAL DISTORTION	NC4242
	C		NC4243
	C		NC4244


```

0077 CALL RADISIC(XPRIME,YPRIME,XP,YP,DISTOR) NC4245
0078 K3=0*INIT/2 NC4247
C NC4248
C ESTABLISH CP(J,K) MATRIX, WHERE J=J-TH POINT, AND K=K-TH TERM NC4249
C FOR K=1 OR 7 PHOTO IDENTIFICATION NUMBER NC4250
C FOR K=2 OR 8 PCINT IDENTIFICATION NUMBER NC4251
C FOR K=3 OR 9 X PRIME WITH THE RADIAL DISTORTION CORRECTION NC4252
C APPLIED NC4253
C Y PRIME WITH THE RADIAL DISTORTION CORRECTION NC4254
C APPLIED NC4255
C STANDARD UNIT ERROR FOR THE FOUR RESEAS UNLY NC4256
C STANDARD ERROR OF ONE OBSERVATION ON THE OBJECT NC4257
C SPACE POINT NC4258
C NC4259
C CP(JPOINT,1,K3)=INED(3*INIT/2) NC4260
C CP(JPOINT,2,K3)=CUI(JPOINT,6,1) NC4261
C CP(JPOINT,3,K3)=XP NC4262
C CP(JPOINT,4,K3)=YP NC4263
C ICUMP=1 NC4264
C GO TO 25 NC4265
C NC4266
C COMPUTE STANDARD ERROR - POINT BY POINT NC4267
C NC4268
C 125 TEMP=0.0 NC4269
C TEMP1=0.0 NC4270
C DO 150 I=1,4 NC4271
C TEMP1=TEMP1*(TFORM(I,1)-XAVG)**2+(TFORM(I,2)-YAVG)**2 NC4272
C TEMP=TEMP+EX(I)**2*EY(I)**2 NC4273
C CP(JPOINT,5,K3)=DSORT(TEMP/2) NC4274
C CP(JPOINT,6,K3)=DSORT(TEMP/48.0) NC4275
C ICUMP=0 NC4276
C IF(COND.NE.DUTH) GO TO 10 NC4277
C JPOINT=JPOINT+INIT/2 NC4278
C N=N+1 NC4279
C INIT=INIT+(-1)**N*2 NC4280
C GO TO 15 NC4281
C 200 WRITE(6,2004) INFO(1) NC4282
C 2004 FORMAT(1,'T52','JOB NUMBER',16,'/T17','PHOTO COORDINATES CORRECTED NC4283
C *FOR LENS AND FILM DISTORTIONS (FAIRCHILD MAPPING CAMERA #003 ),// NC4284
C *T50,'UNIT STANDARD ERROR (MM)',T80,'STANDARD ERROR OF MEAN OF X A NC4285
C *ND Y',T10,'PHOTO',T18,'PCINT',T28,'X (MM)',T39,'Y (MM)',T49,'AFTE NC4286
C *K AFFINE TRANSFORMATION',T81,'ON THE OBJECT SPACE POINT (MM)',// NC4287
C IF(COND.LE.DUTH) GO TO 225 NC4288
C WRITE(6,2005) ((CP(I,J),J=1,6),I=1,NPOINT) NC4289
C DO 210 I=1,NPOINT NC4290
C IPHOTO=CP(I,1) NC4291
C IPGINT=CP(I,2) NC4292
C TEMP=DSORT(CP(I,5)**2+CP(I,6)**2) NC4293

```

```

FORTRAN IV G1  RELEASE 20.0          TRANC4          DATE = 72088          12/50/59          PAGE 0005

0106      210 PUNCH 3000,IPHOTO,IPUNIT,(CP(I,J),J=3,4),TEMP          NC4294
0107      3000 FORMAT(215,3F10.4)          NC4295
0108      IF(COND-50.LEFT) GO TO 250          NC4296
0109      WRITE(6,2005) ((CP(I,J),JJ=7,12),I=1,NPOINT)          NC4297
0110      DO 235 I=1,NPOINT          NC4298
0111      IPHOTO=CP(I,7)          NC4299
0112      IPUNIT=CP(I,8)          NC4300
0113      TEMP=USQRT(CP(I,11)**2+CP(I,12)**2)          NC4301
0114      235 PUNCH 3000,IPHOTO,IPUNIT,(CP(I,J),J=9,10),TEMP          NC4302
0115      2005 FORMAT(110,F6.0,T18,F6.0,T26,F9.4,T37,F9.4,T53,E15.5,T87,E15.5,/IT          NC4303
           *10,F6.0,T18,F6.0,T26,F9.4,T37,F9.4,T53,E15.5,T87,E15.5))          NC4304
0116      250 RETURN          NC4305
0117      END          NC4306

```

Plate If: Main Program for TRANC4

```

FORTRAN IV G1  RELEASE 20.0          RADIS1          DATE = 72088          12/50/59          PAGE 0701

0001      SUBROUTINE RADIS1(XP,YP,XP2,YP2,UISTUR)          RADIS101
0002      IMPLICIT REAL*8 (A-H,O-Z)          RADIS102
0003      REAL XI(2)/-0.002000,0.006000/
0004      REAL *R K(1)/-0.131618500-07,+0.522617570-07,-0.5507283360-13/
0005      REAL *R J(2)/-0.549581950-06,-0.460890-10/
0006      XP=XP*XI(1)
0007      YP=YP*XI(2)
0008      R=USQRT(XP**2+YP**2)
0009      R3=R**3
0010      R5=R**5
0011      R7=R**7
0012      DISTUR=K(1)*R3+K(2)*R5+K(3)*R7
0013      PHI0=2.5655070
0014      K2=XP**2+YP**2
0015      R4=R2**2
0016      R6=R2**3
0017      RUF=1.0+K(1)*R2+K(2)*R4+K(3)*R6
0018      XP2=XP*RUF-(J(1)*R2+J(2)*R4)*DSIN(PHI0)
0019      YP2=YP*RUF-(J(1)*R2+J(2)*R4)*DCOS(PHI0)
0020      RETURN
0021      END

```

Plate Ig: Subroutine RADIS for Computing Radial Distortion

APPENDIX III

PROGRAM FOR CALCULATING ϕ , λ , h FROM X , Y , Z

PURPOSE: The purpose of the program is to solve for latitude, longitude and heights above a lunar sphere of radius 1738.1077 km of points given the selenographic coordinates X , Y , Z .

THEORY: The solution is relatively straight forward for a sphere, however, the program was written to solve for the general case of ellipsoids using the following mathematics:

$$p = \sqrt{X^2 + Y^2} = (N + h) \cos \phi$$

so

$$h = \frac{p}{\cos \phi} - N$$

$$Z = \left(N - \frac{a^2 - b^2}{a^2} N + h \right) \sin \phi = \left(N + h - e^2 N \right) \sin \phi$$

after dividing by p

$$\tan \phi = \frac{Z}{p} \left(1 - e^2 \frac{N}{N + h} \right)^{-1}$$

if $h = 0$ for first approximation

$$\tan \phi = \frac{Z}{p} \left(1 - e^2 \right)^{-1}$$

N is computed

$$N = \sqrt{\frac{a^2}{a^2 \cos^2 \phi + b^2 \sin^2 \phi}}$$

solving for new h

$$h = \frac{p}{\cos \phi} - N$$

inserted into

$$\tan \varphi = \frac{Z}{p} \left(1 - e^2 \frac{N}{N + h} \right)^{-1}$$

using φ improved values are found for N and h. This procedure is repeated until φ and h differ by $< 1 \times 10^{-12}$

Longitude is found directly

$$\tan \lambda = \frac{Y}{X}$$

LANGUAGE AND COMPUTER: Fortran IV IBM system 370/165

AVERAGE COMPUTATION TIME: 5 seconds for 11 points

INPUT PARAMETERS:

A, B	Semi-major and semi-minor axes of the ellipsoid in meters; in this case they are equal.
X, Y, Z	Selenographic coordinates from FORTBLOCK adjustment for control and NEC points.

OUTPUT PARAMETERS:

φ, λ, h	Latitude, longitude and height above or below the radius. Latitude and longitude are given in degrees, minutes, seconds and degrees and tenths. The height is given in meters.
-----------------------	--

```

0001 IMPLICIT REAL*8(A-L,N-Z)
0002 DIMENSION NO(3)
0003 INTEGER NH,I
0004 RHO=57.2957795100
0005 A=1738107.700
0006 B=1738107.700
0007 L=1-NH**2/A**2
0008 OME2=1.-E
0009 1 KLAD(5,5000)(NO(I),I=1,3),X,Y,Z
0010 IF(X.EQ.99) GO TO 25
0011 P=DSQRT(X**2+Y**2)
0012 WP=L/P
0013 TP1=WP/OME2
0014 PHI=DATAN(TP1)
0015 5 TTP=TP1*TP1
0016 SECP=DSQRT(1.-O*TP1)
0017 N=A*SECP/USQRT(1.-O*OME2*TP1)
0018 H=P*SECP-N
0019 TP2=WP/(1.-E*N/(N*H))
0020 PHI=DATAN(TP2)
0021 IF(OABS(PHI-PHI1)).LT.1.-12) GO TO 20
0022 PHI1=PHI
0023 TP1=TP2
0024 GO TO 5
0025 20 LAM=DATAN(2/Y,X)
0026 IF(LAM.LT.0.0) LAM=LAM*6.28318530717968
0027 PHI=PHI*PHI
0028 LAM=LAM*H
0029 CALL CONVRT(PHI,MP,MN,SEC)
0030 CALL CONVRT(LAM,ML,MM,ASEC)
0031 WRITE(5,6000)(NO(I),I=1,3),X,Y,Z,MP,MN,SEC,ML,MM,ASEC,H
0032 WRITE(5,6100) PHI,LAM,H
0033 GO TO 1
0034 5000 FORMAT(2A,4,3X,3D16.8)
0035 6000 FORMAT(1D0,2A4,A2,12X,3G17.9,2I4,G12.4,2I4,2G11.4)
0036 6100 FORMAT(1H ,3G17.9)
0037 25 CONTINUE
0038 STOP
0039 END

```

Reproduced from
best available copy.

Plate II a: Main Program for Computing φ , λ , and h from X , Y , Z

FORTRAN IV G1		RELEASE 20.0	CONVRT	DATE = 72111	15/02/55	PAGE 0001
0001	SUBROUTINE CONVRT(PHI,MP,MN,SEC)					
0002	IMPLICIT REAL*8(A-H,D-Z)					
0003	MP=PHI					
0004	AMN=MP					
0005	AMN=(DABS(PHI)-DABS(AMN))*60.					
0006	MN=AMN					
0007	SEC=(AMN-DFLOAT(MN))*60.					
0008	RETURN					
0009	END					

Plate IIb: Subroutine CONVRT for Converting Degrees